ARMY RESEARCH LABORATORY

U.S. Army Research Laboratory Meteorological Measurements for Joint Urban 2003

by Dennis Garvey, Manny Bustillos, Sam Chang, Ronald Cionco, Ed Creegan, Doyle Scott Elliott, Giap Huynh, Cheryl Klipp, David Ligon, Edward Measure, David Quintis, Mario Torres, Gail Vaucher, Edward Vidal, Jr., Yansen Wang, Chatt Williamson, Jimmy Yarbrough, and Young Yee

ARL-TR-4989 **September 2009**

NOTICES

Disclaimers

The findings in this report are not to be construed as an official Department of the Army position unless so designated by other authorized documents.

Citation of manufacturer's or trade names does not constitute an official endorsement or approval of the use thereof.

Destroy this report when it is no longer needed. Do not return it to the originator.

Army Research Laboratory
Adelphi, MD 20783-1197

ARL-TR-4989 **September 2009**

U.S. Army Research Laboratory Meteorological Measurements for Joint Urban 2003

Dennis Garvey, Manny Bustillos, Sam Chang, Ronald Cionco, Ed Creegan, Doyle Scott Elliott, Giap Huynh, Cheryl Klipp, David Ligon, Edward Measure, David Quintis, Mario Torres, Gail Vaucher, Edward Vidal, Jr., Yansen Wang, Chatt Williamson, Jimmy Yarbrough, and Young Yee,
Computational and Information Sciences Directorate, ARL

REPORT DOCUMENTATION PAGE

Form Approved
OMB No. 0704-0188

1. REPORT DATE *(DD-MM-YYYY)*	2. REPORT TYPE	3. DATES COVERED (From - To)
September 2009	Final	

4. TITLE AND SUBTITLE
U.S. Army Research Laboratory Meteorological Measurements for Joint Urban 2003

5a. CONTRACT NUMBER

5b. GRANT NUMBER

5c. PROGRAM ELEMENT NUMBER

6. AUTHOR(S)
Dennis Garvey**,** Manny Bustillos, Sam Chang, Ronald Cionco, Ed Creegan, Doyle Scott Elliott, Giap Huynh, Cheryl Klipp, David Ligon, Edward Measure, David Quintis, Mario Torres, Gail Vaucher, Edward Vidal, Jr., Yansen Wang, Chatt Williamson, Jimmy Yarbrough, and Young Yee

5d. PROJECT NUMBER

5e. TASK NUMBER

5f. WORK UNIT NUMBER

7. PERFORMING ORGANIZATION NAME(S) AND ADDRESS(ES)
U.S. Army Research Laboratory
ATTN: RDRL-CIE-D
2800 Powder Mill Road
Adelphi, MD 20783-1197

8. PERFORMING ORGANIZATION REPORT NUMBER
ARL-TR-4989

9. SPONSORING/MONITORING AGENCY NAME(S) AND ADDRESS(ES)

10. SPONSOR/MONITOR'S ACRONYM(S)

11. SPONSOR/MONITOR'S REPORT NUMBER(S)

12. DISTRIBUTION/AVAILABILITY STATEMENT
Approved for public release; distribution unlimited.

13. SUPPLEMENTARY NOTES

14. ABSTRACT

The Joint Urban 2003 (JU2003) project, a multi-agency undertaking to study turbulent transport and diffusion in the urban boundary layer, was conducted in Oklahoma City, OK, in summer 2003. The field campaign involved extensive meteorological and gas tracer measurements to investigate the dispersion of simulated contaminants in and around the city. Instrumentation provided by the U.S. Army Research Laboratory's (ARL) Battlefield Environment Division (BED) included a Doppler lidar, a mobile radiosonde system, a temperature/moisture profiling microwave radiometer, and an array of three-dimensional (3D) sonic anemometers mounted on five meteorological towers near and outside the central business district (CBD). In this volume, we describe the temperature, wind, turbulence intensity, and heat and momentum flux measurements obtained by the ARL array of sonic anemometers, all of which were confined to the roughness sub-layer (RSL) of the city. We analyze the temporal and spatial variability of wind and turbulence parameters, focusing on day/night and urban/suburban differences and similarities, and extend the analyses to profiles of turbulence data obtained from sonic anemometers mounted on an 85-m pseudo-tower.

15. SUBJECT TERMS
Urban boundary layer, turbulence, stability, microscale model, sonic anemometer

16. SECURITY CLASSIFICATION OF:			17. LIMITATION OF ABSTRACT	18. NUMBER OF PAGES	19a. NAME OF RESPONSIBLE PERSON
a. REPORT	b. ABSTRACT	c. THIS PAGE			Dennis Garvey
Unclassified	Unclassified	Unclassified	UU	90	19b. TELEPHONE NUMBER (*Include area code*) (301) 394-1771

Standard Form 298 (Rev. 8/98)
Prescribed by ANSI Std. Z39.18

Contents

List of Figures

List of Tables

Acknowledgments

We gratefully acknowledge Douglas Brown, Jon Mercurio, Linda Duchow, Felipe Chavez, Gina Eaton, Nancy Fudge, Mike Mason, Rick Hansen, Felicia Chamberlain, Joseph Trammel, SGT Robert Brice, SGT Steve Morgan, MAJ Raymond Pickering, SGT Alan Mariner, and other military personnel and colleagues at the U.S. Army Research Laboratory (ARL) for their contributions and valuable support. ARL also recognizes and appreciates the cooperation and enthusiastic support of the citizenry of Oklahoma City, OK, particularly the efforts of personnel from Allied Steel, Fleet Pride, Firedog, OKC Metro Transit, and OKC Parks and Recreation. We further recognize the individual contributions of J. R. Caton, Scott Smith, Brenda Michelle, Vernon Banks, and Randy Hume, among others, for their generous cooperation throughout this endeavor.

1. Introduction

1.1 Background

With the continued emphasis on military operations in metropolitan areas, the Army is concerned with the urban environment and its effects on systems, sensors, and personnel. The Joint Urban 2003 (JU2003) project, a cooperative undertaking to study turbulent transport and dispersion in the atmospheric boundary layer, was conducted in Oklahoma City (OKC), OK, in summer 2003 (Allwine et al., 2004). It was sponsored by the U.S. Department of Energy's (DOE) National Nuclear Security Administration (NNSA)–Chemical and Biological National Security Program and the U.S. Department of Defense's Defense Threat Reduction Agency (DTRA). The study involved extensive meteorological (met) measurements as well as gas sampling measurements to accurately track the movement of simulated contaminants in and around the city. The resulting data are being used to better understand the urban boundary layer structure and to evaluate and improve computer models that simulate the atmospheric transport and diffusion of contaminants and toxic agents in urban areas.

To evaluate and improve meteorological and diffusion/dispersion models, researchers need to learn how air flows through the urban area both during the day (generally unstable) and at night (generally stable) and how the turbulence characteristics are affected by the urban morphology in combination with the atmospheric stability. The JU2003 study consisted of a series of experiments and included 10 Intensive Observation Periods (IOPs), conducted during the period June 28 through July 31, 2003. The first six of the IOPs were conducted during daylight hours and the last four at night. The inert tracer gas, SF6 (sulfur hexafluoride), was released for a designated time (up to 6 h) from several outdoor locations. Portable tracer samplers collected outdoor air samples for up to several hours after SF6 was released to track its movement through the city and particularly through the central business district (CBD). More details on sensor placement and instrumentation for the Oklahoma City study can be found in the JU2003 Atmospheric Dispersion Study, Experimental Plan (July 2003).

The field study afforded the Battlefield Environment Division (BED) of the U.S. Army Research Laboratory (ARL) the opportunity to leverage its measurement capabilities to increase our scientific understanding of this complex environment. BED's measurement facilities included a Doppler lidar system, a mobile radiosonde system (the Army's Meteorological Measuring Set [MMS]), a temperature/moisture profiling microwave radiometer, and an array of three-dimensional (3D) sonic anemometers mounted on five meteorological towers near and outside the CBD in surrounding industrial (urban) and semi-rural (suburban) areas. These instruments provided meteorological support throughout the testing period. In combination with the large number of in-situ and remote-sensing instruments operated by multiple agencies, it was

anticipated that we would be able to characterize the effect of the city on the structure and dispersive properties of the atmospheric boundary layer at scales ranging from the whole metropolitan area to individual buildings.

1.2 ARL Test Objectives

The goals of ARL during the JU2003 experiments were (1) to actively cooperate with researchers from other agencies in both the meteorological data collection and subsequent analyses in a full scale urban environment; (2) to use the data sets obtained by the many investigators to perform basic research in boundary layer meteorology and to evaluate both micrometeorological and transport and dispersion models; and (3) to use BED field expertise in support of the JU2003 experiments and to evaluate the performance of various instruments in comparisons among in-situ and remote sensors.

Within the scope of this field study, ARL's specific scientific objectives were as follows:

1. Examine boundary layer structure and characterize mean and turbulent flow interactions in the various sub-layers within and above the urban CBD and surrounding industrial and suburban (residential) domains.
2. Develop a database to test, evaluate, and refine urbanized microscale model/codes, such as the Canopy Coupled to Surface Layer (CCSL) and the Three Dimensional Wind Field (3DWF).
3. Quantify roughness lengths, displacement heights, urban flow indices, coupling ratios, profile behavior, wake effects, and other parameters relevant to the boundary layer over the CBD and suburban regimes.
4. Use the data to better understand dispersion behavior and develop urban diffusion coefficients within, around, and above the urban domain.
5. Perform unique Dual Doppler Lidar Wind Measurements to characterize the 3D wind field above the city and provide input for 3DWF.

This research will yield data sets needed to develop urban characteristics such as flow indices, coupling ratios, and wake parameters, so that BED models such as CCSL and 3DWF can be applied to complex urbanized areas. These same data sets will be used for initialization, comparison, and evaluation of the codes. Figure 1 depicts the flow of data in and out of the urbanized CCSL code, emphasizing which variables are required for comparisons and evaluation. The data must first be analyzed to describe and establish urban characteristics such as velocity deficits and enhancements and the intensity of turbulence as the ambient flow traverses the rural-suburban-downtown zones of the urban domain. The vertical structure of the wind profiles will also be analyzed for these same urban zones. Finally, the meteorological and diffusion/dispersion data sets collected during these trials will be used to support development and validation of urban diffusion/dispersion models.

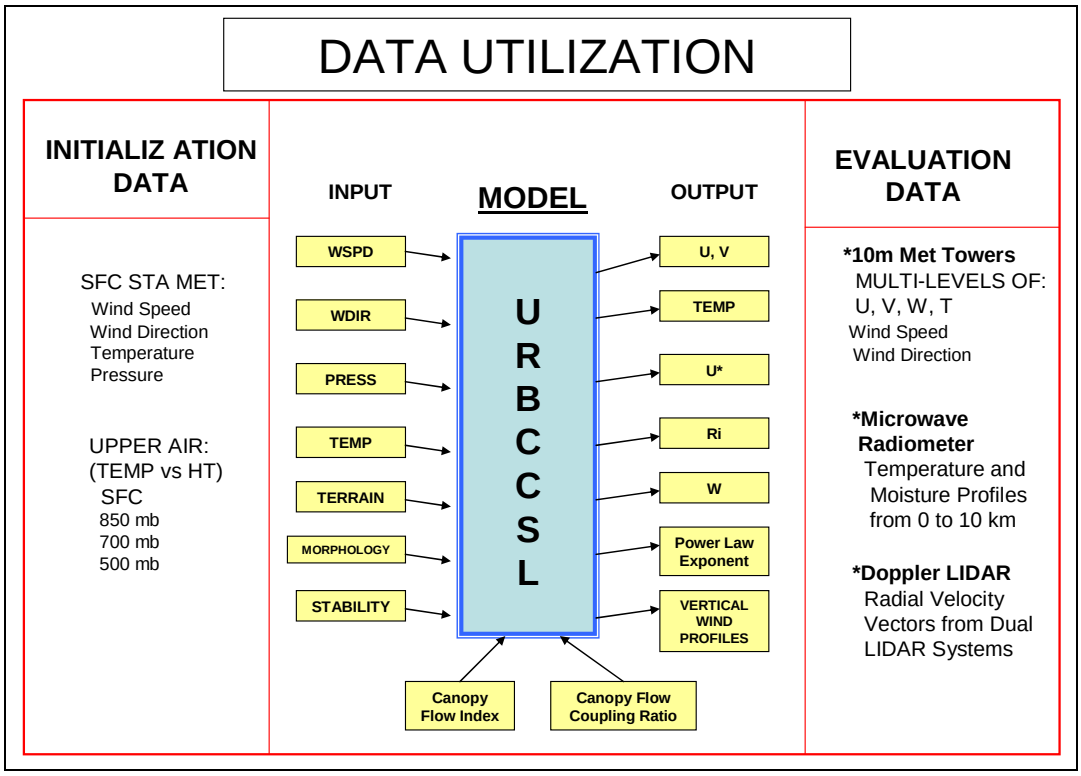

Figure 1. Data utilization and model input and output data for urbanized CCSL (Cionco, 2003).

1.3 Contents of Report

Meteorological data from all of the instruments provided by ARL and other agencies have been archived and are available on the database system maintained by personnel at Dugway Proving Ground (JU2003). This report describes the temperature, wind, turbulence intensity, and heat and momentum flux measurements obtained with the ARL suite of instruments. We first briefly describe the instruments, their site locations within the city, and the data collection and quality control procedures used to process the data.

In this volume, we concentrate on analyses of data obtained using the ARL array of sonic anemometers, all of which were confined to the roughness sub-layer (RSL) of the city. We focus on the spatial variability of wind and turbulence (wind and temperature fluctuations) and describe differences and similarities noted in heat and momentum fluxes and turbulence intensities between urban and suburban regimes. We stratify the measurements by time of day and by wind direction in order to gain insight into the structure of the urban canopy layer as it is affected by stability and surface roughness properties. We also extend the analyses to somewhat higher levels of the boundary layer with data obtained by Lawrence Livermore National Laboratory (LLNL) using sonic anemometers mounted on a pseudo-tower just north of the CBD. These sensors were mounted on a stabilized cable strung from a tall crane; they provided wind and turbulence profiles extending to 85 m above the surface.

In a companion volume, we will examine wind, temperature, and humidity data obtained with the Doppler lidar, the microwave radiometer, and the radiosonde releases. We will consider the height dependence of the various wind and turbulence parameters and extend our analyses to profiles of atmospheric variables up to levels of the troposphere significantly above the urban canopy. In a third volume, we plan to describe how the data has been used to evaluate and refine micro-meteorological and dispersion models. Additional analyses of these data and the large set of meteorological and diffusion measurements obtained by other agencies and investigators will increase our understanding of the urban boundary layer environment and our ability to predict effects within it.

2. ARL Meteorological Measurements

DOE-NNSA and DTRA selected OKC as the experimental site for JU2003 because of its flat terrain, well-defined central city, moderate size, well-characterized climatology, and the world-class supporting meteorological instrumentation already in use throughout the surrounding countryside. The project afforded the ARL the opportunity to leverage the capabilities of the Atmospheric Boundary Layer Exploitation (ABLE) suite of instruments to increase our understanding of the urban boundary layer (Yee et al., 2004). The various locations of the ARL instruments for this campaign are shown in figure 2.

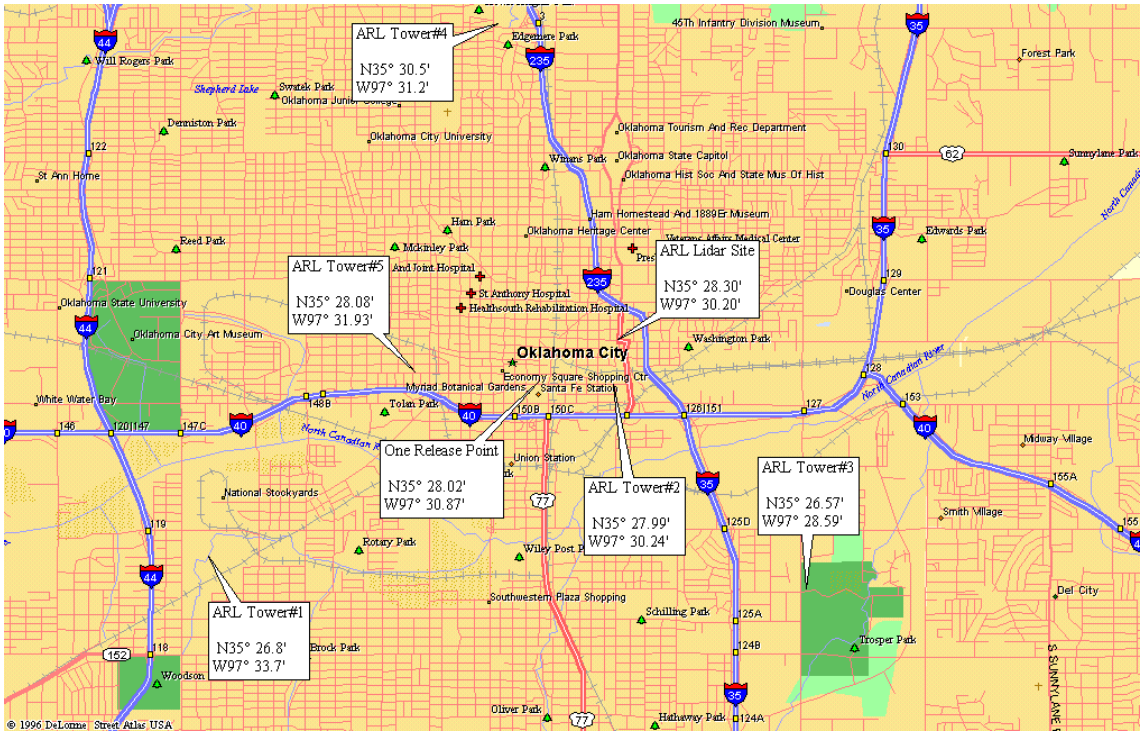

Figure 2. A map of OKC showing the selected ARL meteorological sites with their latitude/longitude coordinates. The radiosonde launch site was co-located with Tower 4.

2.1 3D Sonic Anemometers

An array of multiple-level, micrometeorological (micro-met) masts/towers were located in and about the OKC urban and suburban areas providing both horizontal and vertical spatial coverage spanning the 3DWF model's computational area of simulation. Ten-meter masts with sonic anemometers (R. M. Young, Model 81000) at two or three levels were placed in three suburban area locations to document incoming and outgoing flows. Two other 10-m masts, also with two or three levels of sonic anemometers, were placed in industrial/warehouse locations east and west of the CBD to document the interaction that low-level structures have upon the flow field. On all 5 towers, instruments were mounted at levels 10 and 5 m above the ground; on two of the towers, a third sonic anemometer was mounted at a height of 2.5 m. Instruments mounted on the top of the five towers should not exhibit a "tower shadow" effect or any wind direction. Instruments below the 10-m level were mounted due south of the towers at the end of 2-m booms in anticipation of the prevailing southerly winds in Oklahoma during the summer. Anemometer elevations (heights above the ground) were accurate to about ±0.1 m for 10.0- and 5.0-m instruments and about ±0.05 m for the 2.5-m instruments. All the meteorological instruments on the masts collected data 24 h per day throughout the entire JU2003 test period. All of the sonic anemometers measure or derive the three wind components (u,v,w), the speed of sound, and the ambient (virtual) temperature (T).

Each sonic anemometer was sampled at a rate of 10 Hz, providing turbulence characteristics for frequencies as high as 5 Hz. For sonic anemometer tilt correction, the traditional two angle rotation method (Kaimal and Finnigan, 1994) was used for each time series of 30 min (18,000 data points). After the tilt correction, the three components of the wind vector are u (streamline), v (transverse), and w (normal) with $\bar{v} = \bar{w} = 0$, where the over-bar indicates the 30-min average. For our analysis we adopted the Analysis Package for Time Series (APAK) developed at Oregon State University by Vickers and Mahrt (http://blg.coas.oregonstate.edu/Software/software.html).

Relevant geographic information for the five towers is provided in table 1. Photographs of the tower sites and aerial views of their locations and surrounding morphology (buildings and vegetation) are provided in appendix B. Towers 1 and 3 were sited southwest and southeast of the CBD in relatively open areas belonging to the Metro Transit Station and the Trosper Park Maintenance Facility, respectively. Both sites were affected by the surrounding built-up suburban environment (average height of the houses estimated to be about 5 m) but were expected to exhibit little influence from the CBD under the generally prevailing southerly winds. Tower 1 was erected on a flat gravel parking lot containing a number of weeded patches. The immediate vicinity around Tower 1 was quite open; there were no houses or trees within a distance of 50 m except for a small portable trailer (3.3 m in height) to the south-southwest. There were a number of buses with a height of about 3.5 m to the west of the tower. Towers 2 (Bricktown) and 5 (Fleet Pride) were set up in industrial areas just east and west of the CBD. They were affected by nearby industrial buildings of one or two stories, by the Interstate highway and greater fetch of suburban area to their south, and under some wind directions, by

the CBD itself. Tower 2 was surrounded by industrial buildings with an average height of 10 m within a distance of 30–50 m. Tower 3 was set up in a grassy area with a maintenance building about 50 m to the north and an open fetch to the south sloping off toward a golf course. There were trees with heights of 10–15 m east and west of the tower, with a small house near the trees to the east. Tower 4 (First Christian Church) was sited in an open area about 5 km directly north of the CBD and was co-located with a sodar and a radiosonde launch site. Not too far from Interstate 235, there was a school building on the west and open ground for distances more than 50 m north, east, and south. Tower 5 was surrounded by buildings on the east, south, and west sides, with building heights between 6–8 m. There was a line of fairly tall trees across the alley to the north and a large tree immediately to the southwest.

Table 1. Geographic information for the five ARL meteorological towers. z is the anemometer height above the ground (AGL).

Tower	Latitude (N)	Longitude (W)	Location	Elevation (m)	z (m)
No. 1	35 26.87'	97 33.67'	SW 20th & S Miller	307.85	10,5
No. 2	35 27.99'	97 30.24'	Sheridan Ave & S Byers	381.91	10,5,2.5
No. 3	35 26.57'	97 28.59'	SE 22nd & Eastern Ave	377.34	10,5,2.5
No. 4	35 30.49'	97 31.16'	NW 36th & N Walker St	349.61	10,5
No. 5	35 28.08'	97 31.93'	W Main St & N Klein Ave	368.81	10, 5

Generally speaking, Towers 2 and 5 can be considered typical of industrial or warehouse urban areas while the other three tower locations typify suburban areas. Lundquist et al. (2004) have estimated the mean building height for the urban area of OKC as 5–15 m. Measurements by our sonic anemometers, conducted outside the CBD, can therefore be considered to represent the urban RSL (Roth, 2000) at specific locations.

2.2 MMS Radiosonde

The LORAN radiosonde instrumentation from the Army's MMS (Cogan et al., 1998) was set up north of the CBD to obtain upper air soundings in conjunction with other soundings collected by other agencies. Standard measurements of temperature, pressure, wind speed and direction, and humidity were taken. Each upper air flight measured the temperature-height-pressure profile up to balloon burst or the 400 mb level. The upper air profiles and the surface-based meteorological data were required to supplement the JU2003 science objectives as well as to compute the atmospheric stability as required for input to the CCSL code. A nominal schedule of daily radiosonde flights was at 0600Z (1:00 a.m. Central Daylight Time [CDT]) and 1800Z (1:00 p.m. CDT), thereby, supplementing NOAA's operational schedule of 0000Z and 1200Z radiosonde flights from Norman, OK. Coordination with the DOE teams allowed us to skip flight times when DOE intended to release radiosondes. Those times occurred during the 10 IOPs.

2.3 Wind Tracer Lidar

ARL's Coherent Technology Inc. Wind Tracer Lidar system was sited just east of the CBD and operated in conjunction with a nearly identical system operated by Arizona State University south to southeast of the CBD. The ARL Lidar system was set up atop a four-story parking garage about 1 km east of the CBD (figure 3). On a regular basis, the systems performed coordinated vertical and horizontal scans to obtain wind velocity profiles. The dual lidars also executed an appropriate elevation scan parallel to the mean wind, measuring the radial wind speed as a function of range, elevation, and time.

Figure 3. Photograph of the ARL Microwave Radiometer (right) and the ARL Wind Tracer Lidar (left) set up east of the CND of OKC (Photograph by Young Yee).

The pulsed IR Doppler lidar provides direct measurements of wind velocity vectors at multiple ranges—50–200 m pulses are transmitted 100–500 times per second. The width of the transmitting pencil beam is 10–30 cm. Relative wind induces a Doppler frequency shift in the backscattered light from naturally occurring aerosols; this frequency shift is detected by the sensor. Newsom and Banta (2003) show that these data can be transformed to Cartesian coordinates (distance and height) with estimates of mean speeds and reasonable estimates of wind speed variance. Such a configuration permitted analyses for the air coming toward and away from the lidars, within and peripheral to the city. These data—being three dimensional (r,z,t)—have proved quite valuable in initialization of high resolution diagnostic and computational fluid dynamic (CFD) models of the flows or in assessing the performance of the models as the air leaves the city. With these data sets, questions about the urban drag could be better addressed since the vertical structure of turbulence and wind entering the city can be separated from the same structures downwind of the city.

2.4 Microwave Radiometer

The Microwave Radiometer is a passive remote sensing device that measures the microwave emission from oxygen and water molecules in the atmosphere. The shape and absorption properties of the 60-GHz oxygen band and the 22-GHz water vapor band are exploited to infer atmospheric profiles of temperature and moisture (including liquid water). For the temperature profile determinations, the radiometer measures emission at 7 frequencies between 51–59 GHz. For moisture profile determinations, 5 frequencies between 22–30 GHz are used. Profiles from near the surface up to 10 km AGL are deduced using additional information from archived radiosonde observations and separate surface sensors as inputs for an inversion algorithm using a neural net (Measure et al., 2001). Figure 3 is a photograph of the microwave radiometer and the Wind Tracer Lidar at the OKC measurement site.

2.5 Data Collection and Archival

The recent emphasis on urban warfare requires high-resolution meteorological measurements in complex urban environments. Due to the number of sonic anemometers and the volume of data, data collection of the 3D sonic wind measurements presented special challenges. A methodology for the collection and management of a distributed array of 3D sonic anemometers was developed and implemented for the JU2003 (Vidal and Yee, 2003). Issues that needed to be addressed were sensor interface, databasing, scalability of measurements (number of sonic instruments), distributed processing of loosely coupled systems, and performance of the data acquisition system(s). Two major issues in the management and handling of enormous quantities of micro-met measurements are the time tagging of the data and the location information of each instrument in a micro size grid. Scalability and integration of multiple sonic sensors are currently being investigated using the latest technologies such as loosely coupled Jini/Java Spaces (Torres, 2001).

Because of the complex nature of urban meteorological characterization, high-resolution wind measurements require special collection procedures in these areas. Using microchip technology to collect and process data at the sensor level, the data from individual sensors on a single met tower are networked together. Assembled data from each local network of sensors is transmitted wirelessly to a data collection node on a daily basis.

Meteorological data from all of the instruments provided by ARL and other agencies have been quality controlled and archived on the database system maintained by personnel at Dugway Proving Ground (JU2003). In this volume, we focus on the near surface measurements of wind speed and air temperature fluctuations obtained by the ARL array of sonic anemometers, all of which were confined to the RSL of the city, on five towers set up outside the CBD in surrounding industrial (urban) and semi-rural (suburban) areas. We extend the analyses to somewhat higher levels of the boundary layer in comparisons with data obtained by LLNL using sonic anemometers mounted on a pseudo-tower just north of the CBD. These anemometers were mounted on a stabilized cable strung from a tall crane; they provided wind and turbulence

profiles extending to 85 m above the surface. Turbulent statistics of the three wind components and temperature were calculated using 10-min blocks of data (Garvey et al., 2004). In a companion volume, we will examine wind, temperature, and humidity data obtained with the Doppler lidar, the microwave radiometer, and the radiosonde releases. We will consider the height dependence of the various wind and turbulence parameters and extend our analyses to profiles of atmospheric variables up to levels of the troposphere significantly above the urban canopy.

3. Data Summaries for Intensive Observation Periods (IOPs 1-10)

The dates and start and end times for the 10 IOPs during which tracers were released and tracer concentrations measured are given in table 2. Times shown are local daylight savings time CDT, 5 h behind Universal Time Coordinated (UTC). The first six IOPs were daytime releases, the last four occurred at night.

Table 2. IOPs for JU2003.

Location: Oklahoma City, OK		Times (CDT)		UTC = (CDT + 5)	
Experimental Period: 29 June to 31 July 2003					
IOP No.	**Date**	**Start Time**	**End Time**	**Ordinal Date**	**Comments**
1	Jun 29 03	9:00am		180	
	Jun 29 03		3:00pm		
2	July 2 03	9:00am		183	
	July 2 03		5:00pm		
3	July 7 03	9:00am		188	
	July 7 03		5:00pm		
4	July 9 03	9:00am		190	
	July 9 03		5:00pm		
5	July 13 03	9:00am		194	
	July 13 03		5:00pm		
6	July 16 03	9:00am		197	
	July 16 03		5:00pm		
7	July 18 03	11:00pm			
	July 19 03		7:00am	200	
8	July 24 03	11:00pm			
	July 25 03		7:00am	206	
9	July 26 03	11:00pm			
	July 27 03		7:00am	208	
10	July 28 03	11:00pm			
	July 29 03		4:00am	210	
	July 31 03	end of Joint Urban 2003 experiments end of met measurements			

Data from the 12 ARL sonic anemometers for the 10 days on which IOPs were conducted are presented in figures A-1 through A-30 in appendix A. For each day we have graphed the variables of wind direction, wind speed, temperature, kinematic sensible heat flux, turbulent kinetic energy (TKE), and friction velocity (u^*) as measured at the five tower sites, a total of 30 graphs for each day. When measurements from a single tower are available for more than one level, these are shown on the same graph. Averages of these quantities were calculated for 10-min blocks of data sampled at 10 Hz. Also shown on each page for each day are the time periods during which the IOPs were conducted. Recall that sites 1, 3, and 4 are characteristic of suburban areas while sites 2 and 5 are more urban in nature.

We use the measurements from Tower 1 as representative of the suburban domain and those from Tower 5 as representative of the urban domain. Plots of the temperature, wind direction, wind speed, kinematic heat flux, kinematic momentum flux, and TKE for two levels on the two towers for the period 24 June through 01 August are shown in figures 4 and 5 (Garvey et al., 2004a). The values plotted are averages calculated for 10-min blocks for which the average crosswind (v) and vertical velocity (w) were set equal to zero. Obvious in both sets of plots is the expected diurnal dependence of temperature, heat flux, and TKE; the wind speed and direction as well as the momentum flux also exhibit a diurnal dependence, but their time series are complicated by other factors.

3.1 Temperature

The acoustically measured temperatures were not sufficiently accurate (~1 °C) to distinguish urban heat island effects among the sites nor could they be used to measure vertical temperature gradients at any one of the sites. Data from all five sites, however, reveal the expected diurnal temperature cycle, with a minimum near 1200 UTC (0700 CDT) and a maximum near 2200 UTC (1700 CDT). The daytime IOPs were conducted during periods of rapidly rising temperatures early and a leveling off later. Temperatures during the nighttime IOPs decreased nearly linearly throughout their duration. Measured temperatures during July ranged from a low of about 22 °C to a high of above 38 °C.

It can be seen from figures 4 and 5 that the measured temperatures at 10 m at the two sites correlated extremely well. The calculated correlation for the 10-min averages for times for which temperatures were obtained from both towers was found to be 0.997. Cooler conditions early in the field test, when no measurements were available from Tower 5, were a factor resulting in an average temperature at Tower 1 approximately 1 °C less than that for Tower 5, about 29 °C as opposed to about 30 °C.

3.2 Wind Direction

A quick perusal of figures A-1 through A-30 in appendix A yields a number of noteworthy results. First of all, the winds for all IOPs were generally southerly, as both predicted and anticipated. Only for IOP 1 was there a substantial wind shift from southwest to east during the

course of the IOP. During the nighttime IOPs (7–10), there was a gradual but persistent shift of the wind from east of south to southwesterly. There did not appear to be a substantial change in wind direction from site to site, although the timing of the wind shifts did vary among the sites.

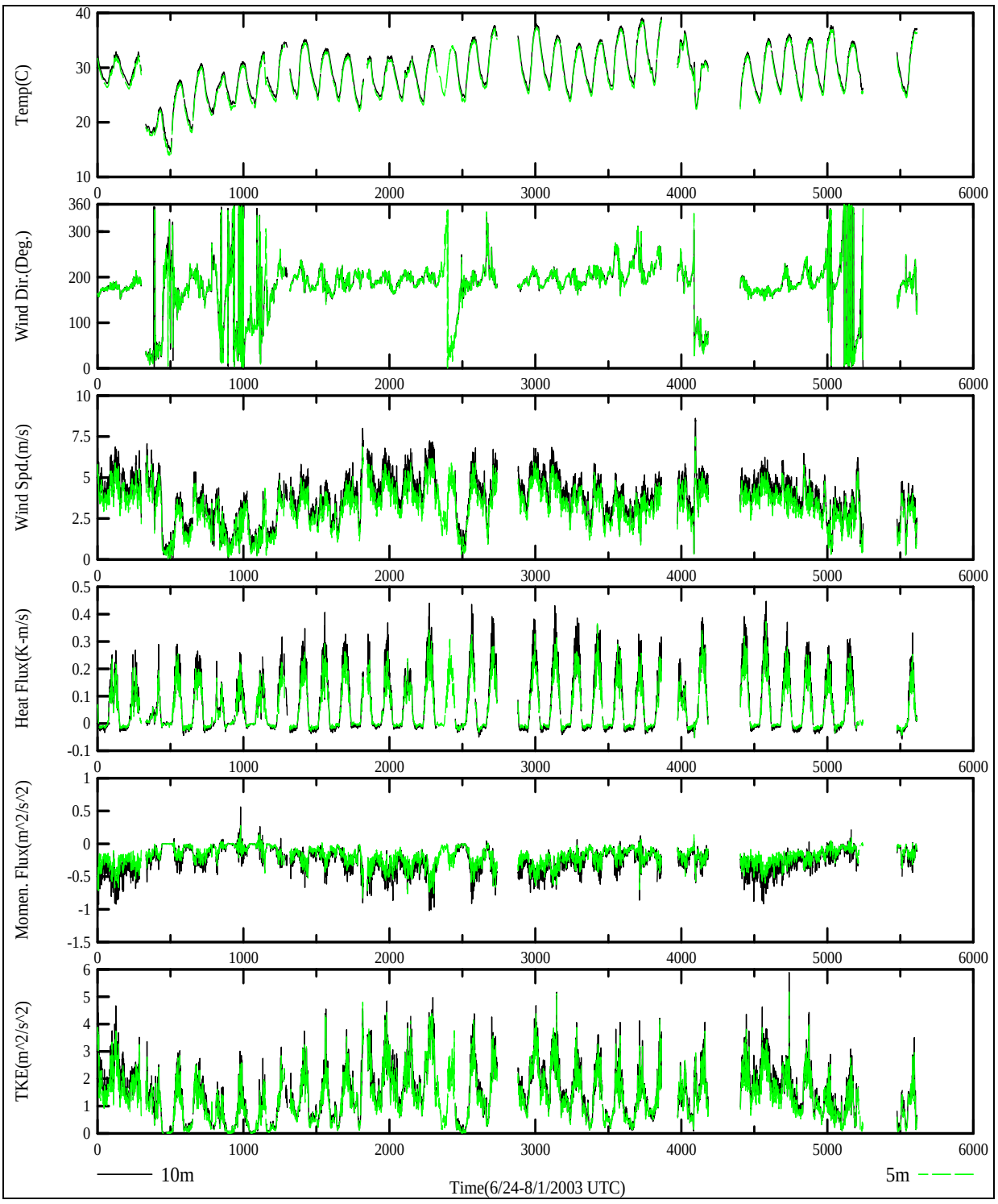

Figure 4. Ten-minute average of temperature, wind direction, wind speed, heat flux, momentum flux, and TKE at 10 m (solid) and 5 m (dash) on Tower 1 (6/24/03–8/1/03).

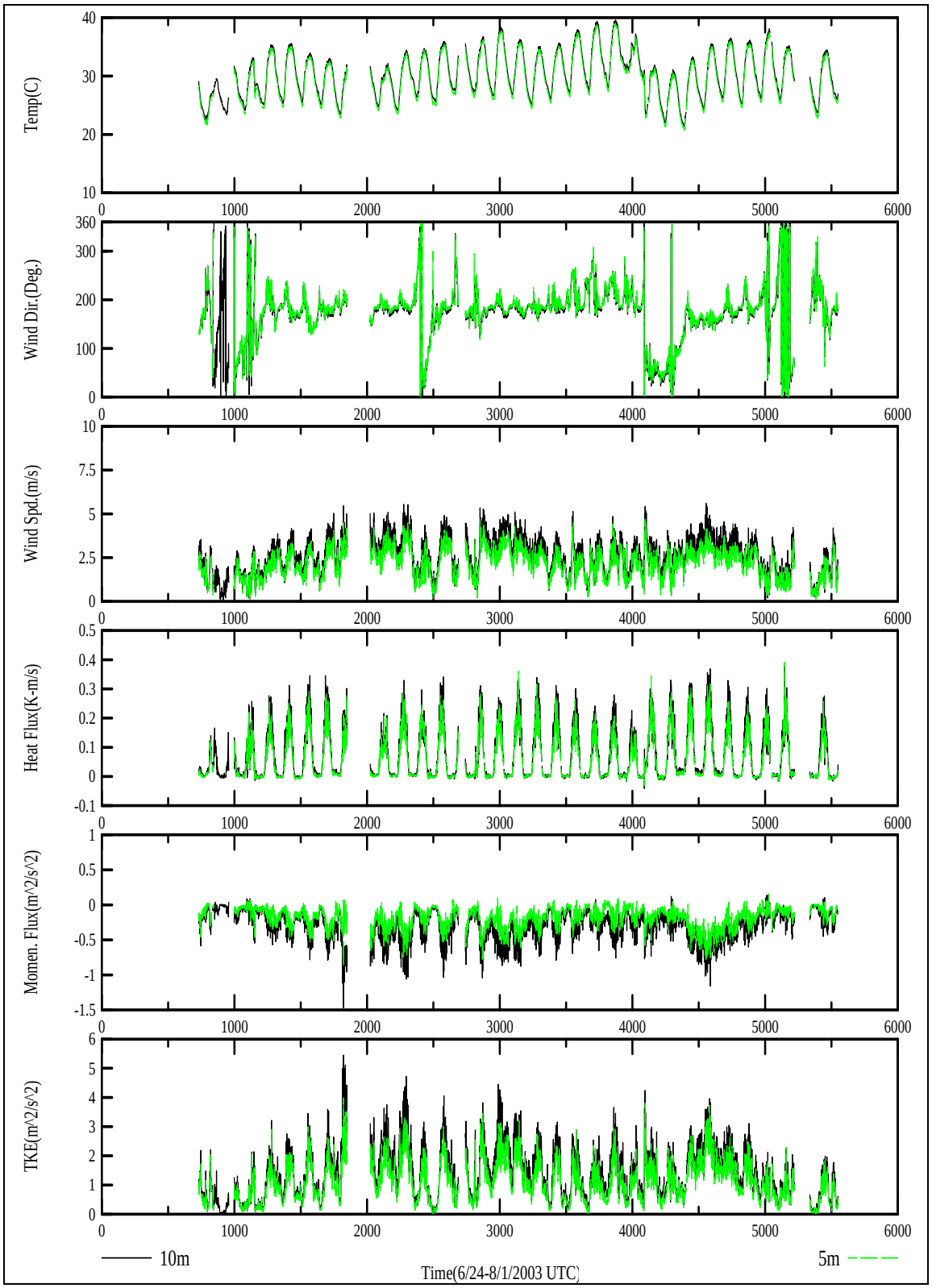

Figure 5. Ten-minute average of temperature, wind direction, wind speed, heat flux, momentum flux, and TKE at 10 m (solid) and 5 m (dash) on Tower 5 (6/24/03–8/1/03).

The measured wind directions at Towers 1 and 5 were generally from the anticipated southerly quadrant. The 10-min mean directions at the two levels at each tower were in very good agreement, showing a correlation of 0.961 at Tower 1 and 0.978 at Tower 5. At 10 m, the average 10-min mean direction at Tower 1 was 181° and at Tower 5 was 173°. The relatively low correlation between the wind directions at the two towers, 0.62, is due in part to times when the northerly winds were west of north at one tower and east of north at the other (figure 6). This scatter plot for the wind directions at the two sites, however, does indicate that there are often times when the mean wind directions are significantly different. We note that not all of the poorly correlated wind directions correspond to periods of light winds; so these times should be looked at to investigate possible turning due to local morphology.

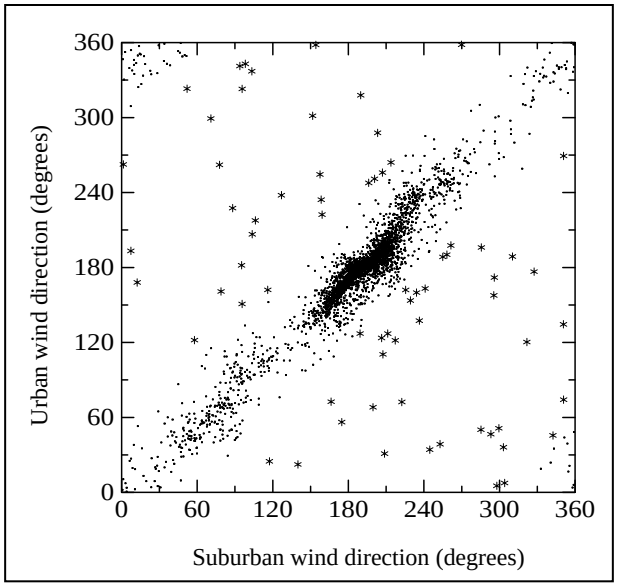

Figure 6. Wind direction in an urban location compared to wind direction in a suburban location about 5 km WSW of the urban location. Points marked with a star (*) are poorly correlated between the two locations.

3.3 Wind Speed

The wind speeds were generally light during JU2003, even for Tower 1 rising above 6 m/s at 10 m only for IOPs 3 and 4. Again the timing of the abrupt changes in wind speed could vary from site to site. The wind speeds were generally lower at the urban sites compared to the suburban sites. At both urban and suburban sites average wind speeds at night were about 15% lower than during the day (Garvey et al., 2004b). The amplitudes of the fluctuations in both the wind directions and the wind speeds were less during nighttime IOPs than during daytime IOPs.

As is evident in figures 4 and 5, the wind speeds measured at the two levels on each tower were also highly correlated, correlation values being about 0.99. Using the slope of regression lines fit to their respective scatter plots, the wind speeds at 5 m on Tower 1 were about 88% of those at

10 m; on Tower 5 the corresponding figure was just 80%. For all of the measurements obtained from 24 June through 01 August, the average wind speed at 10 m on Tower 1 was 3.73 m/s. On Tower 5 the corresponding value was 2.56 m/s, an average reduction of 30% largely due to the drag induced by the roughness of the urban environment.

3.4 Heat Flux

The amount of buoyancy-produced turbulence is proportional to the sensible heat flux ($\overline{w'T'}$) at any given location. Heat flux measurements are also useful for classifying the thermal stability at a location. From our data, the most notable differences in thermal stability from one location to another within the greater urban and suburban area arise at night. The suburban locations have downward nighttime heat fluxes consistent with theoretical expectations for nocturnal conditions. Downward heat flux allows a thermally stable layer to form, which suppresses turbulence. The urban locations, however, maintained upward heat flux throughout most nights; the daytime heat fluxes were generally greater in the urban area than in the suburban area. Both day and night data are evidence of an urban heat island.

We distinguish between daytime and nighttime IOPs. For the daytime IOPs, the heat flux rose from near zero at 1400 UTC (0900 CDT) to its maximum at about 1900 UTC (1400 CDT). With the exception of IOP1, the maximum was above 0.2 K-m/s at all sites and at times approached 0.4 K-m/s on Tower 1. During IOP1 both the diurnal heating and the resulting heat flux were reduced, a result apparently correlated with the wind shift and corresponding drop in wind speed. Sites 1, 2, and 5 generally showed higher maximum heat fluxes than the other two sites. It is thought that this is probably due to the mixture of gravel or bare dirt immediately below the towers and to the presence of nearby buildings and pavement. We conjecture that the relatively low daytime sensible heat flux measured at Tower 3, located just north of a golf course, may have been the result of irrigation. Heat fluxes during the nighttime IOPs were all very close to zero. For the urban sites at Towers 2 and 5, the heat flux never appeared to go negative. For the suburban sites, it went only slightly negative, Towers 3 and 4 appearing more rural in character than Tower 1.

The 10-min kinematic heat fluxes at the two levels on Towers 1 and 5 were highly correlated, values being 0.98 and 0.97, respectively. At Tower 1 the heat flux at 5 m was 78% of that at 10 m; at Tower 5 it was 84%. The average heat flux at 10 m on Tower 1 was 0.071 K-m/s; that on Tower 5 was 0.073 K-m/s. It must be noted, however, that these averages are calculated for the entire period using both the positive and negative values of the heat fluxes. It is barely discernible in figure 5, but the heat fluxes at Tower 5 seldom went negative, while those at Tower 1 always became negative at night. The heat retention by the urban ground surface and surrounding structures at night are almost certainly responsible for this difference. The maximum positive heat flux during the day was always greater at the Tower 1 site, the surrounding gravel surface of the Metro Transit Station being largely responsible for 10-min kinematic sensible heat fluxes very often larger than 0.3 K-m/s.

3.5 Momentum Flux

The loss of momentum from the atmosphere through frictional forces at solid surfaces is measured through the turbulent stress or momentum flux ($-\overline{u'w'}$). The friction velocity (u^*) plotted in appendix A is just the square root of the absolute value of the momentum flux. Values of momentum flux are higher on average at the urban sites than at the suburban sites. Urban values can reach levels 35% higher than suburban values in late afternoon. The amount of momentum loss, which is related to the roughness elements of the surrounding surface, contributes significantly to the uncertainty associated with plume dispersion.

The kinematic momentum fluxes at the two levels on Towers 1 and 5 are not as highly correlated as the other variables, but still 0.92 and 0.85, respectively. At Tower 1 the momentum flux at 5 m was 70% of that at 10 m; at Tower 5 it was only 61%. The average momentum flux at 10 m on Tower 1 was negative 0.25 m^2/s^2; that on Tower 5 was minus 0.30 m^2/s^2.

3.6 Turbulent Kinetic Energy

Turbulent kinetic energy (TKE= $<u'^2 + v'^2 + w'^2>/2$) is a measure of the turbulent velocity scales. Plume or puff spreading as a function of time is proportional to these turbulent velocity scales. Average TKE values were found to be very similar from site to site for both urban and suburban areas. The daytime average values (nearly 2 m^2/s^2) were roughly twice the nighttime averages, implying that daytime dispersion will be greater than at night. Further study is needed to see how close proximity to buildings alters the TKE components. The TKE values at the two levels on both Towers 1 and 5 were very well correlated, greater than 0.97 in each case. On Tower 1 the TKE at 5 m was 92% of that at 10 m; on Tower 5 it was 77%.

Both the TKE and the friction velocity demonstrate a relative minimum around 1200 UTC (0700 CDT) on most IOP days and are significantly higher during the day than at night. At night, the behavior of both is the result of dynamic interactions between the directionally dependent roughness elements and the wind speed profiles. During the day, their behavior is further complicated by the heterogeneity of the radiative properties of the surface and the resulting convective cells of different sizes. Both variables demonstrate large amplitude fluctuations. The mean TKE is not significantly different at the urban and suburban sites, averaging 1.45 m^2/s^2 at 10 m on Tower 1 and 1.39 m^2/s^2 on Tower 5 for the period 24 June through 01 August. The average friction velocity or vertical momentum flux is also roughly similar for the two sites during this period. Both variables correlate well with the magnitude of the wind. For example, during the nighttime of the day on which IOP2 was conducted, the 10-m wind speeds at all sites are lower than on any other night shown, generally less than 2 m/s, whereas for all other nights and almost all sites the wind speed at 10 m is greater than 4 m/s for at least part of the night. The TKE corresponding to this period is generally less than 0.2 m^2/s^2 at all sites, significantly less than for all other nights.

3.7 Turbulence Spectra

Spectral analyses of the sonic anemometer data (figure 7) show a consistent shift in the temporal/ spatial scales of the dominant turbulent eddies between the urban and suburban locations (Chang et al., 2004). The shift is from larger spatial (lower frequency) scales at the suburban locations to smaller spatial (higher frequency) scales at the urban locations. This shift in scale is observed at all hours and for all variables (the three components of the velocity vector and temperature), indicating that the integral time scales within the city are smaller than in the suburban area.

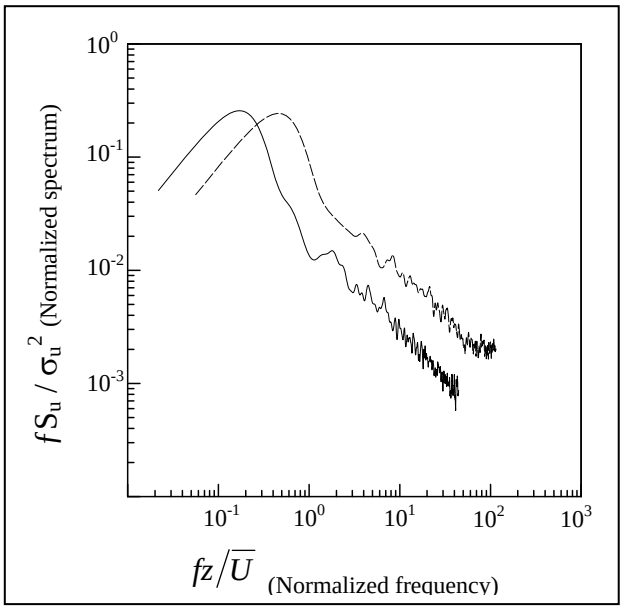

Figure 7. Normalized Fourier spectra of longitudinal wind speed fluctuation data at urban (---) and suburban (—) locations with frequency f (Hz), observation height z (m), mean wind speed $\overline{U}$ (m/s), and variance of the wind speed fluctuations σ_u^2 (m^2/s^2) as the scaling factors. Data are for 1 July, 2003, at noon CDT.

3.8 Statistical Summary

We first note that the correlation between values of any one of the variables derived from the sonic anemometers at the 5- and 10-m levels on either of the towers was very high, better than 0.96 for all variables except the kinematic momentum flux, where it dropped just below 0.85 on Tower 5. Both the heat flux and momentum flux at these two levels on each tower, however, differed by more than the 10% nominal value often used to define the surface layer. Therefore, while the values measured at 10 m can be used to describe roughness layer characteristics at each site, caution must be exercised when surface layer vertical gradients of any of the variables are considered.

Table 3 provides a summary comparison of the wind speed, heat flux, momentum flux, and TKE measured at 10 m for the two sites. The first row of numbers is the average and the second row the standard deviation of each of these variables calculated for all times for which data is available. The last row shows both the correlation and the slope of the regression line for each of the variables at the two sites. The slope is calculated using the Tower 1 data as the independent (unaffected) value. The correlation is highest for the heat flux (a result that might be expected because of the dominant effect of solar heating), intermediate for the TKE and momentum flux, and lowest for wind speed. The absence of a downward heat flux at night on Tower 5, already pointed out previously, is not evident in these numbers, but the stronger positive heat flux during the day at Tower 1 manifests itself in the relatively small value of the slope of the regression line. The momentum fluxes at the two sites are on the average not greatly different, but because of the intermediate correlation value and the relatively large standard deviations, this variable needs to be investigated on an individual case basis to determine the relative effects of buoyancy and surface roughness for different conditions of wind and solar heating. The reduced wind speed for the more urban site (Tower 5) is borne out by both the average values and the slope of the regression line, though the correlation value for this line is only 0.74. The value of the slope is less than the ratio of the average value, 0.60 compared to 0.69. For TKE, the corresponding values are 0.81 and 0.96, indicating a slightly reduced turbulent kinetic energy for the urban site. We note, too, that if the average values of the TKE are divided by the squares of the average wind speeds for the two sites, the magnitude of the normalized turbulence intensity for the suburban site is about half that for the urban site.

Table 3. Summary comparison of wind speed, heat flux, momentum flux, and TKE at two sites.

u_T1	**u_T5**	**<wT>_T1**	**<wT>_T5**	**<uw>_T1**	**<uw>_T5**	**TKE_T1**	**TKE_T5**
3.73	2.56	0.071	0.073	–0.25	–0.30	1.45	1.39
1.37	1.06	0.105	0.087	0.18	0.20	0.93	0.87
Correl.	Slope	Correl.	Slope	Correl.	Slope	Correl.	Slope
0.74	0.60	0.93	0.76	0.80	0.97	0.87	0.81

We conclude this section by pointing out that only average urban/suburban and day/night differences for the tower locations are discussed herein. Much more analysis of the data for all the sites stratified by time of day and by wind speed and direction remains to be done. Klipp et al. (2004) report on a method for distinguishing between necessary sonic anemometer tilt corrections and real directional dependencies on local slopes and structures. This is a necessary step in attempting to estimate directionally dependent diffusion coefficients for dispersion modeling. We emphasize that since a principal motivation for performing the field experiment was to relate the urban meteorological conditions to the resulting atmospheric dispersion in the boundary layer, future analyses will necessitate looking at all of the data obtained by the many investigators (e.g., Lundquist et al., 2004, and Grimmond et al., 2004), concentrating particularly on times for which intensive operations were conducted.

4. Analysis and Discussion

In this section, we provide further analysis of the sonic anemometer data presented in section 3 and appendix A. In particular, we examine the horizontal inhomogeneities in the wind and turbulence properties of the RSL and characterize their height dependence. Values of the displacement height (d) for the five tower locations are shown to vary both with location and wind direction. We next examine the profiles of TKE, sensible heat flux, and momentum flux obtained at the various locations. We stratify the measurements by time of day and wind direction in order to gain insight into the structure of this layer as it is affected by stability and surface roughness properties. We look, too, at profiles obtained from measurements on a much taller tower (85 m) instrumented by LLNL to see whether a constant flux layer (CFL) might be identified at higher levels above the city.

4.1 Spatial Variability of Turbulence Characteristics in the RSL

Roth (2000) divides the urban boundary layer into the following sub-layers or regions:

1. Urban canopy layer (UCL)
2. Roughness sub-layer (RSL)
3. Constant flux layer (CFL)
4. Mixed layer (ML)

The UCL extends from the ground to about roof level (z_h) and is usually characterized by the zero plane displacement height (d), which may vary from about 0.5 to 0.8 z_h. The RSL, also called the transition or interfacial layer, includes the UCL and extends above it to a height (z_r), estimated by Raupach et al. (1991) to vary from about 2 to 5 times z_h. The CFL, also called the inertial sub-layer, extends from the top of the RSL to about 0.1 times the height of the boundary layer and corresponds to the surface layer over homogeneous terrain. Oke et al. (1989) have noted that it may happen that the depth of the RSL exceeds the potential depth of the CFL and that no such layer exists. Extending above the CFL to the height of the boundary layer is the ML.

In a number of presentations (Chang et al., 2004; Garvey et al., 2004; Klipp et al., 2004; Yee et al., 2004; Garvey et al., 2005; Huynh et al., 2005), we have described the experimental setup, quality control, and analysis procedures followed in examining wind and turbulence properties obtained from sonic anemometers mounted on the five 10-m towers fielded by ARL in the OKC metropolitan area during the summer of 2003. Klipp (2007) has focused on the dependence of turbulence parameters on wind direction. Generally, these analyses have focused on data obtained 10 m above the ground at sites characterized as suburban or urban (industrial) and have

emphasized the heterogeneity of the urban surface properties and the resulting wind and turbulent characteristics. Following a method proposed by Rotach (1994) and described herein, we have shown values of the displacement height for the five tower locations to vary both with location and wind direction. Values for the suburban locations obtained from measurements at 10 m varied from as little as 1.4 m to as much as 6.1 m; values for the urban locations varied from 4.2 to 7.5 m. It is evident then that, for the urban locations, the sonic anemometer measurements at 10 m (and below) were entirely within the RSL, while even those at suburban locations were often within this layer.

Lundquist et al. (2004) have estimated the mean building height for the urban area of OKC as 5–15 m. Measurements by the ARL sonic anemometers, conducted outside the CBD, can therefore be considered to represent the urban RSL at specific locations. The sonic anemometer data consist of three wind components (u,v,w) and sonic temperature (T). In this analysis, we use the data from the 10-m sonic anemometers only. Mounted on the top of the five towers, these sensors should not exhibit a "tower shadow" effect for any wind direction. The sampling rate of the sonic anemometers was 10 Hz. For sonic anemometer tilt correction, the traditional two angle rotation method (Kaimal and Finnigan, 1994) was used for each time series of 30 min (18,000 data points). After the tilt correction, the three components of the wind vector are: u (streamline), v (transverse), and w (normal), with vbar = wbar = 0, where the over-bar indicates the 30-min average. For our analysis we adopted the APAK developed at Oregon State University by Vickers and Mahrt (http://blg.coas.oregonstate.edu/Software/software.html).

4.1.1 Zero Plane Displacement Height (d)

Rotach (1994) has presented the temperature variance method to estimate the zero plane displacement height (d) over urban surfaces. This method assumes (perhaps optimistically, though the results seem to justify it) that the classic Monin-Obukhov similarity formula for the temperature variance can be applied to the urban surface layer. Specifically, the non-dimensional temperature variance for the unstable surface layer can be expressed as

$$\sigma_T' = \sigma_T/|T_*| = C_1[1 - C_2\,(z\text{-}d)/L]^{-1/3}, \quad (1)$$

where σ_T is the standard deviation of temperature and T_* denotes the temperature scale. Here

$$T_* = -H/u_* = -\langle w'T'\rangle/u_* \ ; \quad (2)$$

$$u_*^2 = [(\langle u'w'\rangle)^2 + (\langle v'w'\rangle)^2]^{1/2} \ ; \text{ and} \quad (3)$$

$$L = -u_*^3/[k\,(g/T)\,H] \ , \quad (4)$$

where u_* is the friction velocity, k the von Karman constant, g the acceleration of gravity, H the kinematic heat flux, and L the Monin-Obukhov length. The constants C_1 and C_2 are estimated to be 2.9 and 28.4, respectively (Wyngaard et al., 1971; Tillmann, 1972; De Bruin et al., 1993; Feigenwinter et al., 1999). To obtain an estimate of d, the differences between the estimated

value of σ_T' with a specific value of d from equation 1 and the measured value $(\sigma_T')_m$ are to be minimized from the following equation by varying the d value in equation 1.

$$E^2 = (1/N)\sum_{i=1}^{N}[\sigma_T' - (\sigma_T')_m]^2, \quad i = 1, 2, \ldots N \tag{5}$$

where E represents the root-mean square error for a specific value of d and N is the number of measurements. The value of d for the minimum E is adopted as the estimated value of d. Table 4 lists estimated values of d for the five tower locations.

Table 4. Estimated values of d (m) with respect to the wind direction for the five ARL tower locations. The number in the parentheses denotes N in equation 5. The last line indicates the N-weighted values of d for all wind directions.

Wind Dir. (degree)	Tower 1 d (N)	Tower 2 d (N)	Tower 3 d (N)	Tower 4 d (N)	Tower 5 d (N)
0–90	1.4 (44)	4.7 (64)	6.8 (30)	4.8 (46)	5.7 (57)
90–180	1.7 (68)	5.7 (106)	1.8 (48)	4.0 (49)	4.2 (138)
180–270	2.9 (253)	5.6 (273)	6.6 (183)	2.5 (221)	5.3 (186)
270–360	5.3 (13)	5.9 (16)	5.3 (8)	6.1 (13)	7.4 (14)
0–360	2.6 (378)	5.5 (459)	5.7 (269)	3.2 (329)	5.0 (395)

As emphasized by Rotach (1994), the zero plane displacement (d) at an urban site can vary considerably with wind direction. From table 4, we see that d varies with wind direction at each location. For example, depending on wind direction, d can vary from 1.4 m to 5.3 m for the Tower 1 site and from 4.7 m to 5.9 m for the Tower 2 site. Feigenwinter et al. (1999) have also found significant variation of d values with wind direction over the city of Basel, Switzerland. Those authors used eight wind direction sectors. We felt we had too few data points in some of the sectors to present a corresponding analysis here.

The reason for the significant variation of d with wind direction for the five tower sites is generally understandable if we examine the significant variation of urban roughness elements (buildings, structures, and trees) with wind direction at the five sites shown in appendix B. It can be seen, for example, that there were many more roughness elements to the west of Tower 1 than to the east. Consequently, the d values are larger for westerly winds than for easterly winds. Likewise, the d values are larger for the sites at Towers 2 and 5 than for the sites at Towers 1 and 4 due to the fact that the former two were more closely surrounded by taller buildings, as seen in the aerial views of those sites. The large values of d for northeasterly and southwesterly winds (6.8 and 6.6 m, respectively) for the Tower 3 site are believed to be due to the effects of the nearby trees; we speculate that if a southerly sector had been chosen for analysis, a smaller value of d would have resulted.

The measurements by the sonic anemometers at the five towers do not allow us to estimate the roughness length z_0 for the five locations because the heights of the instruments are not high enough to be considered in the inertial (constant flux) sub-layer (Roth, 2000). Grimmond and

Oke (1999) have reviewed several methods to determine the aerodynamic characteristics of a surface, including the zero plane displacement height d and roughness length z_0. An approximate relation between z_0 and d can be derived as a simple rule of thumb. Based on the common morphometric approach, z_0 can be expressed as a fraction of d, say $z_0 = C_z * d$, where C_z is about 0.1–0.2; see section 2 of Grimmond and Oke (1999). Hence we can estimate the values of z_0 for the five locations from the d values in table 4. Burian et al. (2003) have estimated the values of d and z_0 for the OKC downtown core area as around 13 and 2.5 m, respectively, as cited by De Wekker et al. (2004). Because the downtown core area has taller buildings than the rest of the city, the values of d and z_0 from Burian et al. (2003) are significantly larger than our estimated values for the five ARL tower sites, which are not in the downtown area.

4.1.2 Normalized Standard Deviations of Velocity Components and Temperature

The standard deviations of longitudinal (σ_u), transverse (σ_v), and vertical (σ_w) wind velocity components normalized by the friction velocity (u_*) for unstable conditions can be expressed as (Roth, 2000)

$$\sigma_v' = \sigma_v/u_* \sim \sigma_u' = \sigma_u/u_* = C_3\,[1 - C_4\,(z\text{-}d)/L]^{1/3} \;; \tag{6}$$

$$\sigma_w' = \sigma_w/u_* = C_5\,[1 - C_6\,(z\text{-}d)/L\,]^{1/3} \;; \tag{7}$$

where C_3, C_4, C_5, and C_6 are empirical constants. Over flat terrain,

$$C_3 = 2.2, \quad C_4 = 3.0, \quad C_5 = 1.25, \quad C_6 = 3.0 \;; \tag{8}$$

see, e.g., Panofsky and Dutton (1984) and De Bruin et al. (1993). Based on the d values for the five tower locations at the four quadrants in table 4, the measured normalized standard deviations for the three wind velocity components and for the temperature are plotted versus (z-d)/L in figure 8. The solid lines in figure 8 represent the empirical relations of equations 1, 6, and 7 using the empirical constants we have cited. Figure 8 shows that σ_w' (third row in figure 8) over OKC seems to exhibit the same behavior as over flat terrain, where d in equation 7 is close to zero. The reason is probably that the vertical velocity fluctuations are produced by small eddies, the diameters of which are of the order of the reduced height (z-d) over the urban area instead of the height above the ground (z) over flat terrain. In contrast, the normalized standard deviations of the horizontal wind components (σ_u' and σ_v') are primarily produced by large quasi-horizontal eddies. Their diameters are typically a few hundred meters and tend to be influenced and distorted by urban buildings and trees. Consequently, σ_u' and σ_v' over an urban area are larger and more scattered, especially under unstable conditions, as compared to their counterparts over flat terrain. The mean values of the normalized standard deviations for near-neutral conditions, defined as $|(z\text{-}d)/L| < 0.05$, are listed in table 5.

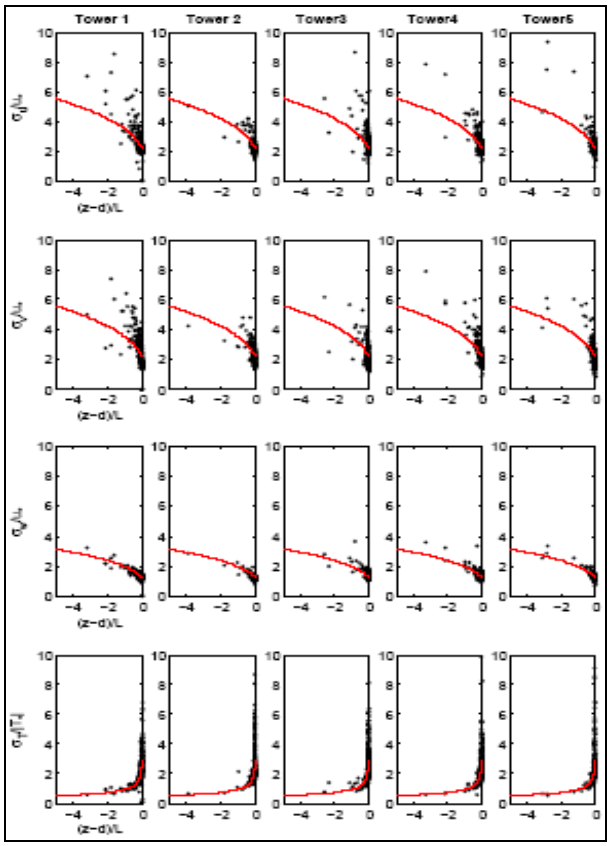

Figure 8. Normalized standard deviations from five ARL tower measurements. The lines show the empirical relations of equations 6 and 7 with equation 8 for (u,v,w) and of equation 1 for (T), respectively.

Table 5. Mean values and their standard deviations (in parentheses) of the normalized standard deviations for near neutral condition defined as $|(z-d)/L|<0.05$ measured at five ARL towers. N is the number of data points.

Tower	N	σ_u/u_*	σ_v/u_*	σ_w/u_*	$\sigma_T/\lvert T_*\rvert$
No. 1	182	2.15 (0.37)	1.80 (0.42)	1.25 (0.21)	2.73 (1.00)
No. 2	304	2.13 (0.22)	1.93 (0.35)	1.19 (0.10)	2.69 (1.23)
No. 3	386	2.31 (0.41)	1.84 (0.38)	1.32 (0.14)	2.70 (0.92)
No. 4	276	2.15 (0.23)	1.84 (0.29)	1.34 (0.12)	2.69 (1.01)
No. 5	255	2.23 (0.26)	1.73 (0.32)	1.21 (0.11)	2.73 (1.36)
All	1403	2.20	1.84	1.27	2.71
(Panofsky & Dutton)		2.39	1.92	1.25	

As the surface layer similarity theory suggests, the normalized standard deviations for the three wind components (σ_u', σ_v', σ_w') under neutral conditions are "constants." From table 5, we obtain values of 2.20, 1.84, and 1.27 when measurements from all five towers are considered. These values are very close to the corresponding values over flat terrain (Panofsky and Dutton, 1984), as indicated in table 5. It is seen, too, that near-neutral values of these normalized standard deviations are very similar among the five tower locations.

Finally, the σ_T' data are plotted using the calculated d values and compared to equation 1, shown in the bottom row of figure 8. The good agreement between the two is reassuring. As pointed out by Roth (2000), large variations in σ_T' are expected at near-neutral stability, where the heat flux becomes close to zero but production of temperature fluctuations does not cease. As a result of this, the estimated neutral limit values of σ_T' are dependent more on the definition of near-neutral than on the initial choice of parameters in equation 1, since the d values only affect the z/L scaling, not the magnitudes of σ_T'. Our estimates in table 5 are based on $|(z-d)/L|<0.05$. Further restricting the definition of near-neutral stability results in larger values for the neutral limits of σ_T' and in larger standard deviations.

4.2 Profiles of TKE and Sensible Heat and Momentum Fluxes in the RSL

We next focus on the profiles of turbulent properties, in particular, the sensible heat and momentum fluxes and TKE and TKE flux. In addition to the 10-m measurements, we use data obtained at levels of 2.5 and 5 m. Recognizing that for northerly wind directions, these data may be affected by the towers themselves and noting that just a sixth of the wind measurements had a northerly component, we have only included data with wind directions having a southerly component in this analysis. In order to identify the top of the RSL and see whether a CFL might exist at higher levels above the city, we also examine data obtained with similar sonic anemometers mounted on an 85-m crane-supported cable fielded by co-investigators from LLNL north of the central business district (Lundquist et al., 2004).

4.2.1 Vertical Variation of Turbulent Heat Flux

Figure 9 shows a typical diurnal variation of the turbulent kinematic heat flux ($H = \overline{w'T'}$) observed at 3 levels (10, 5, and 2.5 m) from Tower 2 on 29 July 2003. Note that the local time (CDT) is 5 h earlier than UTC. As expected, *H* is usually small, though rarely negative, at night and in the early morning. In the day time, *H* increases with time at all three levels until it reaches a maximum in the early afternoon. Significantly, *H* increases with height from 2.5 to 5 m, and from 5 to 10 m during most of the daytime period. To further illustrate the vertical variation of *H*, scatter diagrams of *H* between 2 levels from both Tower 2 (industrial) and Tower 3 (suburban) are plotted in figure 10. This figure shows that a general trend of slightly increasing *H* within the lowest 10 m exists for both Tower 2 and Tower 3.

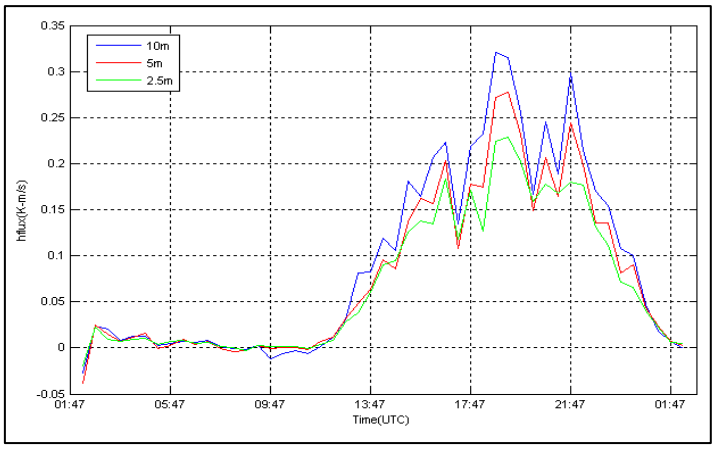

Figure 9. Heat flux at 10, 5, and 2.5 m levels from Tower 2 on 29 July 2003.

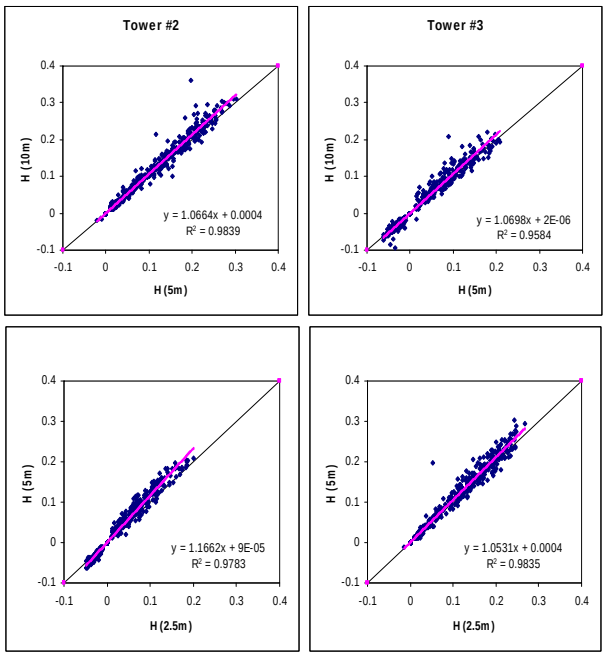

Figure 10. Scatter diagrams of heat flux, *H*, for Tower 2 and Tower 3.

Figure 11 presents the vertical variation of the averaged heat flux, <*H*>, for all five 10-m towers. The values of <*H*> plotted are those for the 2.5, 5, and 10 m levels for the two wind direction quadrants having a southerly component. In the first plot, these averages are plotted against z, the level at which the measurements were made. In the second plot, the reduced height ($z - d$) has been used in order to include the effect of the displacement height. The positive value of the slope of the linear regression indicates the general trend of slightly increasing *H* with height from 2.5 to 10 m in the RSL.

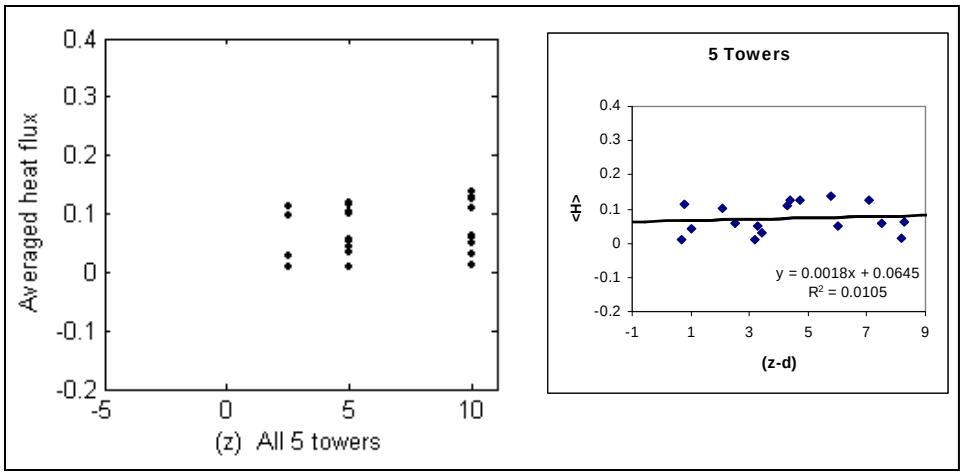

Figure 11. Vertical variation of averaged heat flux, <*H*>, for the five ARL towers.

4.2.2 Vertical Variation of Momentum Flux (u_*)

Similar to figure 10, figure 12 provides scatter diagrams of the friction velocity (u_*) between 5 and 10 m as well as between 2.5 and 5 m from Tower 2 and Tower 3. This figure also indicates a general trend of the increase of u_* within the lowest 10 m of the RSL. This general trend of u_* is much stronger than the trend for the turbulent heat flux, the positive value of the slope of the linear regression being larger than that in figure 10.

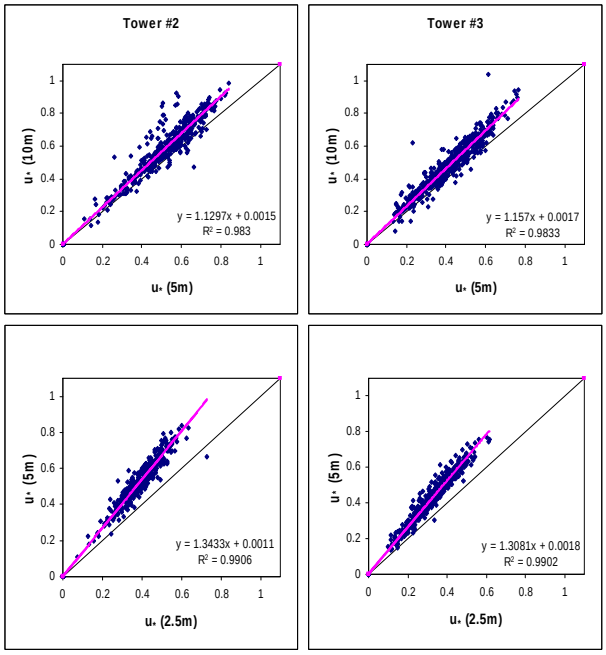

Figure 12. Scatter diagram of friction velocity, u_*, for Tower 2 and Tower 3.

Similar to figure 11, figure 13 further shows the increase of the averaged friction velocity, $< u_* >$, with z and with the reduced height $(z - d)$ for the 5 towers together. The increase of $< u_* >$ with $(z - d)$ is larger than the increase of $<H>$ with $(z - d)$. Rotach (1993) has analyzed the vertical variation of Reynolds stress for the lowest few tens of meters of an urban RSL. He also found that the Reynolds stress (u_*) increased with height in the RSL. Our results from the five tower measurements as shown by figures 12 and 13 appear to agree with his results.

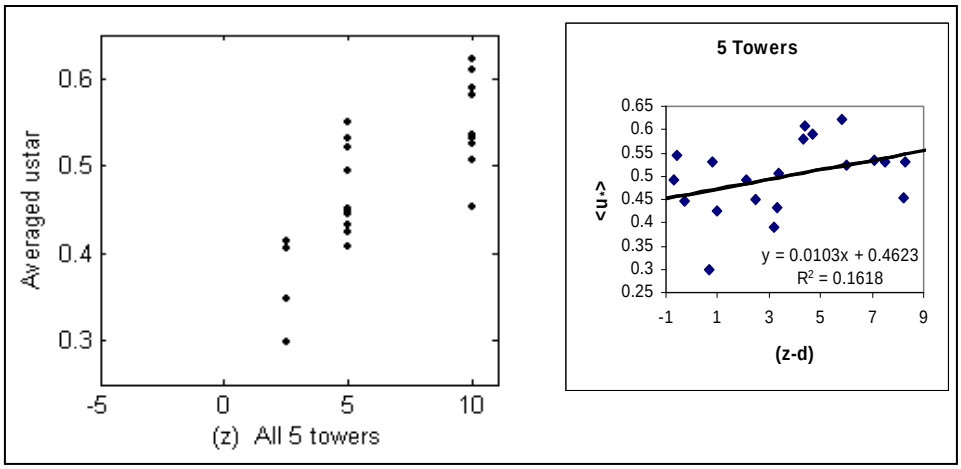

Figure 13. Vertical variation of averaged friction velocity, $<u_*>$, for the five ARL towers.

4.2.3 Vertical Variation of TKE

As shown in figure 14, the TKE also increases with height from 2.5 to 10 m on the towers at both urban and suburban sites. The rate of increase is greater than that for the kinematic heat flux and comparable to that for the friction velocity.

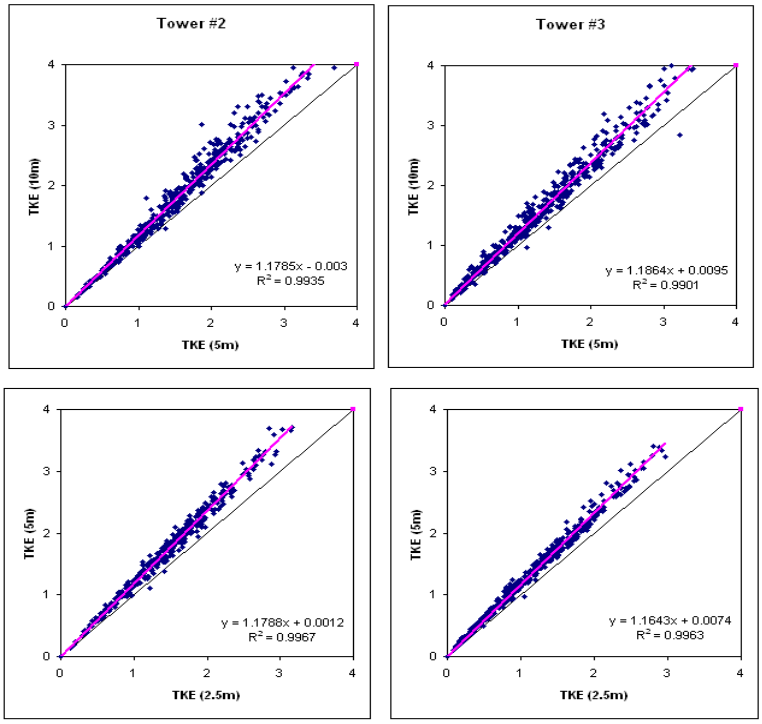

Figure 14. Scatter diagram of TKE for Tower 2 and Tower 3.

4.2.4 Vertical Profiles of TKE and Turbulent Fluxes up to 80 m

We also examined profiles of TKE above the 10-m level. For four of the IOPs during JU2003, two daytime and two nighttime, we have analyzed hourly averages of profiles of wind and TKE as measured by sonic anemometers mounted on cables supported by a 90-m crane instrumented by LLNL and located just north of the CBD. The results for IOPs 2, 3, 7, and 8 are shown in figure 15.

For daytime IOPs 2 and 3, the magnitudes of the TKE increased with height from the lowest level (~8 m) to 20 m, only slightly for IOP2 and more sharply for IOP3. During IOP2, the TKE above 20 m was relatively constant up to 80 m, at times showing a small decrease, at others a small increase; there was an increase in TKE with time at all levels during the first two hours. During IOP3, the TKE above 20 m continued to increase with height, though more slowly than below, up to 40 or 70 m, above which it decreased slightly. These profiles would suggest that there was a source of TKE at about 20 m during IOP2 and a more elevated source varying from 40 to 70 m during IOP3. The magnitudes of the TKE were larger during IOP3 than during IOP2, probably related to the higher wind speeds during IOP3. But the relative maximum in the TKE at 40 to 60 m during IOP3 would indicate enhanced conversion of mean kinetic energy to TKE at levels below that of the maximum wind speed, perhaps due to wake effects induced downwind of the CBD.

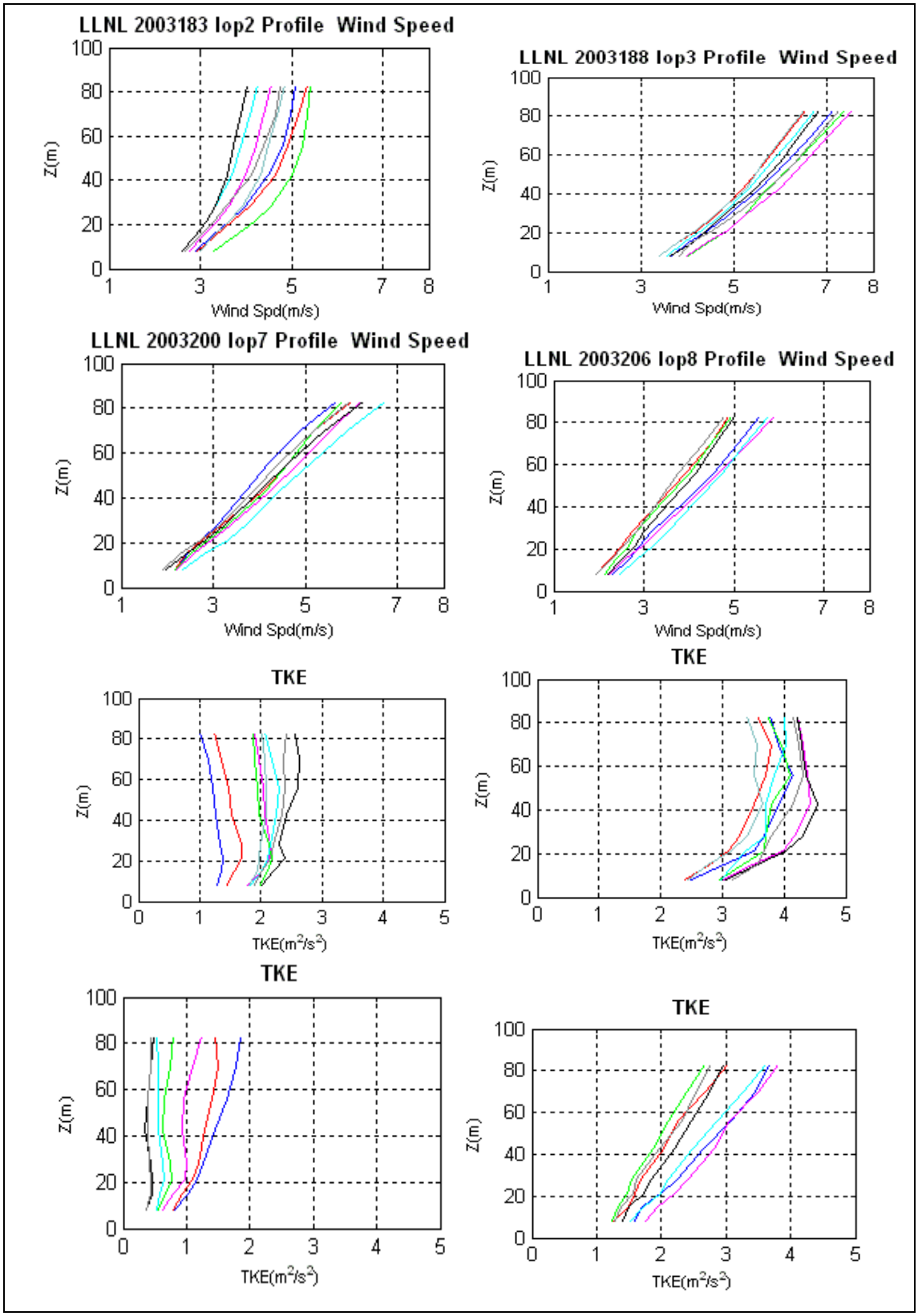

Figure 15. Hourly average profiles of wind speed (left) and TKE (right) for two daytime IOPs (2 and 3) and two nighttime IOPs (7 and 8) measured at the LLNL tower. The times for each of the colored curves are given in figures 16 and 17.

For nighttime IOPs 7 and 8, potential source levels of TKE were hard to identify. During IOP7, the TKE was nearly constant or slightly increasing with height all the way up to 80 m; during IOP8, the TKE increased upwards at all levels at all times.

In figures 16 and 17 we have plotted hourly averages of profiles of friction velocity (square root of momentum flux), kinematic heat flux, and the vertical flux of TKE up to 80 m for the two daytime IOPs (2 and 3) and the two nighttime IOPs (7 and 8). We looked for evidence of the top of the RSL and the existence of a CFL in these profiles.

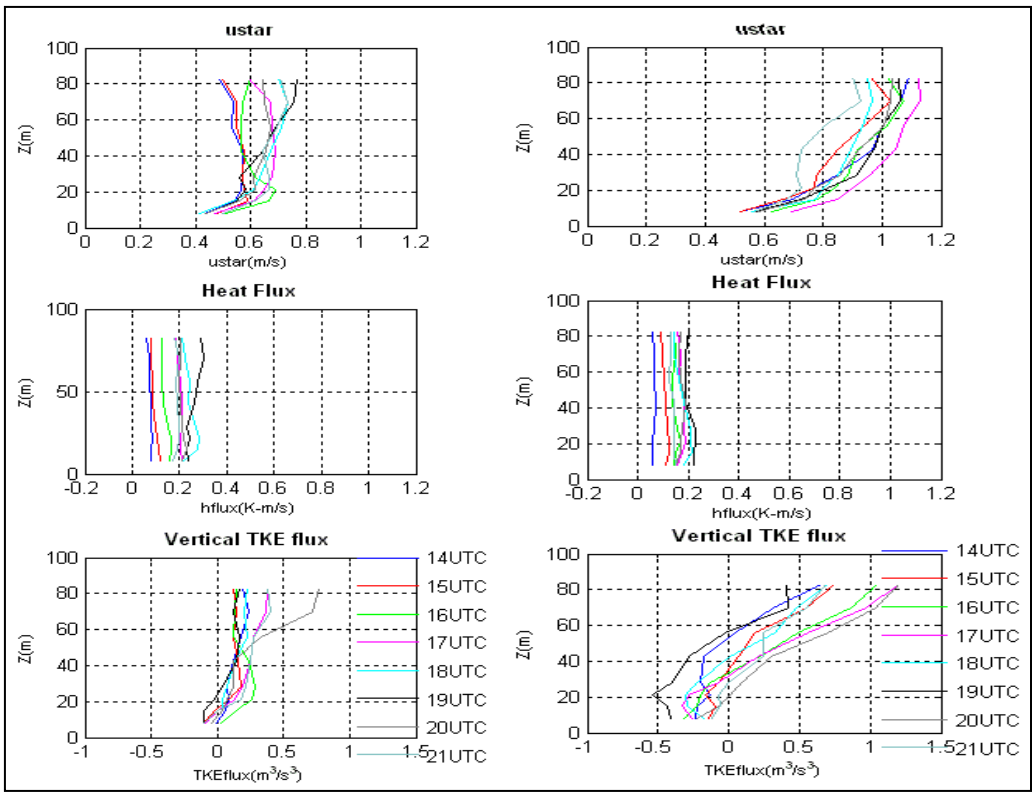

Figure 16. Hourly average profiles of u_*, heat flux, and vertical TKE flux for two daytime IOPs (2-left and 3-right) measured at the LLNL tower The times for each of the colored curves are given in the plots for TKE fluxes.

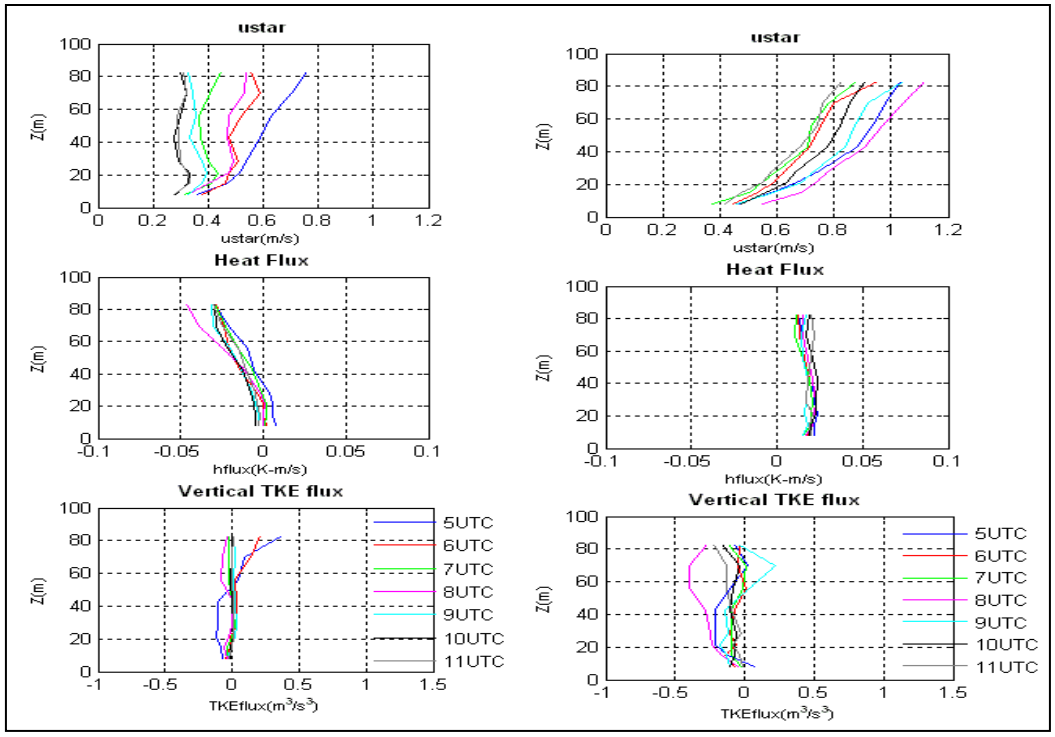

Figure 17. Hourly average profiles of u_*, heat flux, and vertical TKE flux for two nighttime IOPs (7-left and 8-right) measured at the LLNL tower. The times for each of the colored curves are given in the plots for TKE fluxes.

The heat fluxes were relatively constant throughout the 80 m extent of the profiles, showing the expected more positive values during the day (figure16) as solar insolation increased. The nighttime heat fluxes (figure 17, note the expanded scale) were close to zero but exhibited some interesting features. For IOP7, they were near-zero close to the surface but became negative at about 30 m and more negative above that level; for IOP8, they remained slightly positive and nearly constant throughout the 80 m.

The friction velocity profiles all increase with height up to about 20 m. Above that level for IOPs 2 and 7, they show no regular trend and are relatively constant; for IOPs 3 and 8, on the other hand, they continue to increase with height, up to 60 m during IOP3 and all the way up to 80 m for IOP8.

During IOP2, the vertical fluxes of TKE below 20 m were at times negative but always positive above that level. During IOP3, the fluxes were negative from 20 to 60 m, depending on the time, and positive above those levels. Both the magnitudes of the TKE and the TKE fluxes were larger during IOP3 than during IOP2. During IOP7, the vertical fluxes were near zero or slightly negative at least up to 60 m; for two of the hours during this IOP, the flux was positive above 60 m. During IOP8, the vertical flux was negative or near zero at all levels at all times, indicating a more elevated source level for TKE.

4.3 Summary of RSL Analyses

A considerable amount of sonic anemometer data from ARL's five meteorological towers during the JU2003 OKC field experiment has been collected and processed. Using the temperature variance method, the displacement heights (d) for the five tower locations have been estimated. The estimated values of d exhibit significant heterogeneity and depend strongly on wind direction, as shown by table 4; and so does the roughness length. On the other hand, the normalized standard deviations for the three wind components and temperature appear to follow more or less the empirical relations derived for flat terrain (rural area). In particular, the near neutral values of these normalized standard deviations are very close to the values observed over flat terrain as documented in the literature.

Kinematic heat fluxes and friction velocities calculated from measurements of eddy correlations on both the 10-m towers and the 85-m tower just downwind of the CBD indicate that while the lowest layers (RSL and CFL) of the urban boundary layer may be considered a constant flux layer (varying by less than 10%) for sensible heat, the momentum fluxes in this region are far more complex. Both night and day, the maximum gradient in the friction velocity with height occurs in the lowest 20 m; above that level u_* can be relatively constant but often continues to increase, at times all the way up to the 80-m level. Therefore, the classical concept of a constant flux layer as in a homogeneous surface layer cannot be applied.

Both the profiles of TKE and their vertical fluxes indicate various source regions for turbulent kinetic energy. The data from the 10-m towers indicate that there is generally a source of turbulence above 10 m even in the suburban areas, probably resulting from the shear associated with the tops of buildings, trees, and other structures. At least downwind of the CBD, there can exist more elevated source regions of TKE at levels below that of the maximum wind speed. In this domain the RSL can extend at least to 60 m, and there is little evidence of a CFL for momentum above that level.

5. Summary and Conclusions

As emphasized in the introduction (sections 1–2) of this report, the goals of ARL during the JU2003 experiments were (1) to actively cooperate with researchers from other agencies in both the meteorological data collection and subsequent analyses in a full-scale urban environment; (2) to use the data sets obtained by the many investigators to perform basic research in boundary layer meteorology and to evaluate both micrometeorological and transport and dispersion models; and (3) to use BED field expertise in support of the JU2003 experiments and to evaluate the performance of various instruments in comparisons among in-situ and remote sensors.

Within the scope of this field study, ARL's specific scientific objectives were as follows:

1. Examine boundary layer structure and characterize mean and turbulent flow interactions in the various sub-layers within and above the urban CBD and surrounding industrial and suburban (residential) domains.
2. Develop a database to test, evaluate, and refine urbanized microscale model/codes, such as CCSL and especially 3DWF.
3. Quantify roughness lengths, displacement heights, urban flow indices, coupling ratios, profile behavior, wake effects, and other parameters relevant to the boundary layer over the CBD and suburban regimes.
4. Use the data to better understand dispersion behavior and develop urban diffusion coefficients within, around, and above the urban domain.
5. Perform unique Dual Doppler Lidar Wind Measurements to characterize the 3D wind field above the city and to provide input for 3DWF.

As documented in this volume, in subsequent volumes of this report, and in the literature cited in the references, these goals and objectives have been met. Collaborative efforts with researchers from LLNL and Arizona State University have been particularly fruitful in enhancing our understanding of the urban boundary layer environment, particularly the RSL, and in enabling us to initiate and evaluate the diagnostic wind model 3DWF and associated dispersion models. Continued improvement of these models for urban areas in complex terrain has been realized in BED's subsequent work plans. In-depth analysis procedures for data obtained with the sonic anemometers and the dual lidars have been developed. Combining these data with data from other instruments has given us a more complete picture of the boundary layer under near-neutral and unstable conditions. Wave/turbulence interactions have been investigated. We have found that a RSL of considerable depth and complexity cannot be simply parameterized with Monin-Obukhov similarity theory.

Specific findings include the following:

1. The displacement heights (d) for the five ARL tower locations have been estimated. The estimated values of d exhibit significant heterogeneity and depend strongly on wind direction; and so does the roughness length.
2. Kinematic heat fluxes and friction velocities indicate that while the lowest layers of the urban boundary layer may be considered a constant flux layer (varying by less than 10%) for sensible heat, the momentum fluxes in this region are far more complex. The classical concept of a constant flux layer as in a homogeneous surface layer cannot be applied.

3. Both the profiles of TKE and their vertical fluxes indicate various source regions for turbulent kinetic energy. Downwind of the CBD there can exist elevated source regions of TKE at levels below that of the maximum wind speed. In this domain the RSL can extend at least to 60 m, and there is little evidence of a classical CFL above that level.

We conclude this report by pointing out that much more analysis of the data for all the sites stratified by time of day and by wind speed and direction remains to be done. A first step, but only a first step, has been taken in attempting to estimate the effects of local terrain features and structures on directionally dependent diffusion coefficients. We must continue to relate the data from the in-situ sensors with the remote sensors probing the boundary layer depth to gain a more complete picture of the interactions among the various sub-layers as a function of stability and wind direction. While the investigation of wave/turbulence interactions has been initiated, much more work in this area remains to be done. We emphasize that since a principal motivation for performing the field experiment was to relate the urban meteorological conditions to the resulting atmospheric dispersion in the boundary layer, future analyses will necessitate looking at all of the data obtained by the many investigators (e.g., Lundquist et al., 2004, and Grimmond et al., 2004), concentrating particularly on times for which intensive observations were conducted.

6. References

Allwine, K. J.; Leach, M. J.; Stockham, L. W.; Shinn, J. S.; Hosker, R. P.; Bowers, J. F.; Pace, J. C. Overview of Joint Urban 2003, an Atmospheric Dispersion Study in Oklahoma City. *AMS Symposium on Planning, Nowcasting, and Forecasting in the Urban Zone*, Seattle, WA, 11–15 Jan. 2004.

Bach, W.; Ligon, D.; Creegan, E. Private communications, Dual Lidar proposal, 2003.

Burian, S. J.; Han, W. S.; Brown, M. J. M*orphological Analyses Using 3D Building Databases: Oklahoma City, Oklahoma*; Los Alamos National Laboratory: Los Alamos, NM, 2003, 63.

Campbell, G. G. Asynchronous Stereo Height and Motion Analysis: Applications, Fourth Winds Workshop, WMO, 1998.

Chang, S. S.; Huynh, G. D.; Klipp, C. L.; Williamson, C. C.; Garvey, D. M.; Wang, Y. Observational Study of Turbulence Spectra for Joint Urban 2003. Preprints, *5th Symposium on Urban Environment*, Vancouver, BC, Canada, 3.5, 23–27 Aug. 2004.

Cionco, R. M.; Vaucher, G. T.; Yee, Y. P.; Bustillos, M.; Brice, R.; Elliott, D. S.; Creegan, E.; Yarbrough, J.; Vidal, E. Measurements of Airflow about a Building. *Proceedings Battlefield Atmospheric and Cloud Impacts on Military Operations (BACIMO) Conf.*, Monterey, CA, 9–11 Sep. 2003.

Cogan, J.; Measure, E.; Vidal, E.; Creegan, E.; Vaucher, G. The MMS-Profiler: Present and Future. *Proceedings, Battlefield Atmospheric and Cloud Impacts on Military Operations (BACIMO) Conf.*, 1–3 Dec. 1998,

De Bruin, H.A.R.; Kohsek, W.; Van Den Hurk, J.J.M. A Verification of Some Methods to Determine the Fluxes of Momentum, Sensible Heat, and Water Vapour Using Standard Deviation and Structure Parameter of Scalar Meteorological Quantities. *Boundary-Layer Meteor.* **1993**, *63*, 231–257.

De Wekker, S.F.J.; Berg, L. K.; Allwine, K. J.; Doran, J. C.; Shaw, W. J. Boundary Layer Structure Upwind and Downwind of Oklahoma City During the Joint Urban 2003 Field Study. *Amer. Meteor. Soc. 5th Conf. on Urban Environment*,Vancouver, BC, Canada, 23–27 August 2004.

Feigenwinter, C.; Vogt, R.; Parlow, E. Vertical Structure of Selected Turbulence Characteristics above an Urban Canopy. *Theoretical and Applied Climatology* **1999**, *62*, 51–63.

Garvey, D. M.; Klipp, C. L.; Williamson, C. C.; Huynh, G. D.; Chang, S. S. Comparison of Surface Layer Turbulence in Urban and Suburban Domains during Joint Urban 2003. Preprints, *16th Symposium on Boundary Layers and Turbulence*, Amer. Meteor. Soc., Portland, ME, 9.9, 2004.

Garvey, D. M.; Klipp, C. L.; Chang, S. S.; Huynh, G. D.; Williamson, C. C. Urban Effects on Transport and Diffusion of Smokes and Toxic Agents. Summary preprints, *24th Army Science Conference*, Orlando, FL, 2004.

Garvey, D. M.; Huynh, G.; Klipp, C. L.; Chang, S.; Williamson, C. C.; Wang, Y. Profiles of TKE and Sensible Heat and Momentum Fluxes in the Roughness Sub-layer of a City. *AMS Sixth Symposium on the Urban Environment*, Atlanta, GA, 30 Jan.–2 Feb. 2005.

Grimmond, C.S.B.; Oke, T. R. Aerodynamic Properties of Urban Areas Derived from Analysis of Surface Form. *J. Applied Meteor.* **1999**, *38*, 1262–1292.

Hanna, S.; Britter, R. *Wind Flow and Vapor Cloud Dispersion at Industrial and Urban Sites*. American Institute of Chemical Engineers, publication G-75, 2002.

Huynh, G. D.; Chang, S. S.; Klipp, C. L.; Williamson, C. C.; Wang, Y. Spatial Variability of Turbulence Characteristics in an Urban Roughness Sublayer. *AMS Sixth Symposium on the Urban Environment*, Atlanta, GA, 30 Jan.–2 Feb. 2005.

Joint Urban 2003 Atmospheric Dispersion Study, Oklahoma City, July 2003, Experimental Plan, U.S. DoD Defense Threat Reduction Agency (DTRA), U.S. DOE National Nuclear Safety Administration – Chemical and Biological National Security Program (CBNP).

Kaimal, J. C.; Finnigan, J. J. *Atmospheric Boundary Layer Flows, Their Structure and Measurement*. Oxford University Press, 289, 1994.

Klipp, C. L.; Chang, S. S.; Williamson, C. C.; Huynh, G. D.; Garvey, D. M.; Wang, Y. A Generalized Planar Fit Method for Sonic Anemometer Tilt Correction. Preprints, *16th Symposium on Boundary Layers and Turbulence*, Amer. Meteor. Soc., Portland, ME, 11.11, 2004.

Klipp, C. L. Wind Direction Dependence of Atmospheric Boundary Layer Turbulence Parameters in the Urban Roughness Sublayer. *J. Appl. Meteorol.* **2007**, *46*, 2086–2089.

Lundquist, J. K.; Shinn, J. H.; Gouveia, F. Observations of Turbulent Kinetic Energy Dissipation in the Urban Environment. *84th AMS Annual Meeting*, Seattle, WA, 11–15 Jan. 2004.

Measure, E.; Yee, Y.; Cogan, J.; Bleiweiss, M. Neural Network Based Retrieval of Wind and Temperature Profiles from Combined Surface and Satellite Observations, Preprints, *17th International Conference on Interactive Information and Processing Systems for Meteorology, Oceanography, and Hydrology*Albuquerque, NM, 14–18 Jan. 2001, 287–.

Newsom, R.; Banta, R. Sensitivity Analysis of Wind and Temperature Retrievals from Coherent Doppler Lidar Data. Proceedings, *Battlefield Atmospheric and Cloud Impacts on Military Operations (BACIMO) Conf.*, Monterey, CA, 9–11 Sep. 2003.

Newsom, R.K.; Ligon, D. A.; Calhoun, R.; Heap, R.; Creegan, E.; Princevac, M. Retrieval of Microscale Wind and Temperature Fields from Single- and Dual-Doppler Lidar Data. *J. Appl. Meteorol.* **2005**, 44, 1324–1345.

Oke, T. R.; Cleugh, H. A.; Grimmond, S.; Schmid, H. P.; Roth, M. Evaluation of Spatially-averaged Fluxes of Heat, Mass, and Momentum in the Urban Boundary Layer. *Weather and Climate* **1989**, *9*, 14–21.

Panofsky, H.A.; Dutton, J. A. *Atmospheric Turbulence – Models and Methods for Engineering Applications*. John Wiley and Sons, New York, 1984, p. 397.

Raupach, M.R.; Antonia, R. A.; Rajagopalan, S. Rough-wall Turbulent Boundary Layers. *Appl. Mech. Review* **1991**, *44*, 1–25.

Rotach, M. W. Determination of the Zero Plane Displacement in an Urban Environment. *Boundary-Layer Meteorology* **1994**, *67*, 187–193.

Roth, M. Review of Atmospheric Turbulence Over Cities. *Q. J. R. Meteorol. Soc.* **2000**, *126*, 941–990.

Tillman, J. E. The Indirect Determination of Stability, Heat and Momentum Fluxes in the Atmospheric Boundary Layer from Simple Scalar Variables during Dry Unstable Conditions. *J. Appl. Meteorol.* **1972**, *11*, 783–792.

Torres, Mario. Developing Scalable Distributed Applications, A Generic Model Implemented in Java. *Dr. Dobb's Journal,* Sept 2001.

USARL Research Proposal for Joint Urban 2003 Field Study, DTC Project No. 8-CO-160-000-052, DPG Document No. WDTC-TP-01-028.

Vickers D.; Mahrt, L. Quality Control and Flux Sampling Problems from Tower and Aircraft Data. *J. of Atmos. and Oceanic Technology* **1997**, *14*, 512–526.

Vidal, Jr, E.; Yee, Y. Data Collection of High Resolution 3D Sonic Anemometer Measurements. Preprints, *19th International Conf. on Interactive Information Processing Systems (IIPS) for Meteorology, Oceanography, and Hydrology,* Long Beach, CA, 2003.

Wang, Y.; Mercurio, J. J.; Williamson, C. C.; Garvey, D. M.; Chang, S. S. *A High Resolution, Three-dimensional, Computationally Efficient, Diagnostic Wind Model: Initial Development Report*; ARL-TR-3094; U.S. Army Research Laboratory: Adelphi, MD, 2003.

Wang, Y.; Williamson, C. C.; Huynh, G.; Chang, S.; Ligon, D. A.; Garvey, D. M. Measured and Modeled Wind Fields in an Urban Environment. Preprints, *84th Meeting of Amer. Meteor. Soc.*, Seattle, WA, 2004.

Wang, Y.; Ligon, D. A.; Creegan, E.; Williamson, C. C.; Klipp, C. L.; Felton, M. Turbulence Characteristics over an Urban Domain Observed by Doppler Lidars. Preprints, *16th Symposium on Boundary Layers and Turbulence*, Amer. Meteor. Soc., Portland, ME, 6.3, 2004.

Wang, Y.; Williamson, C. C.; Garvey, D. M.; Chang, S. S.; Cogan, J. L. Application of a Multigrid Method to a Mass Consistent Diagnostic Wind Model. *J. Appl. Meteor.* **2005**, *44*, 1078–1089.

Wang, Y.; Klipp, C. L.; Garvey, D. M.; Ligon, D. A.; Williamson, C. C.; Chang, S. S.; Newsom, R. K.; Calhoun, R. Nocturnal Low-level-jet Dominated Atmospheric Boundary Layer Observed by Doppler Lidars over Oklahoma City during JU2003. *J. Appl. Meteor.* **2007**, *46*, 2098–2109.

Ware, R.; Carpenter, R.; Guldner, J.; Liljegren, J.; Nehrkorn, T.; Solheim, F.; Vandenberghe, A Multi-channel Radiometric Profiler of Temperature, Humidity, and Cloud Liquid. *Radio Science* **2003**, *38*, 8079, doi:10.1029/2002RS002856.

Wyngaard, J. C.; Cote, O. R.; Izumi, Y. Local Free Convection, Similarity and the Budgets of Shear Stress and Heat Flux. *J. Atmos. Sci.* **1971**, *28*, 1171–1182.

Yee, Y.; Bustillos, M.; Chang, S.; Cionco, R.; Creegan, E.; Elliott, D. S.; Garvey, D.; Huynh, G.; Ligon, D.; Measure, E.; Quintis, D.; Torres, M.; Vaucher, G.; Vidal, Jr, E.; Williamson, C.; Yarbrough, J. Wind and Turbulence Observations in Joint Urban 2003. Preprints, *Symposium on Planning, Nowcasting, and Forecasting in the Urban Zone*, *84th Meeting of Amer. Meteor. Soc.*, Seattle, WA, J7.5, 2004.

INTENTIONALLY LEFT BLANK.

Appendix A. ARL Sonic Anemometer Data for 10 IOP Days

Data from the 12 ARL sonic anemometers for the 10 days on which IOPs were conducted are presented in figures A-1 through A-30 of this appendix. For each day we have graphed the following variables as measured at the five tower sites, a total of 30 graphs for each day:

- wind direction,
- wind speed,
- temperature (T),
- kinematic sensible heat flux (H),
- turbulent kinetic energy (TKE), and
- friction velocity (u_*).

When measurements from a single tower are available for more than one level, these are shown on the same graph. Averages of these quantities were calculated for 10-min blocks of data sampled at 10 Hz. In cases where one or more of the input measurements did not meet quality control criteria or there were interruptions in the data stream, the figures show missing data. Also shown on each page for each day are the time periods during which the IOPs were conducted. Recall that sites 1, 3, and 4 are characteristic of suburban areas while sites 2 and 5 are more urban in nature.

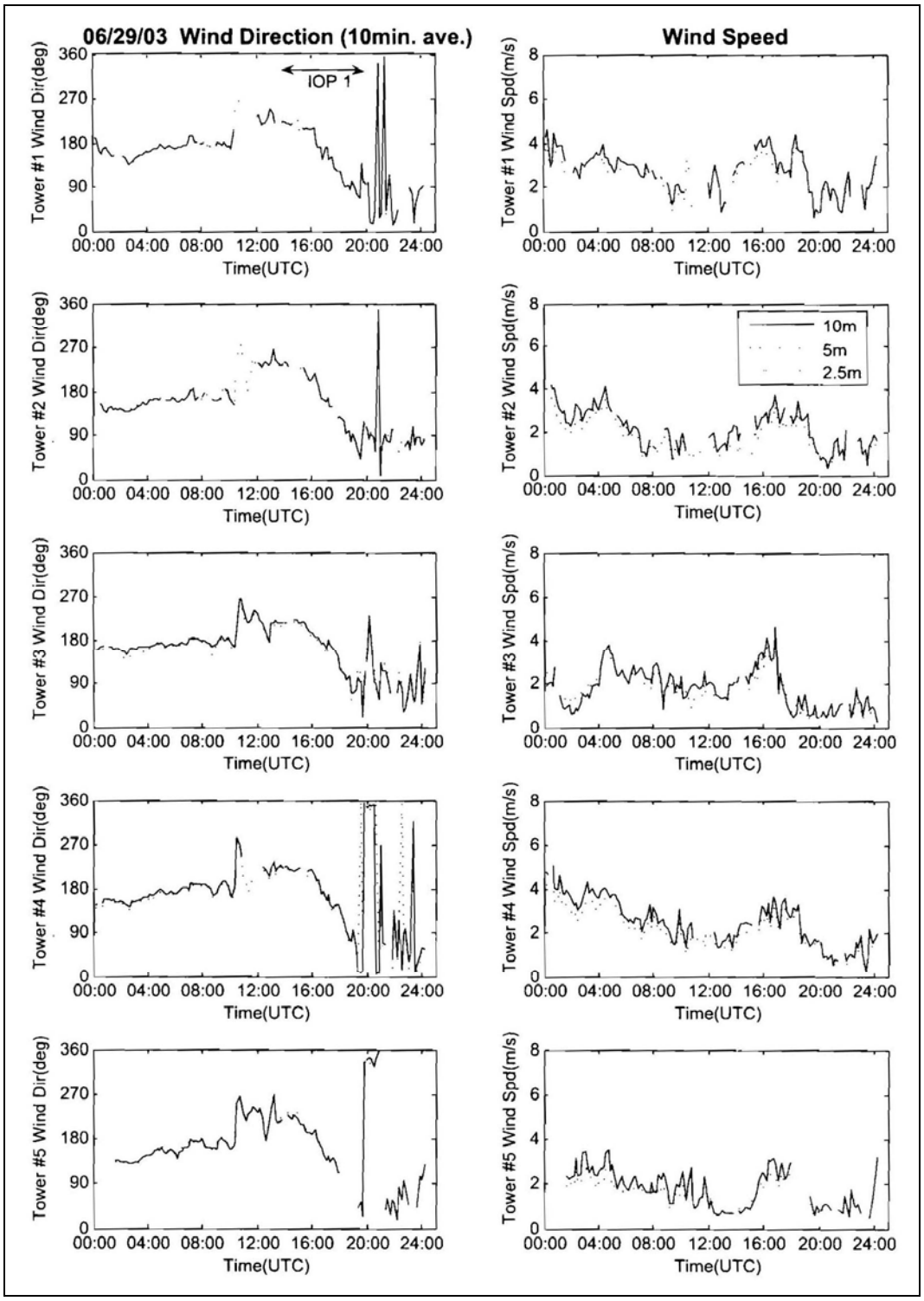

Figure A-1. Wind direction and wind speed, 29 June 2003.

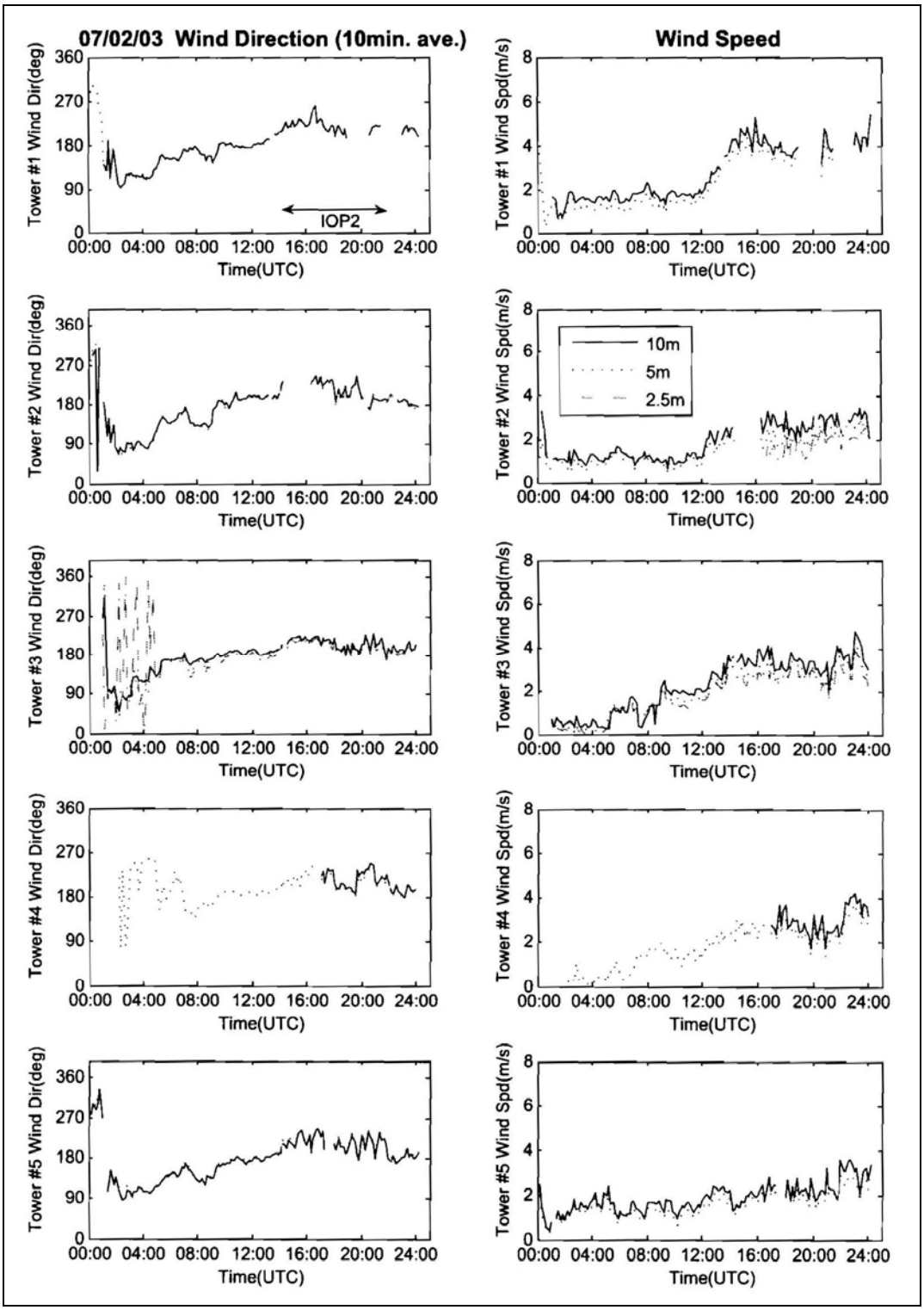

Figure A-2. Wind direction and wind speed, 2 July 2003.

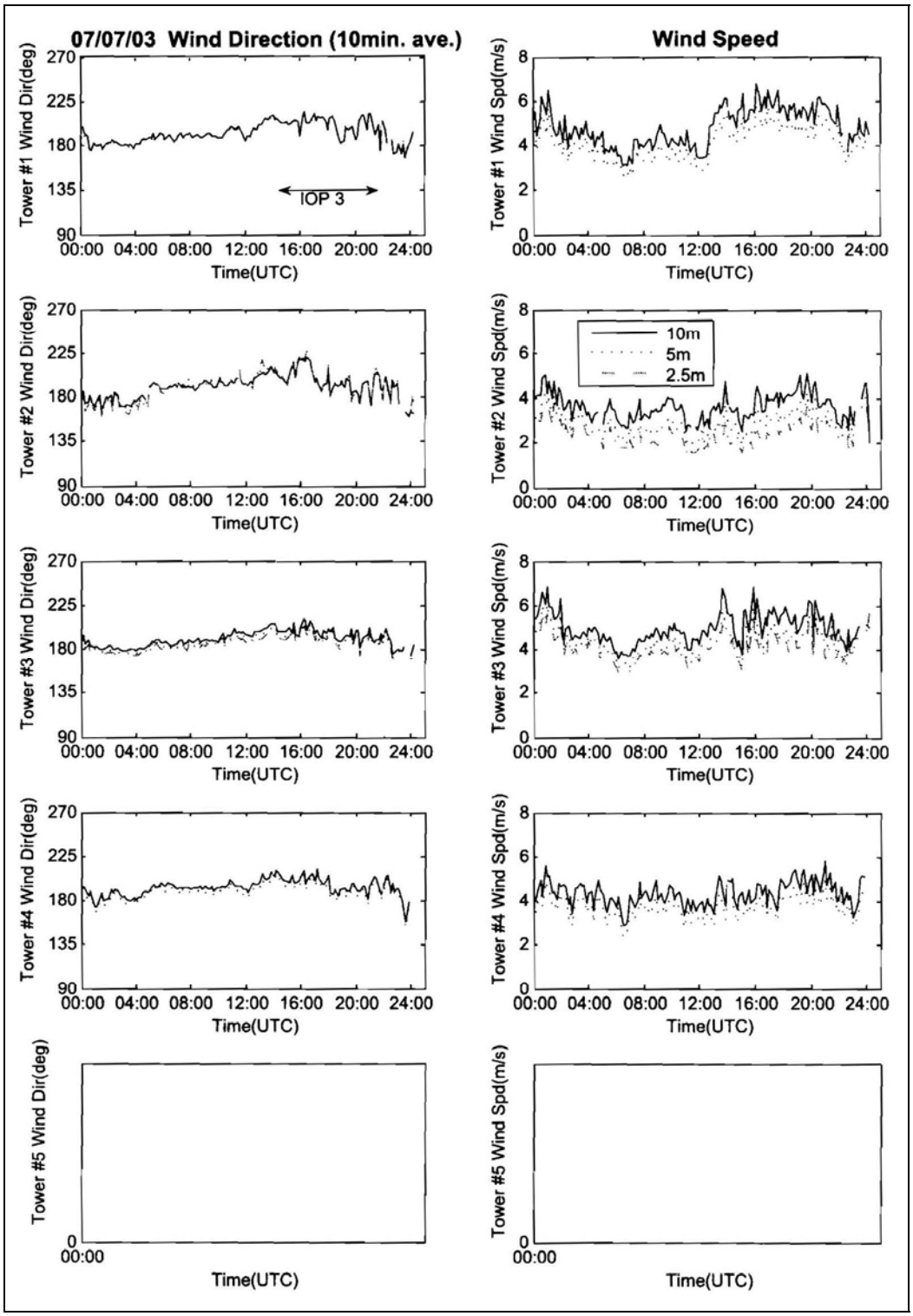

Figure A-3. Wind direction and wind speed, 7 July 2003.

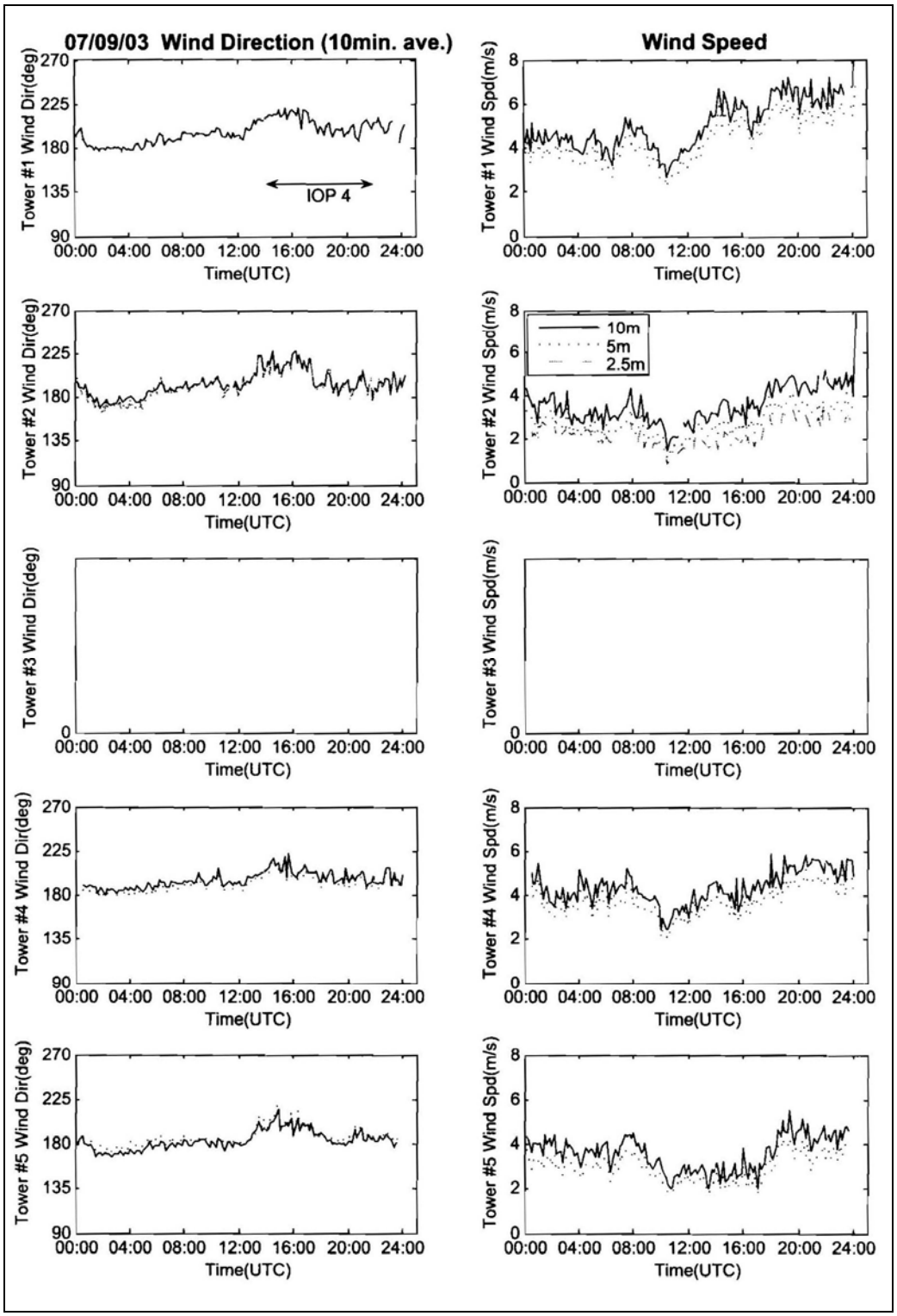

Figure A-4. Wind direction and wind speed, 9 July 2003.

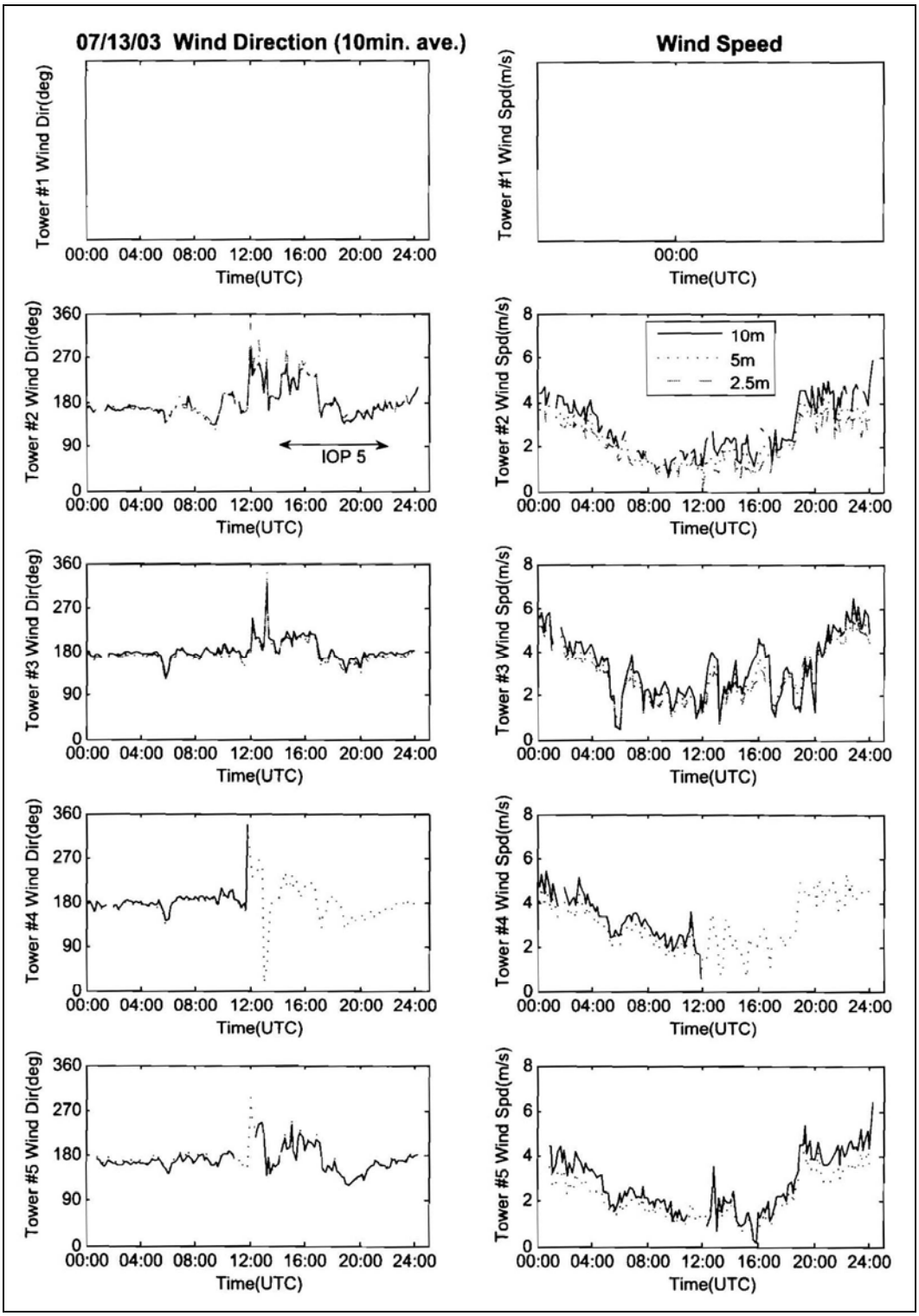

Figure A-5. Wind direction and wind speed, 13 July 2003.

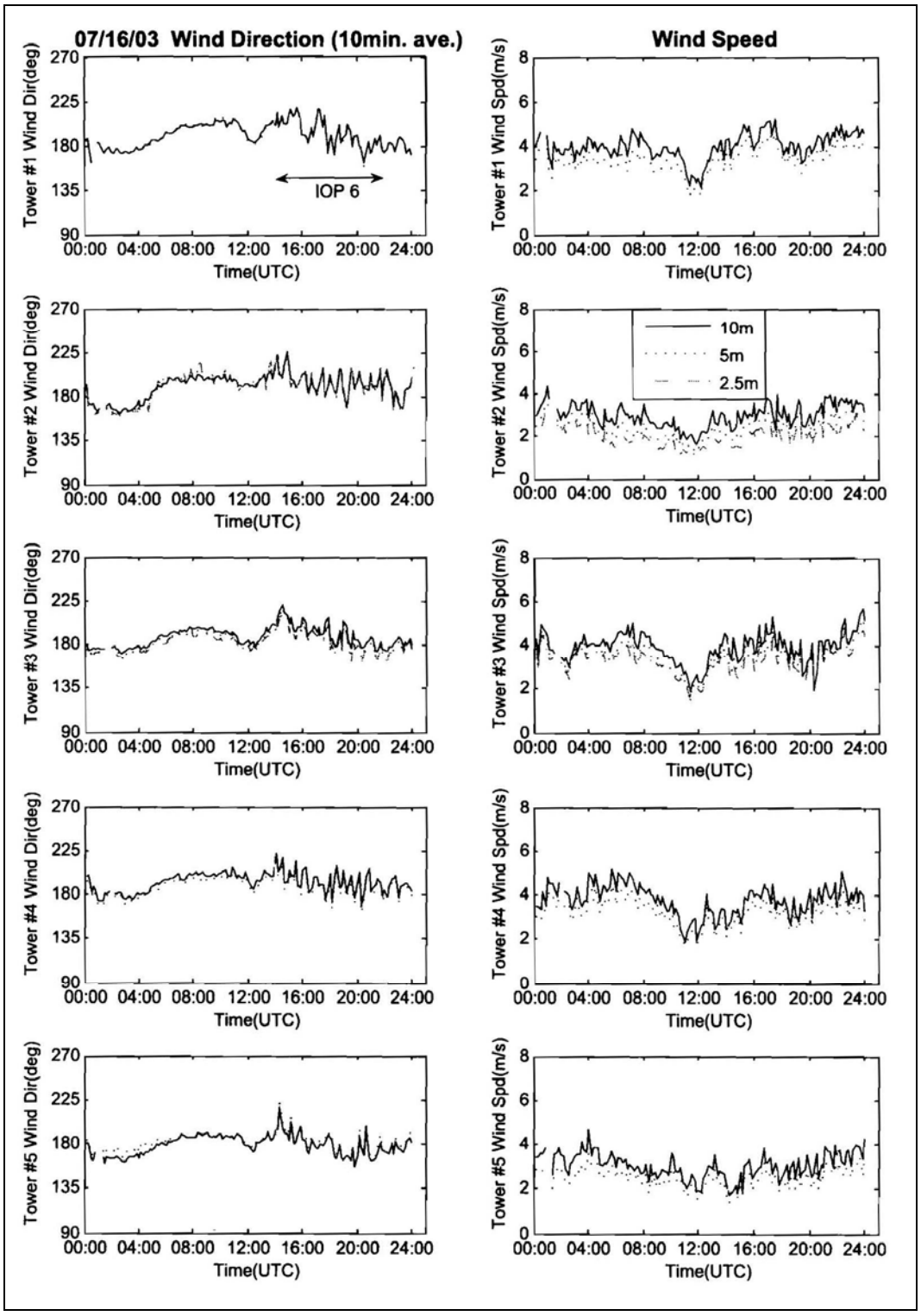

Figure A-6. Wind direction and wind speed, 16 July 2003.

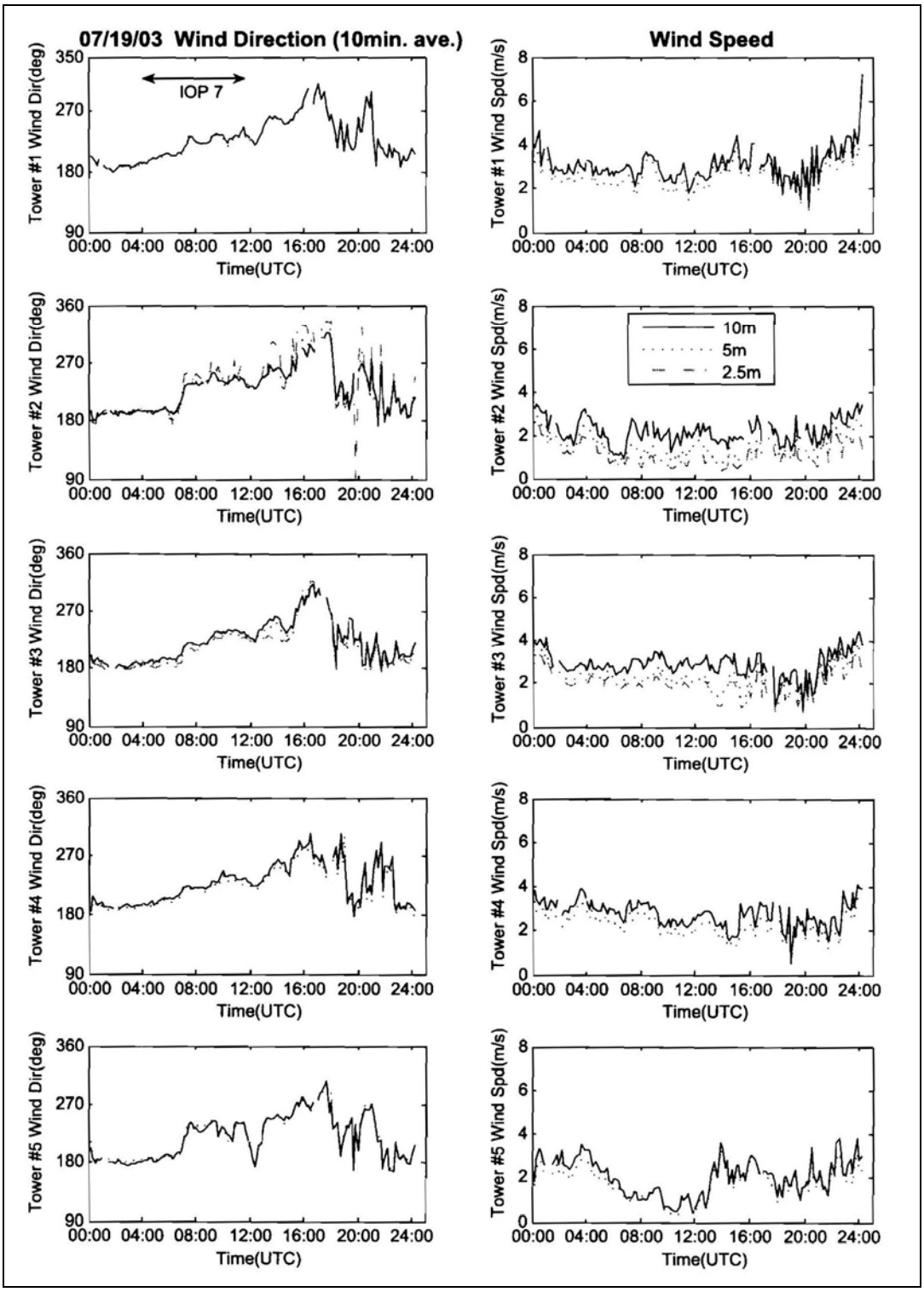

Figure A-7. Wind direction and wind speed, 19 July 2003.

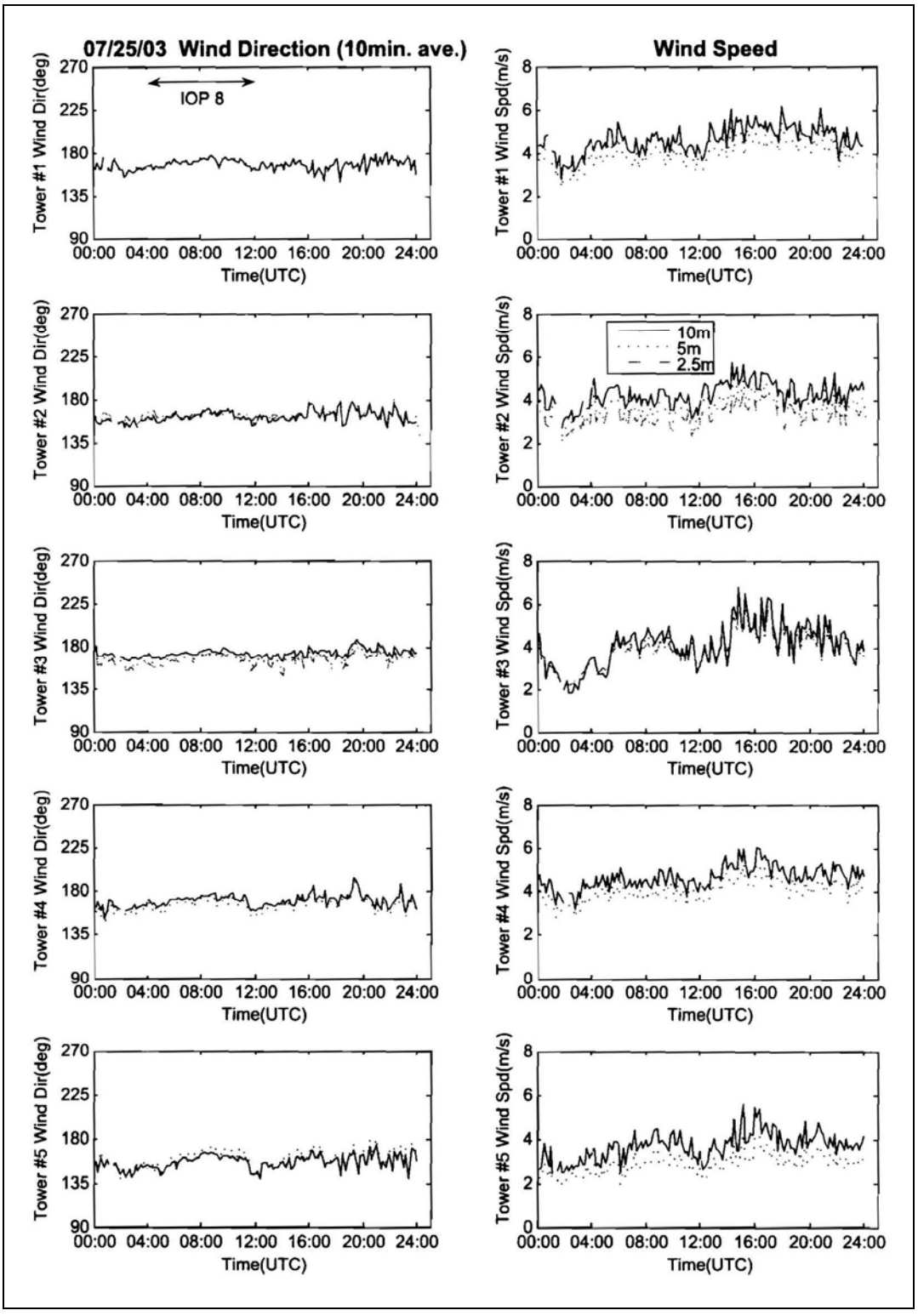

Figure A-8. Wind direction and wind speed, 25 July 2003.

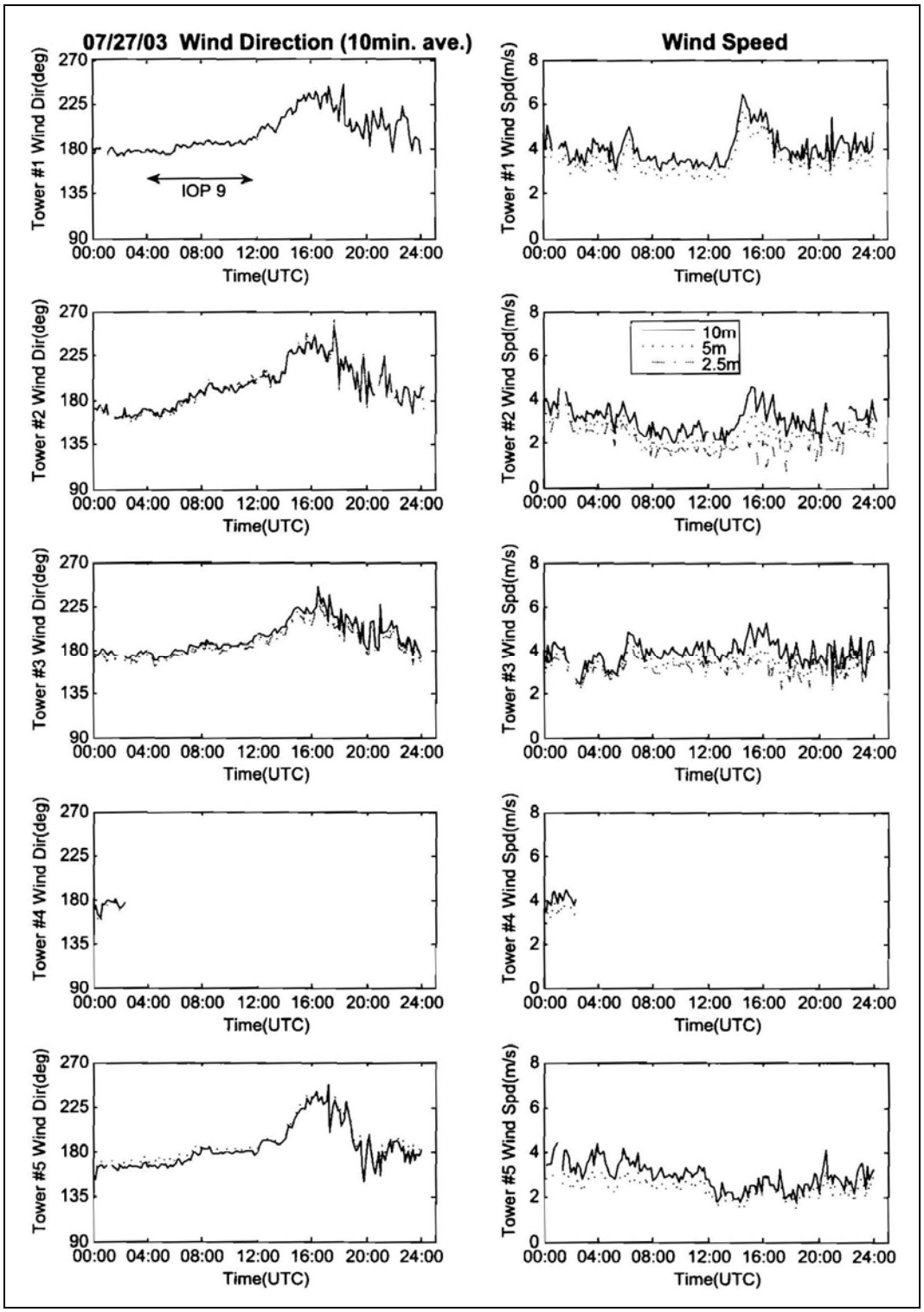

Figure A-9. Wind direction and speed, 27 July 2003.

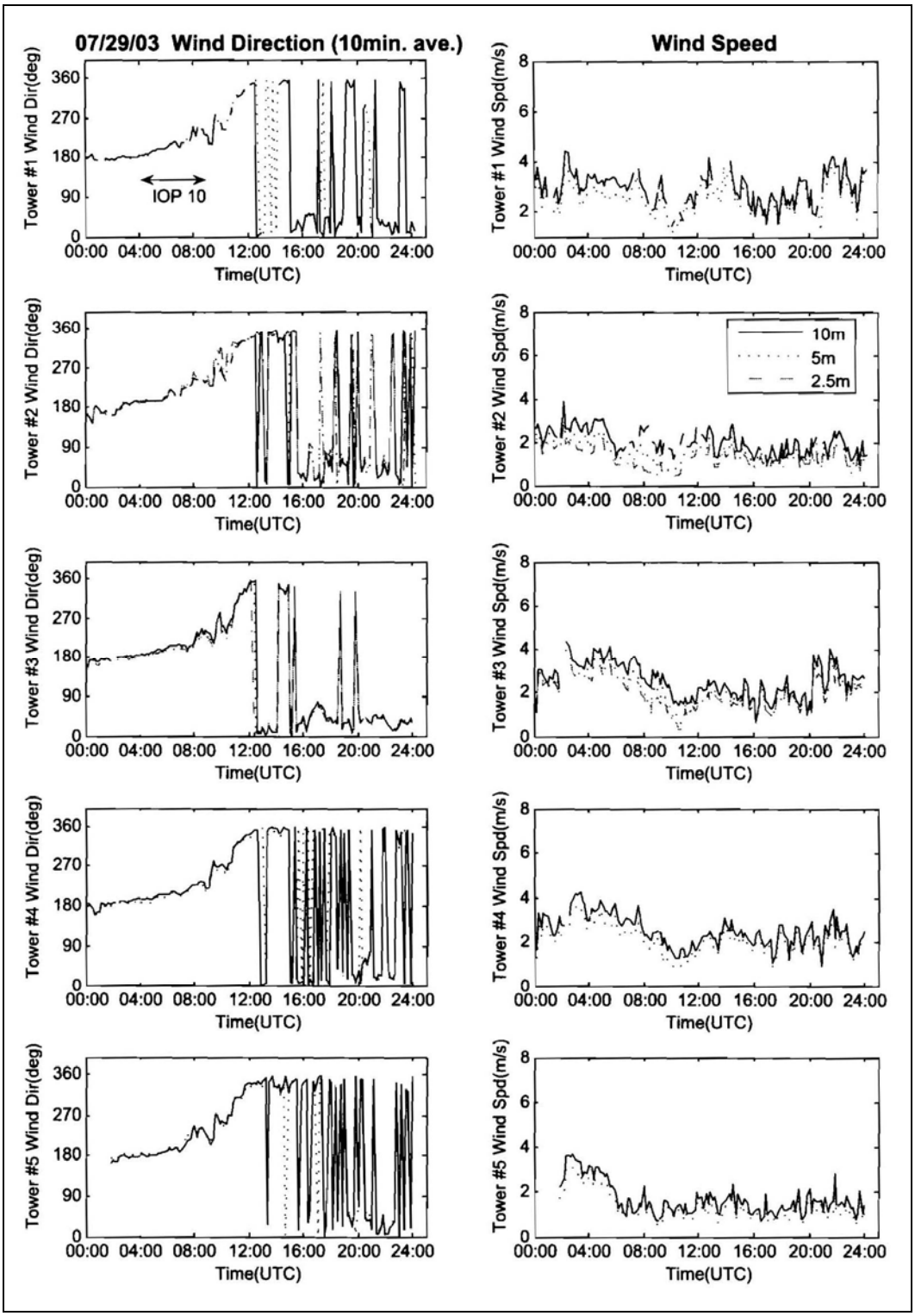

Figure A-10. Wind direction and speed, 29 July 2003.

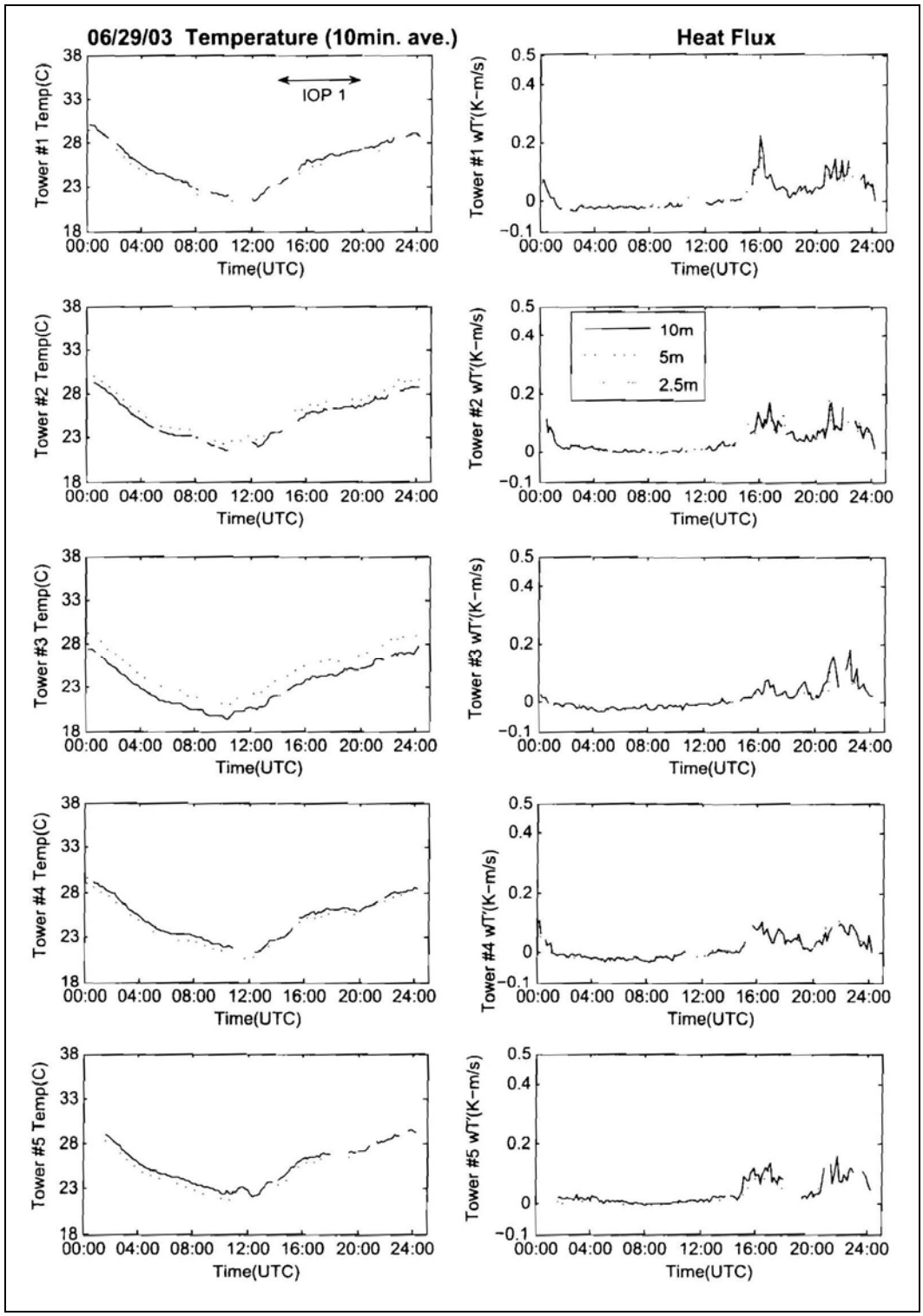

Figure A-11. Temperature and kinematic sensible heat flux, 29 June 2003.

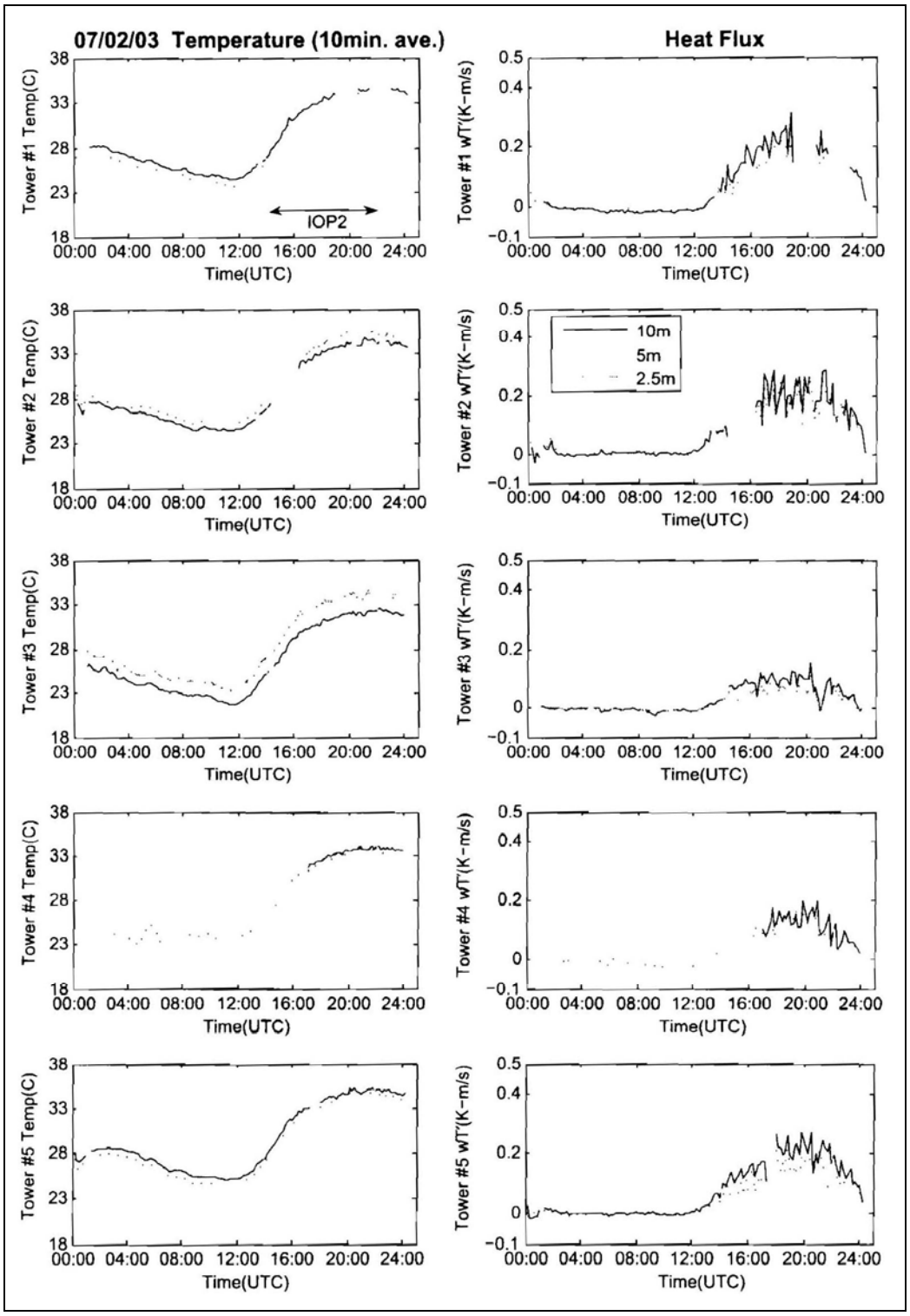

Figure A-12. Temperature and kinematic sensible heat flux, 2 July 2003.

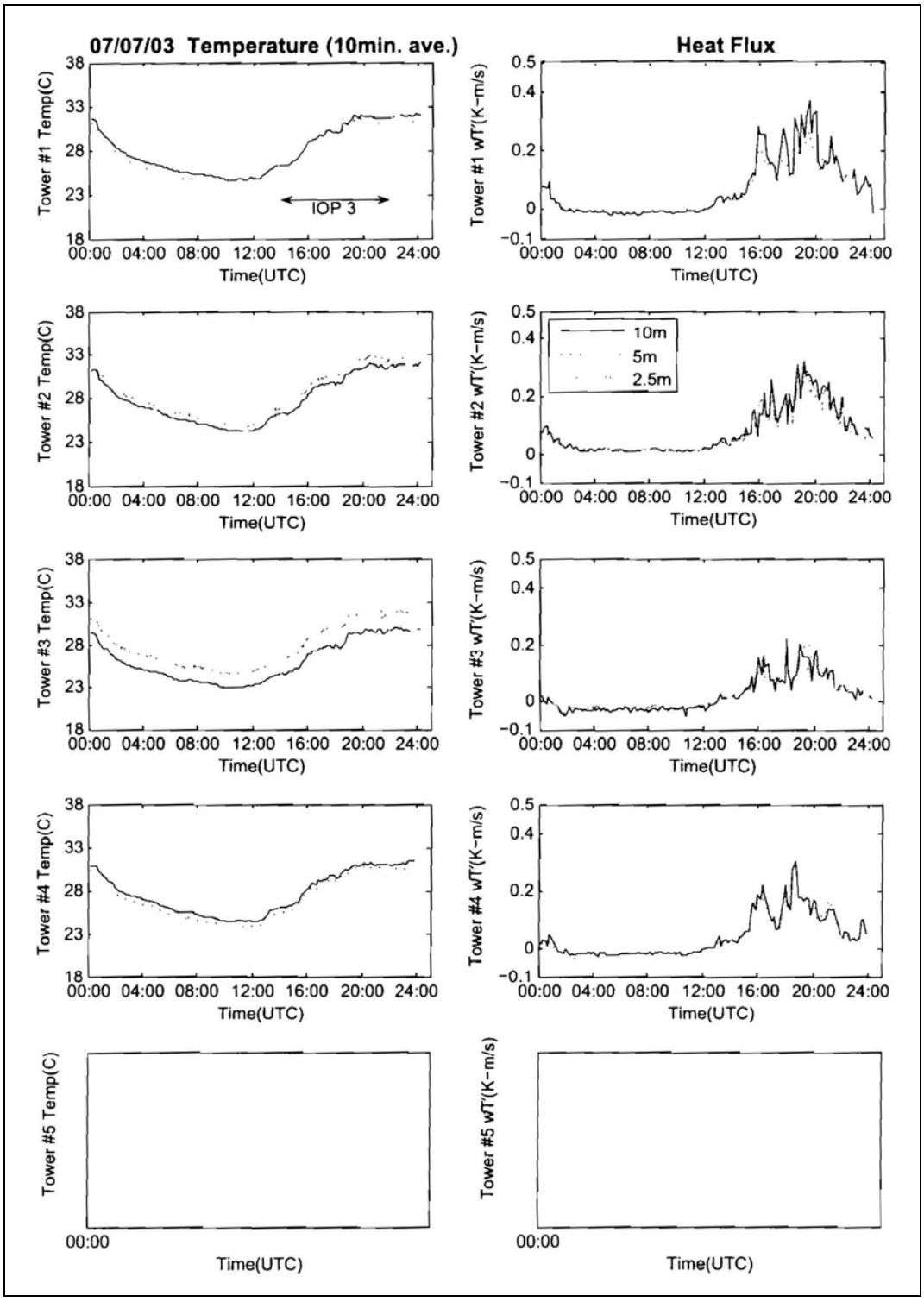

Figure A-13. Temperature and kinematic sensible heat flux, 7 July 2003.

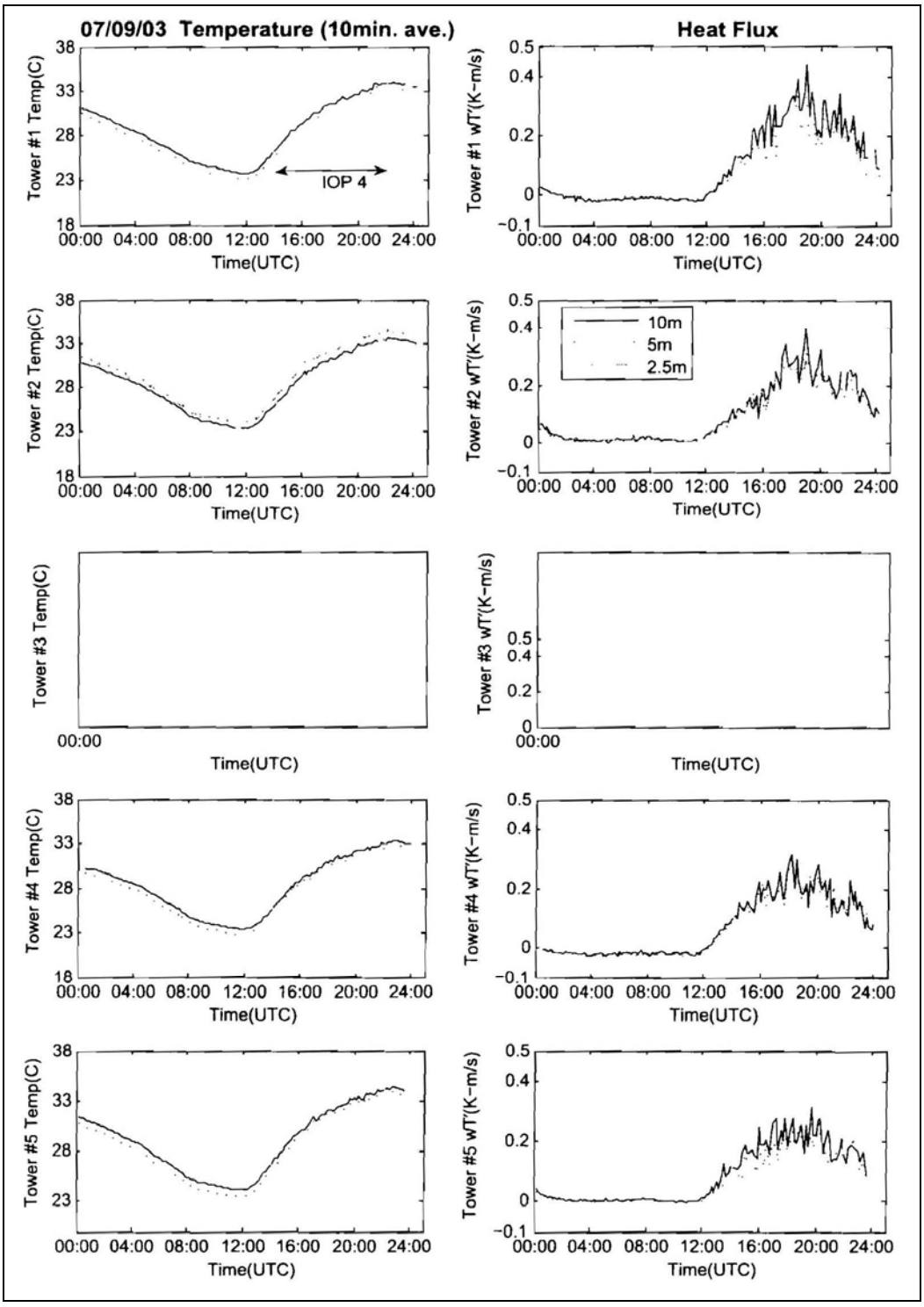

Figure A-14. Temperature and kinematic sensible heat flux, 9 July 2003.

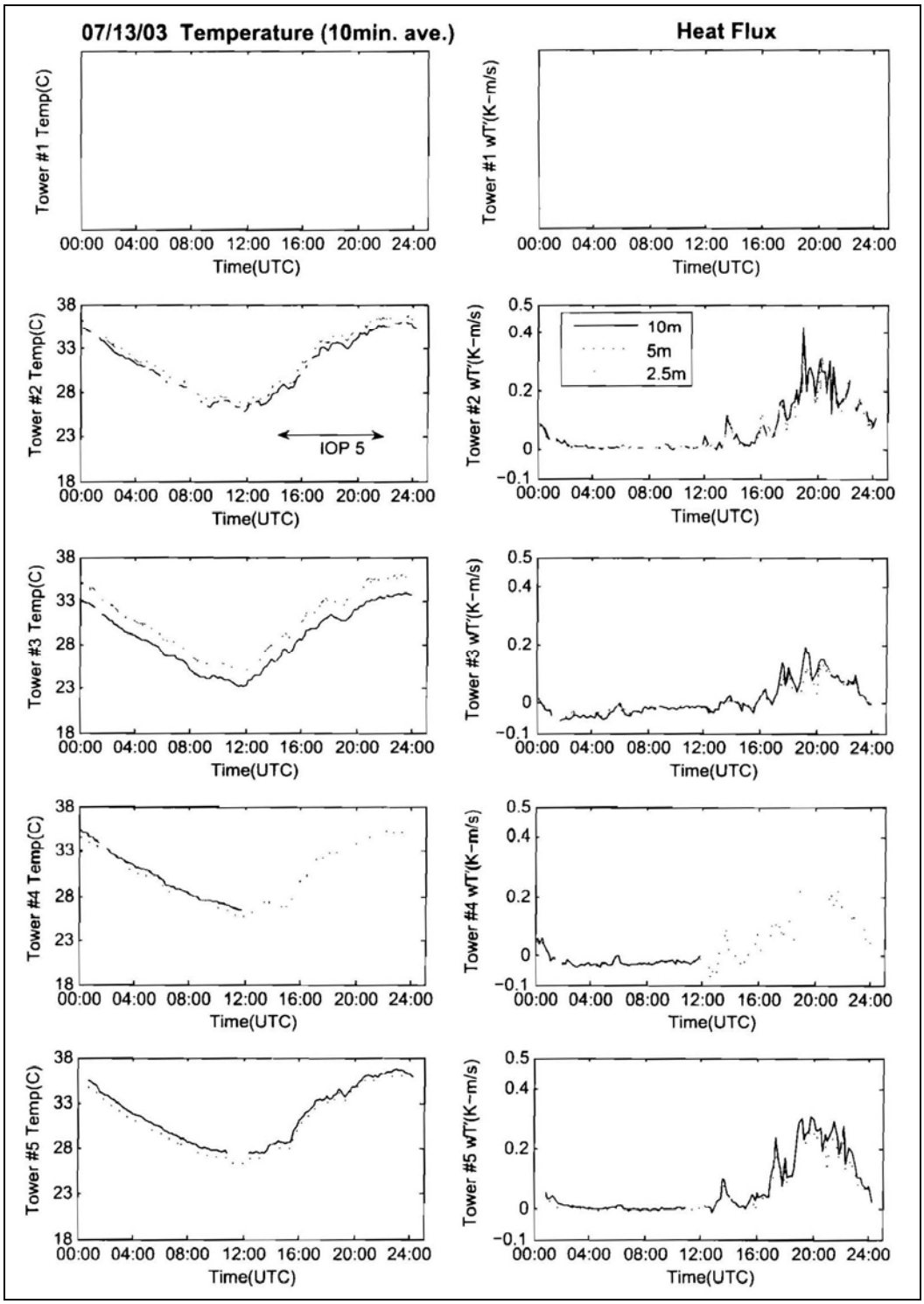

Figure A-15. Temperature and kinematic sensible heat flux, 13 July 2003.

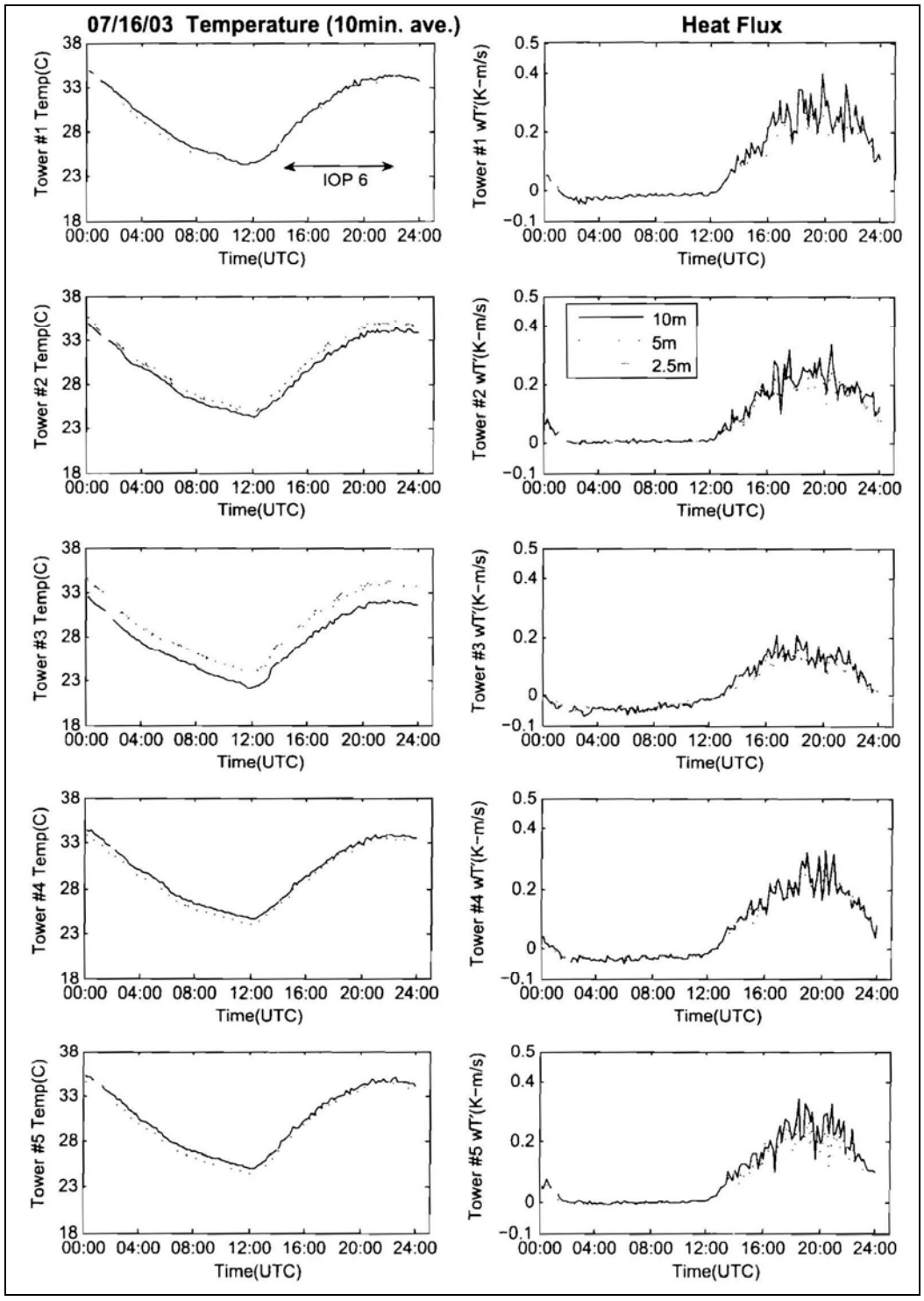

Figure A-16. Temperature and kinematic sensible heat flux, 16 July 2003.

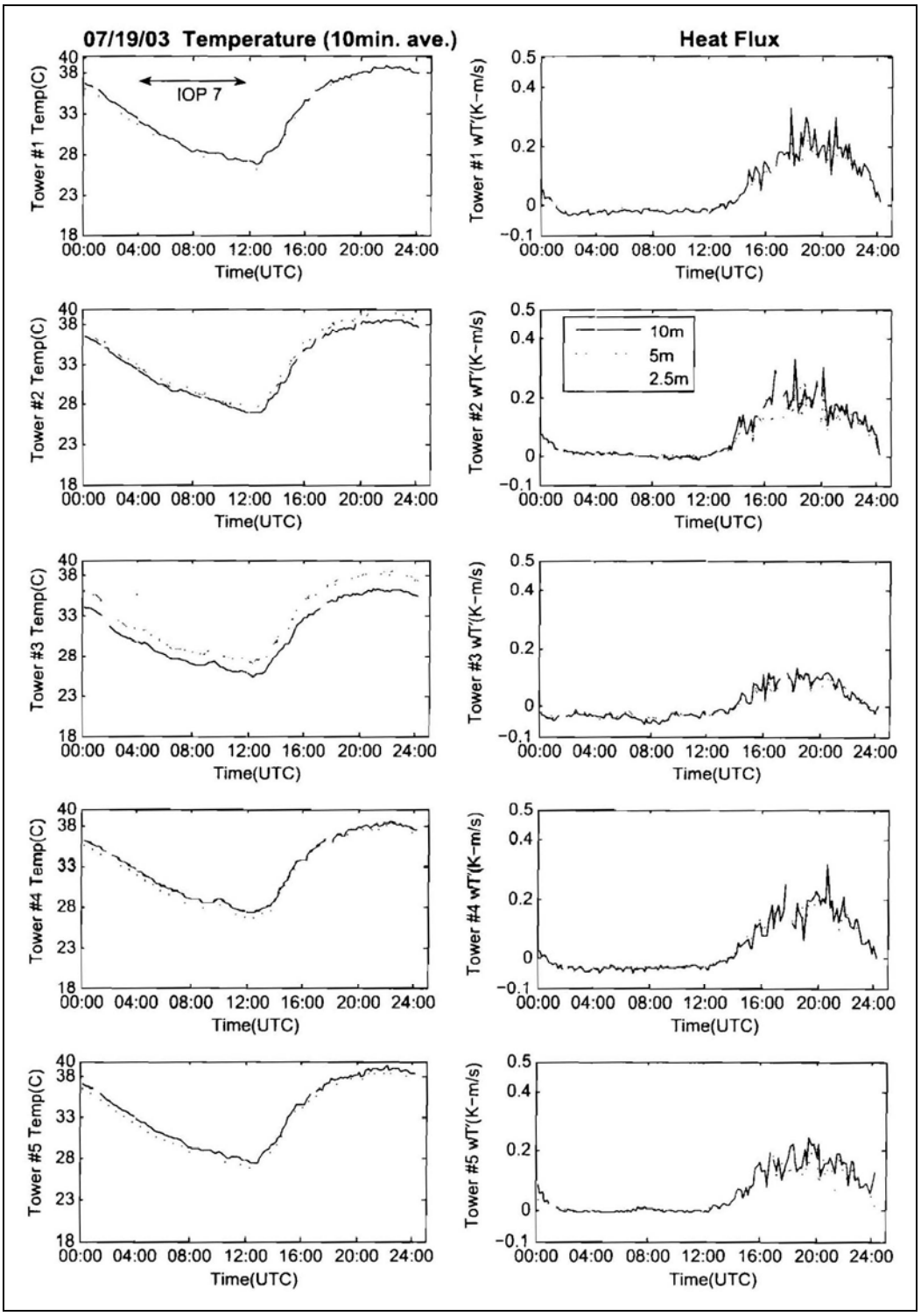

Figure A-17. Temperature and kinematic sensible heat flux, 19 July 2003.

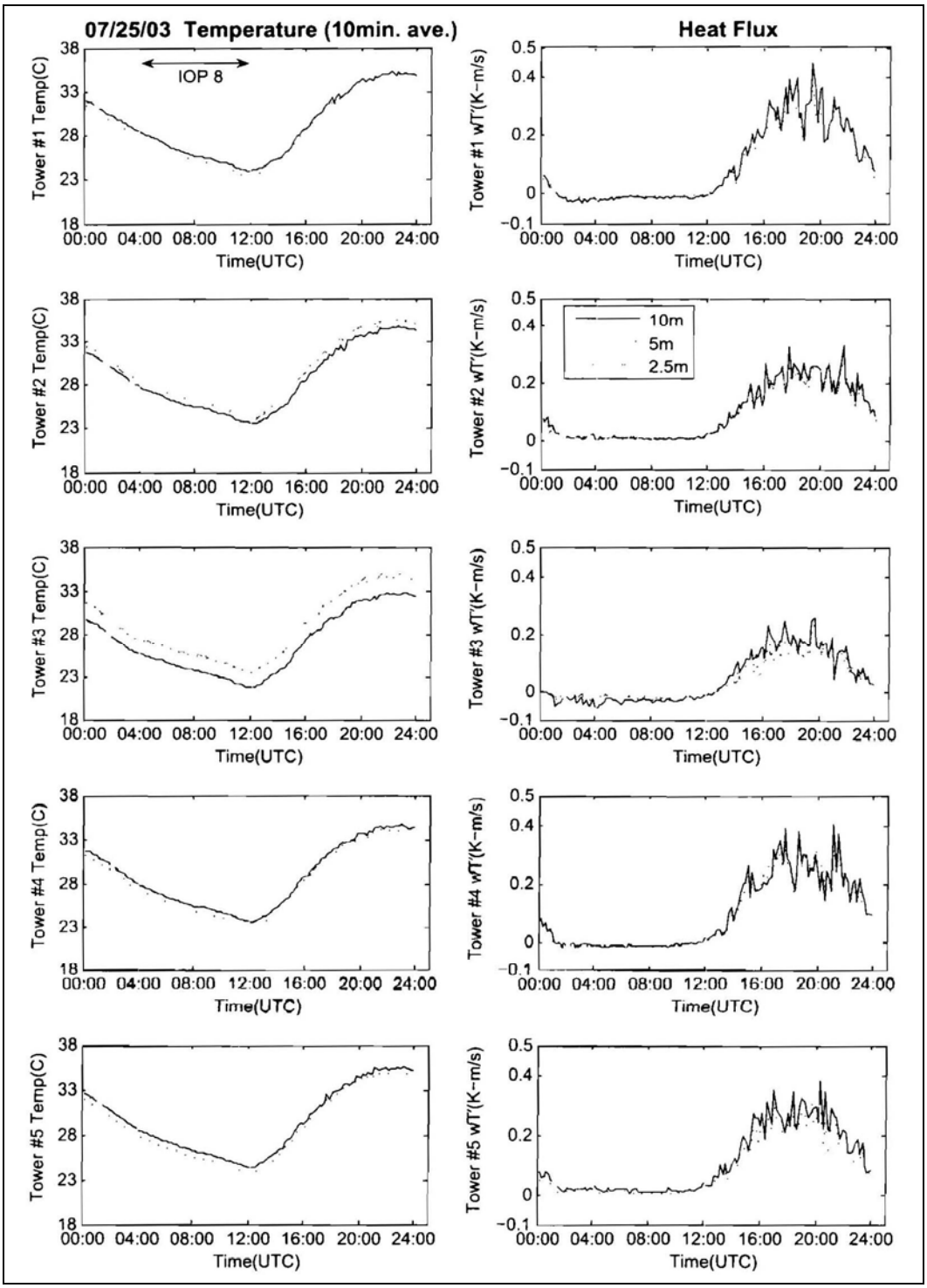

Figure A-18. Temperature and kinematic sensible heat flux, 25 July 2003.

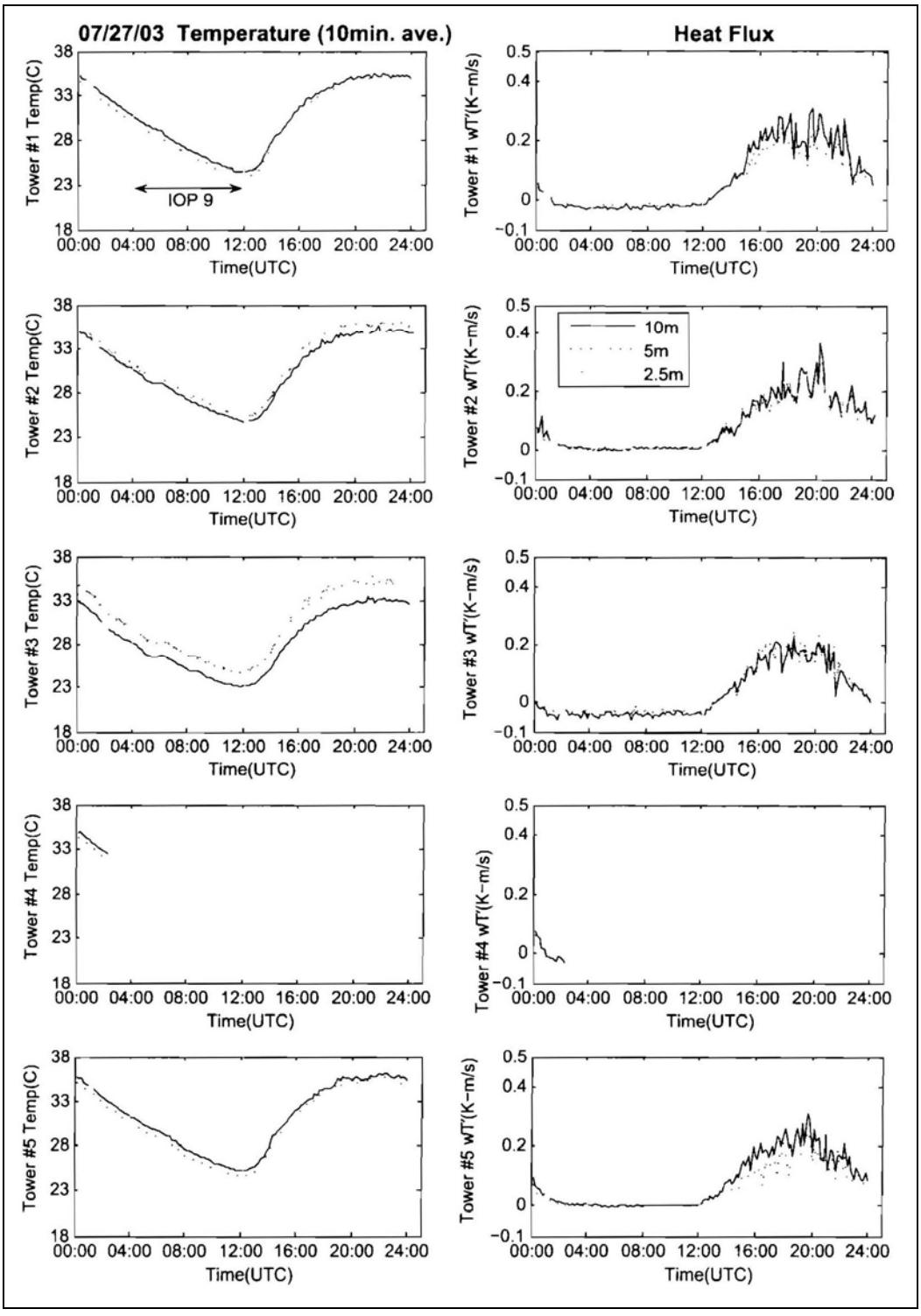

Figure A-19. Temperature and kinematic sensible heat flux, 27 July 2003.

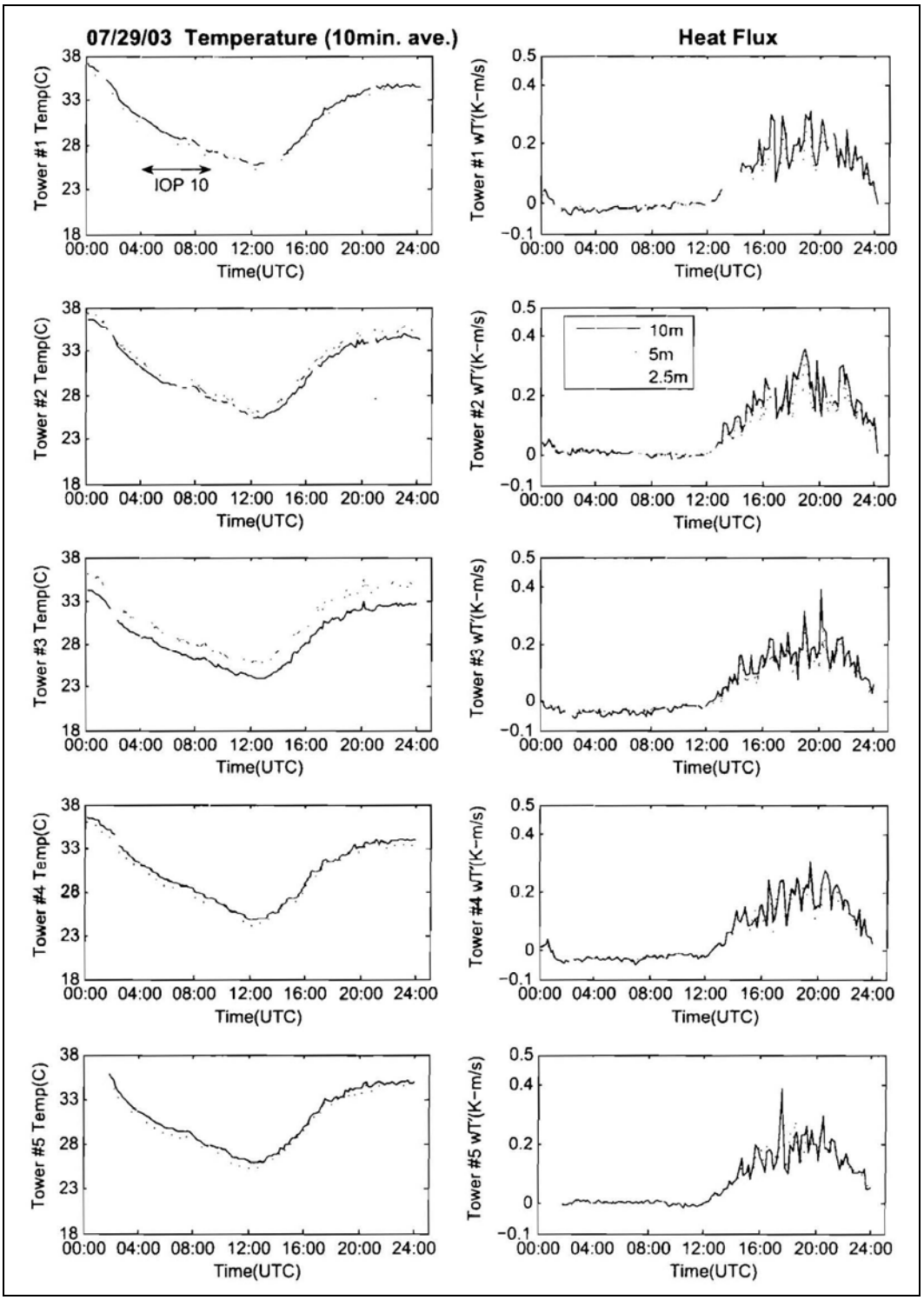

Figure A-20. Temperature and kinematic sensible heat flux, 29 July 2003.

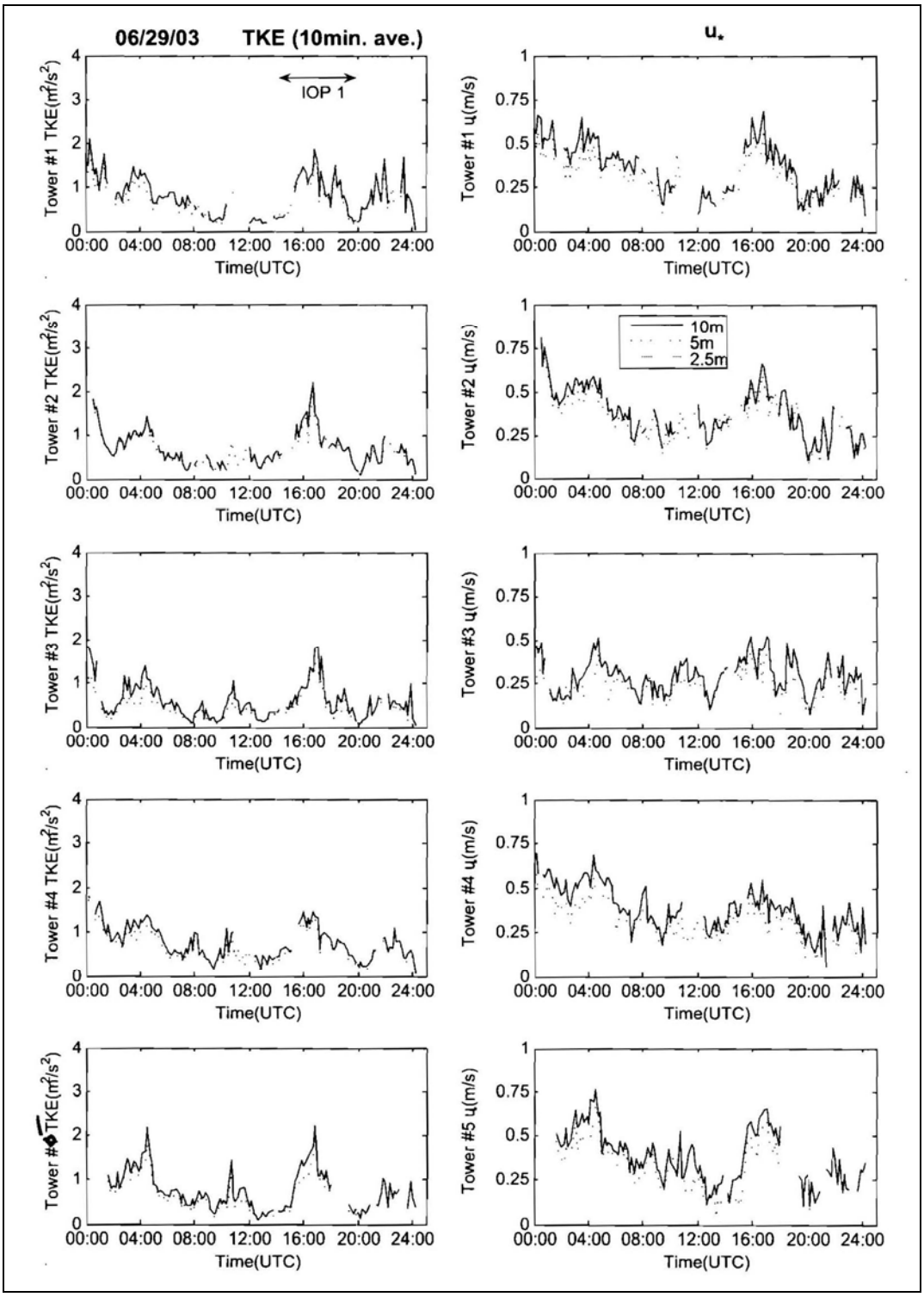

Figure A-21. TKE and friction velocity, 29 June 2003.

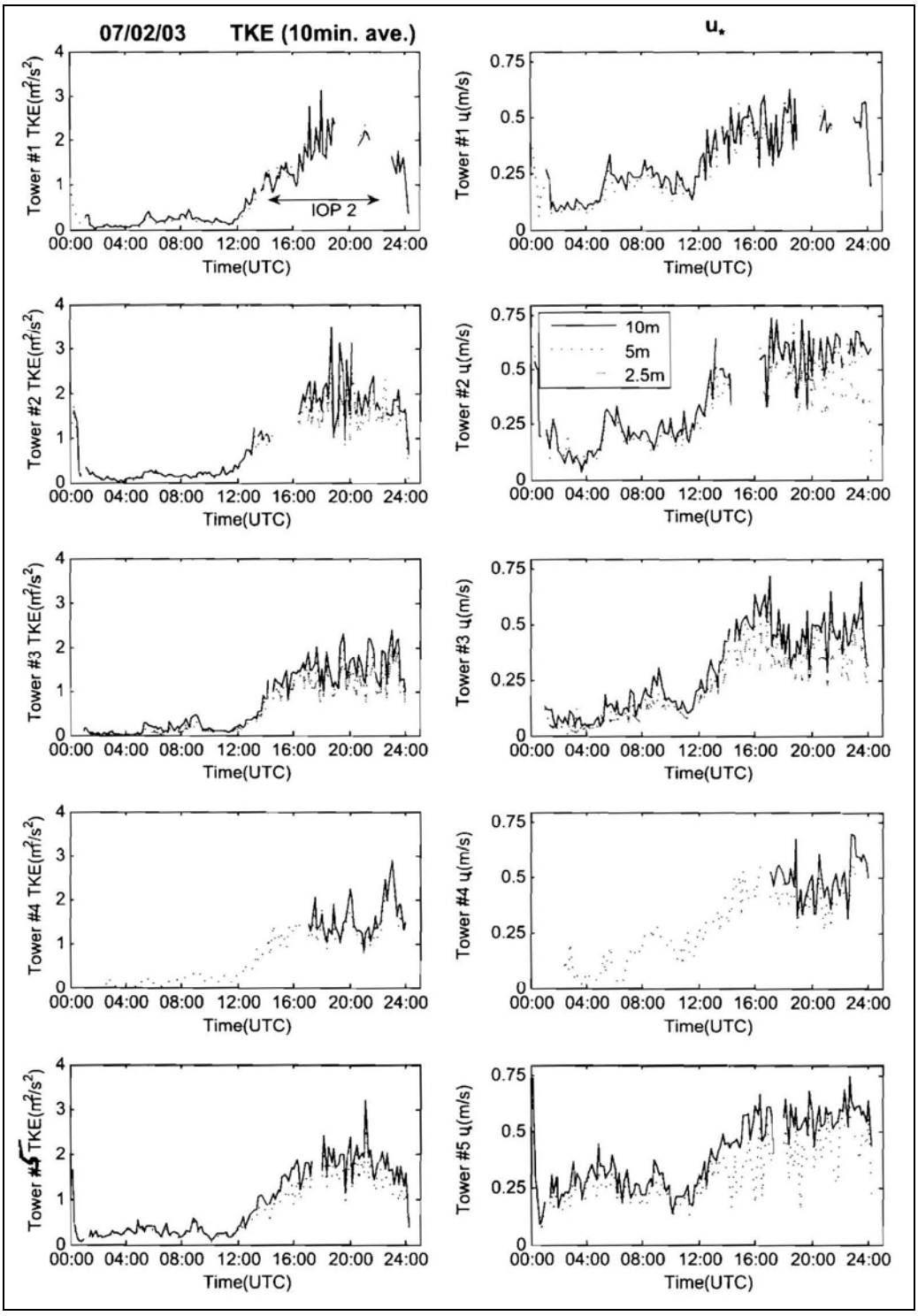

Figure A-22. TKE and friction velocity, 2 July 2003.

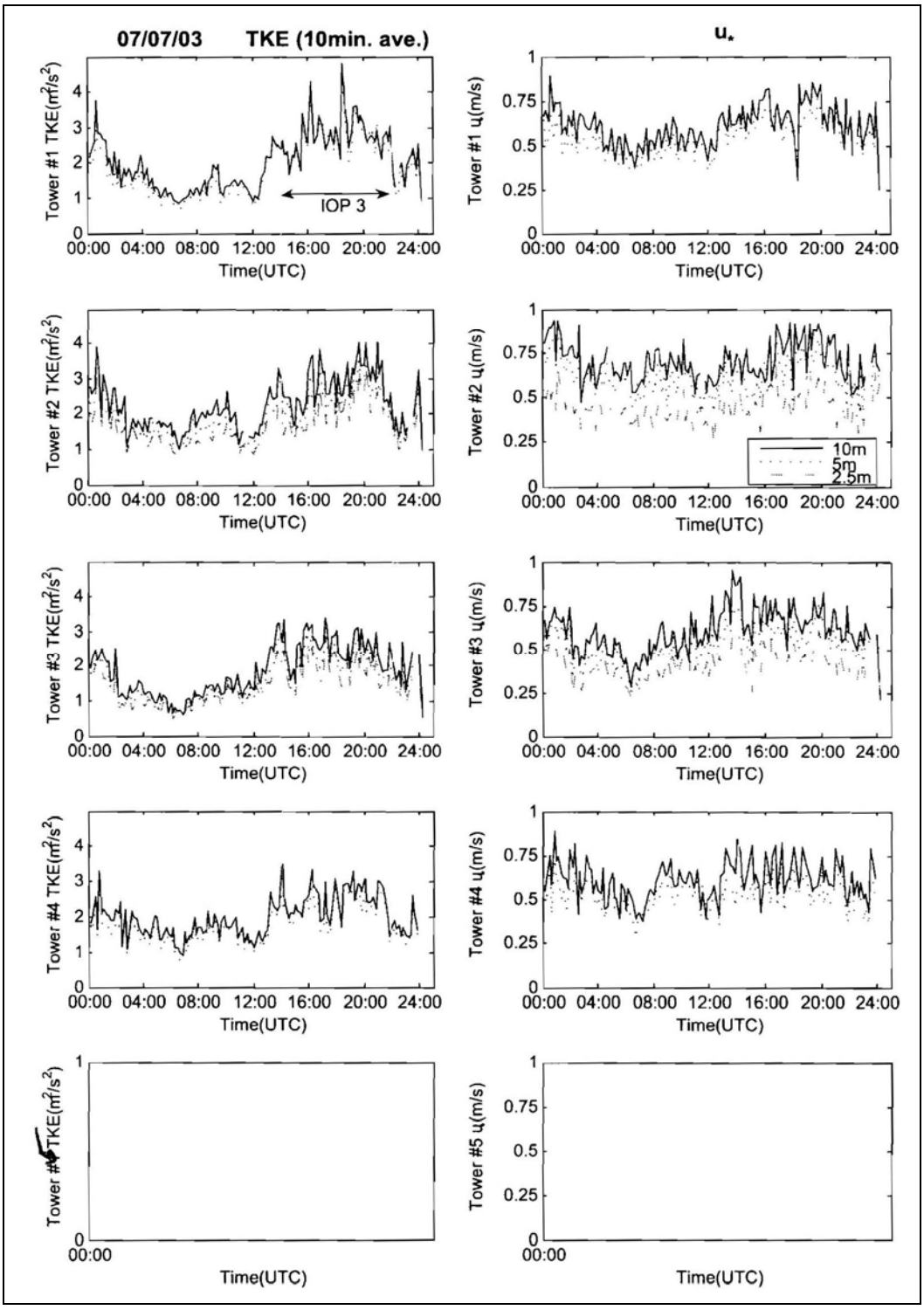

Figure A-23. TKE and friction velocity, 7 July 2003.

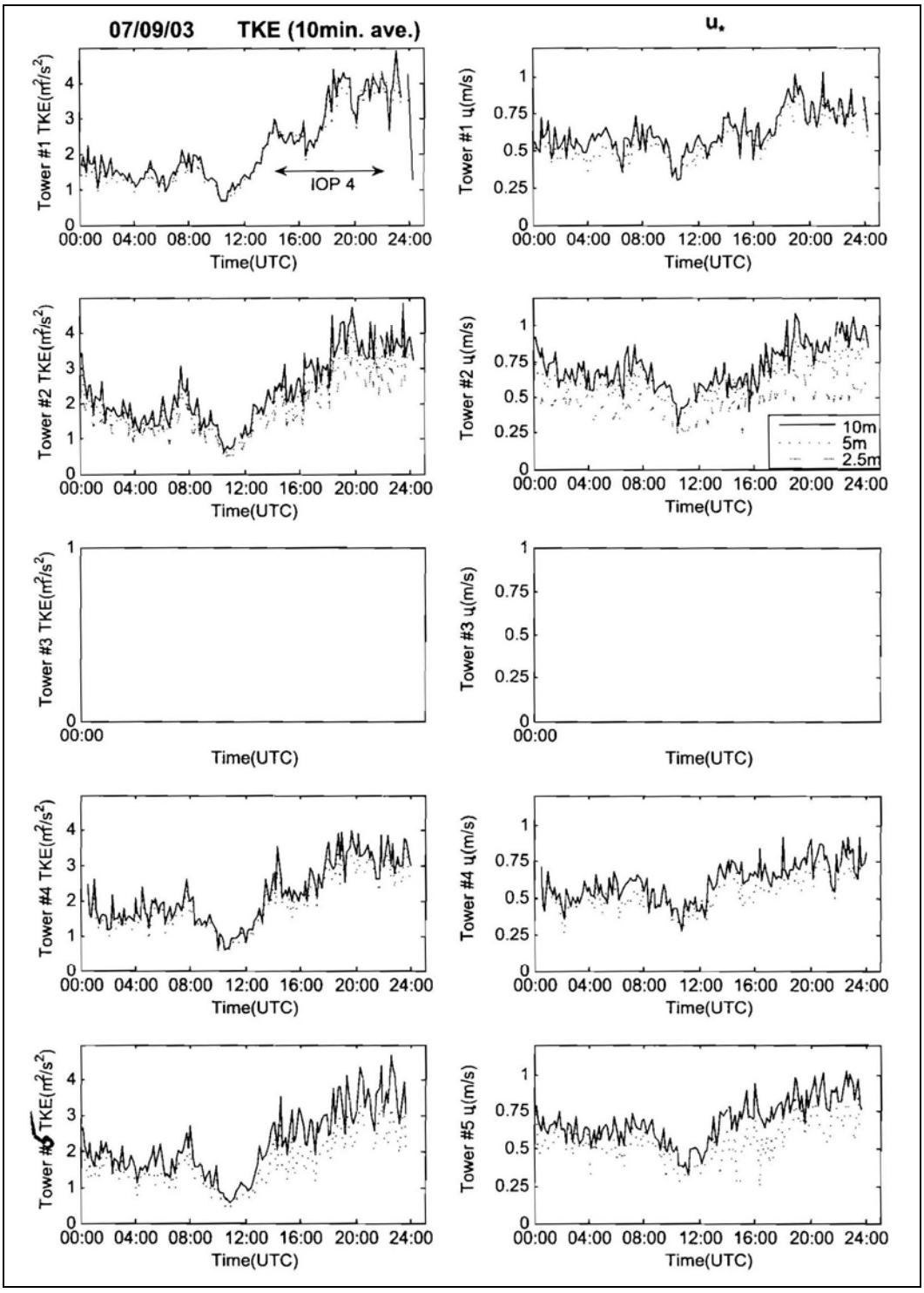

Figure A-24. TKE and friction velocity, 9 July 2003.

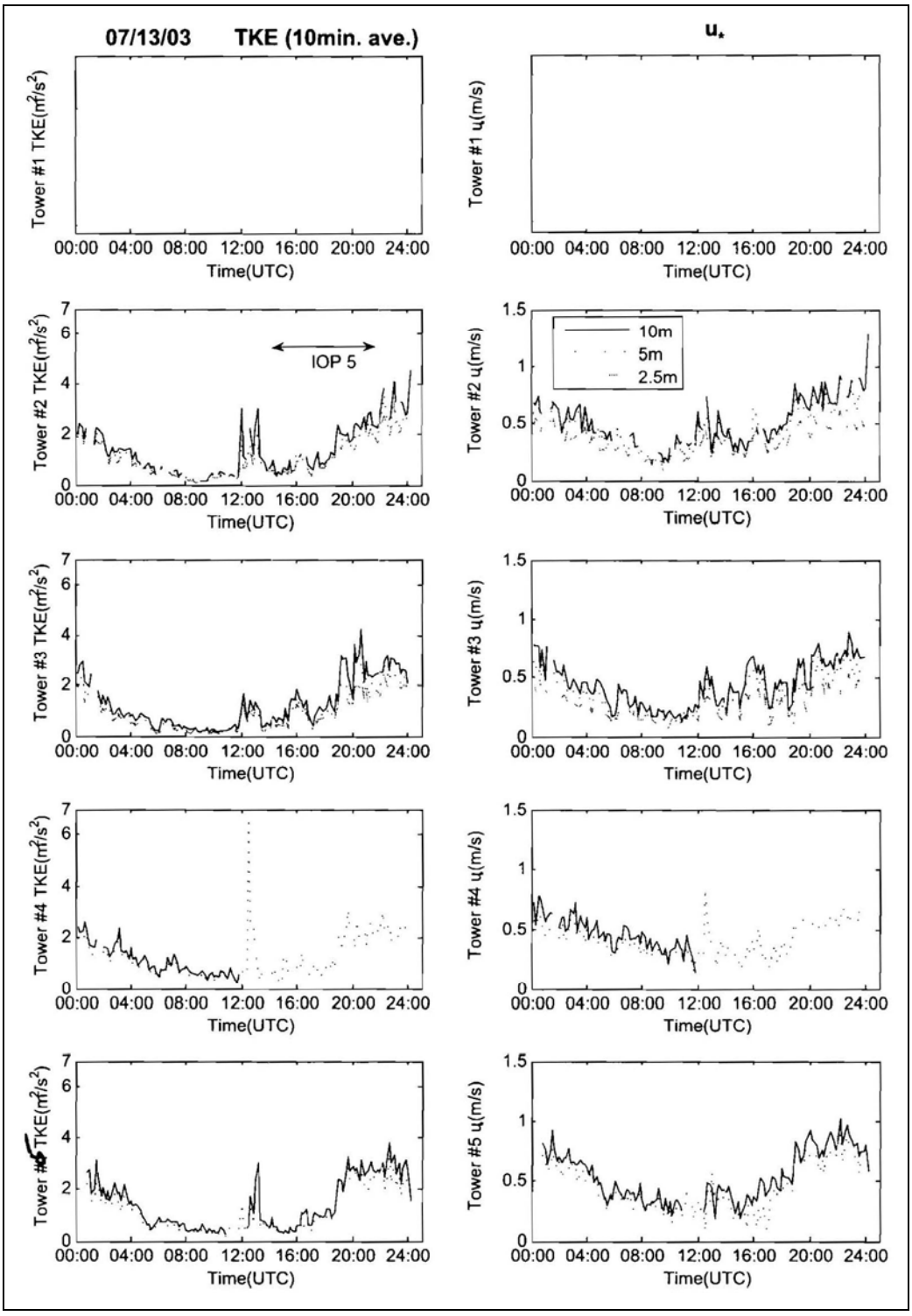

Figure A-25. TKE and friction velocity, 13 July 2003.

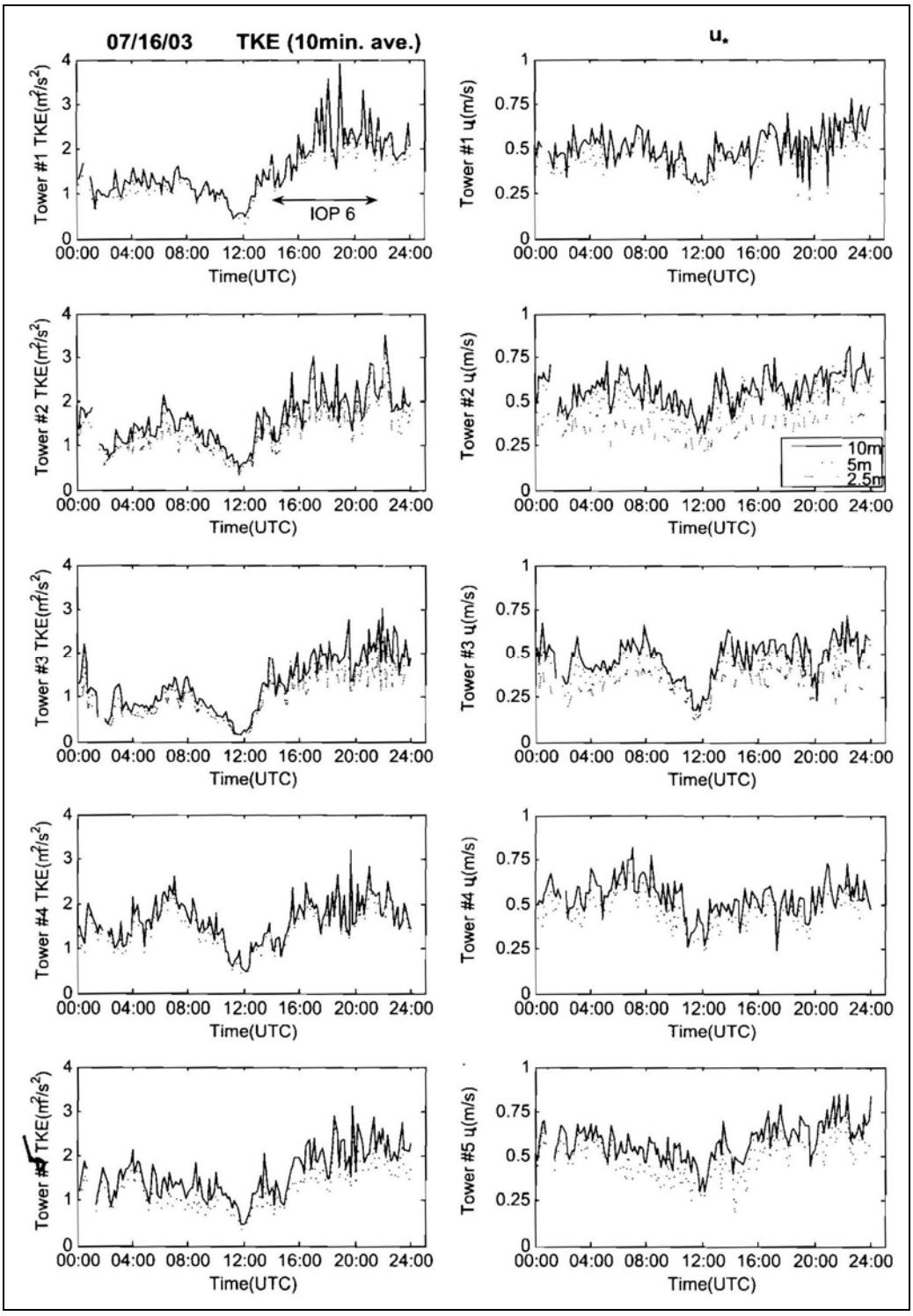

Figure A-26. TKE and friction velocity, 16 July 2003.

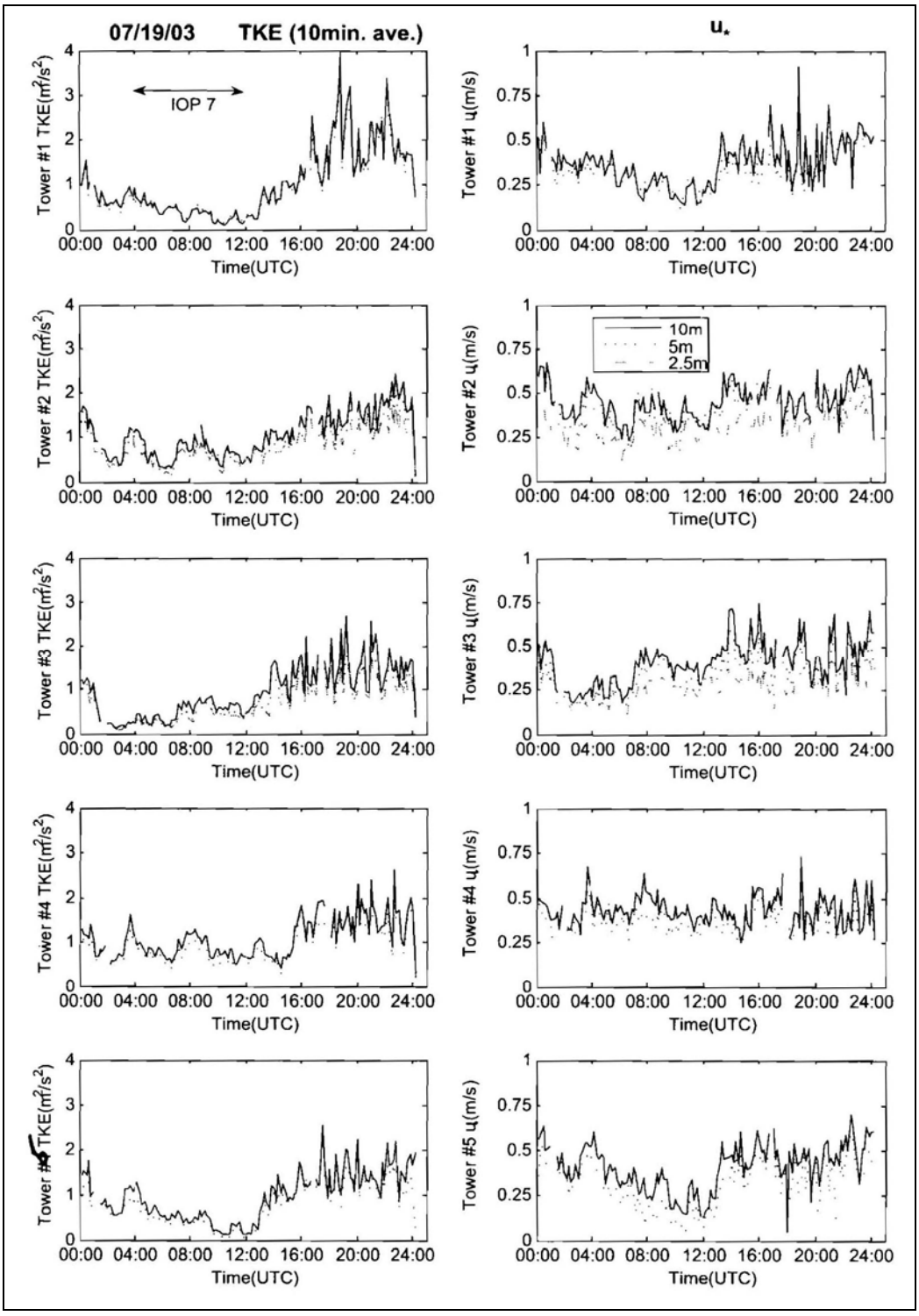

Figure A-27. TKE and friction velocity, 19 July 2003.

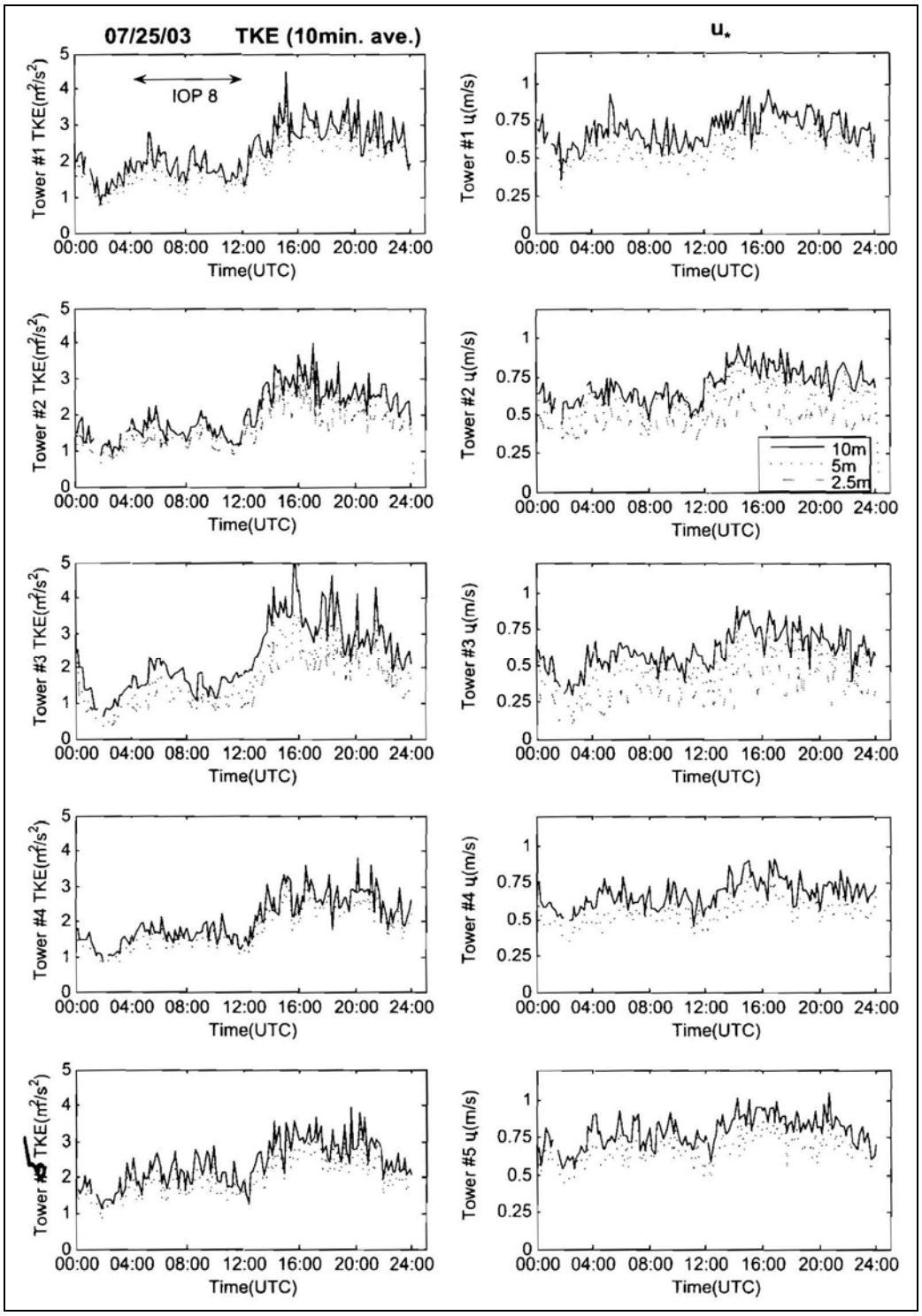

Figure A-28. TKE and friction velocity, 25 July 2003.

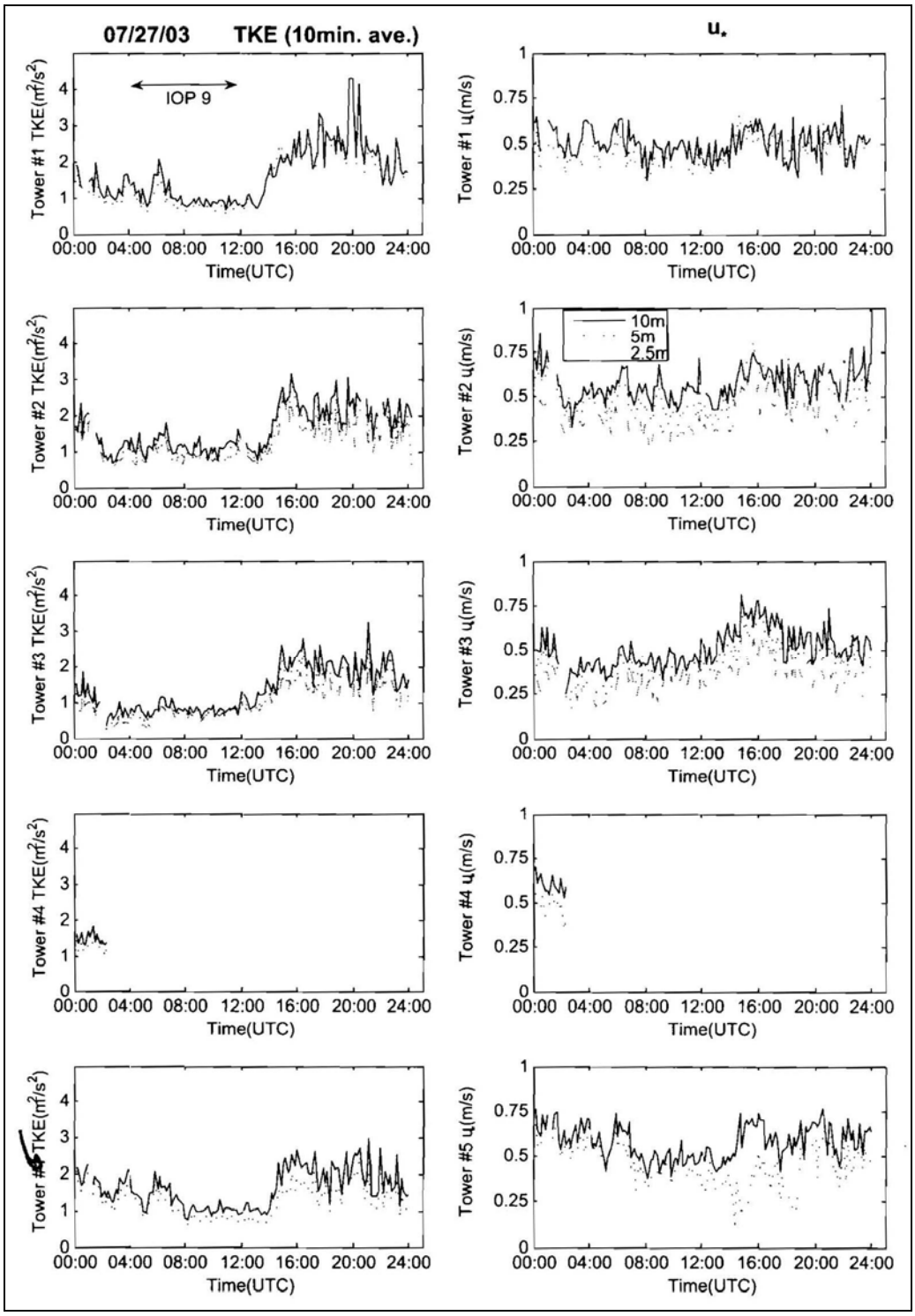

Figure A-29. TKE and friction velocity, 27 July 2003.

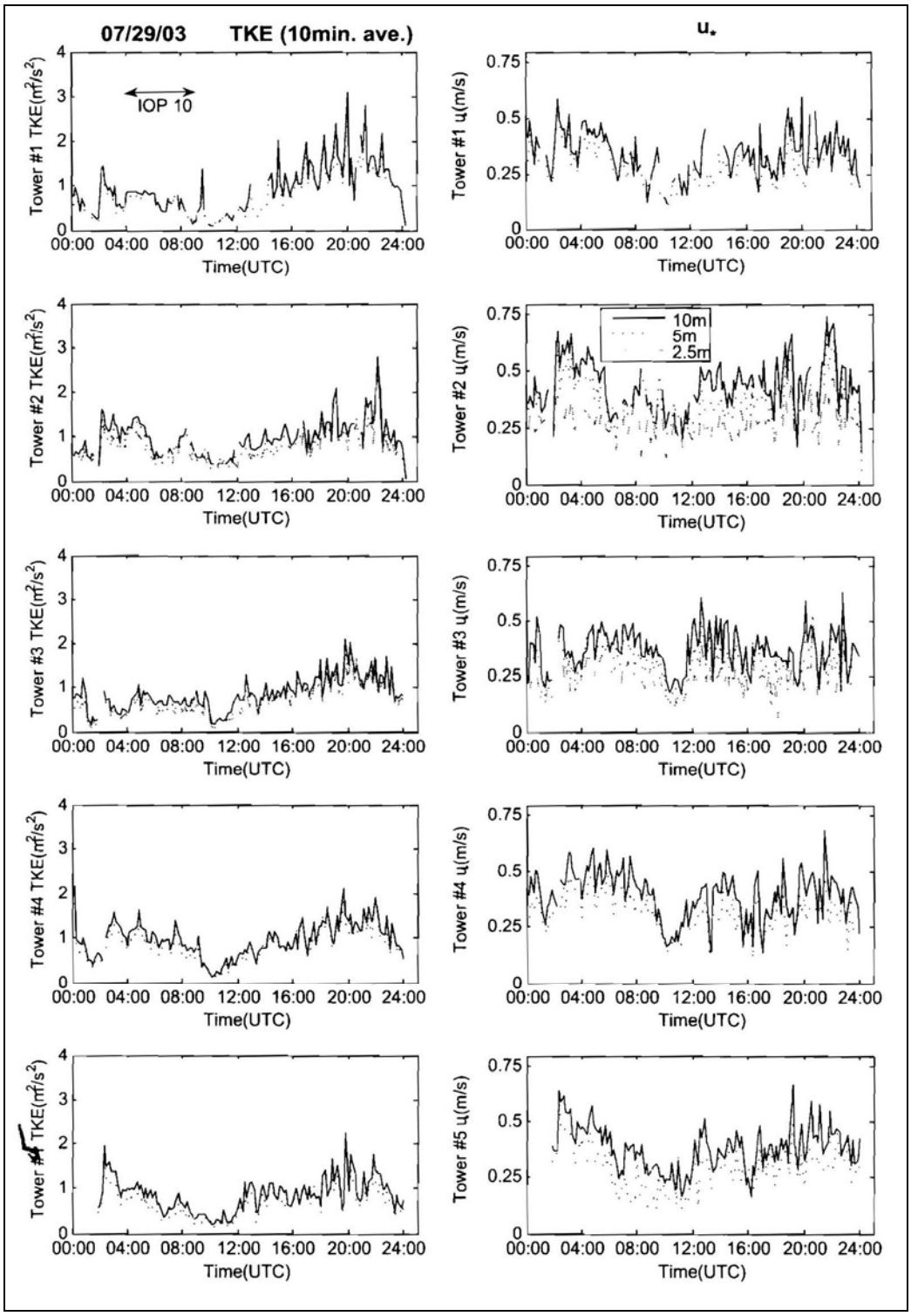

Figure A-30. TKE and friction velocity, 29 July 2003.

INTENTIONALLY LEFT BLANK.

Appendix B. Photographs of ARL Tower Sites and Aerial Views of their Locations

TOWER 1 SITE
Rural-SW: SW 15th & So. Miller
N35° 26.87' W97° 33.67' @1010 Ft (est)

Figure B-1. Tower 1 site.

TOWER 2 SITE
Urban-E: Sheridan St & Byers St
N35° 27.99' W97° 30.24' @1253 Ft (est)

Figure B-2. Tower 2 site.

TOWER 3 SITE
Rural-SE: SE 22nd & Eastern Ave.
N35° 26.57' W97° 28.59' @1238 Ft (est)

Figure B-3. Tower 3 site.

TOWER 4 SITE
10 meter met tower & ARL UPPER AIR STATION
Rural-N: NW 36th & N. Walker
N35° 30.49' W97° 31.16'@1147 Ft(est)

Figure B-4. Tower 4 site.

TOWER 5 SITE
Urban-W: Main St & Klein St
N35° 28.08' W97° 31.93' @1210 Ft (est)

Figure B-5. Tower 5 site.

ARL WIND TRACER LIDAR SITE:
4th Street & Lincoln Street
N35° 28.30' W97° 30.20' @1234 FT(est)

Figure B-6. ARL Wind Tracer Lidar and Microwave Radiometer site.

Aerial photos are available from U.S. Geological Survey, EROS Data Center, Sioux Falls, SD. (http://seamless.usgs.gov).

List of Symbols, Abbreviations, and Acronyms

3D	three-dimensional
3DWF	Three Dimensional Wind Field
ABLE	Atmospheric Boundary Layer Exploitation
AGL	above the ground
APAK	Analysis Package for Time Series
ARL	U.S. Army Research Laboratory
BED	Battlefield Environment Division
CBD	central business district
CCSL	Canopy Coupled to Surface Layer
CDT	Central Daylight Time
CFD	computational fluid dynamic
CFL	constant flux layer
DOE	Department of Energy's
DTRA	Defense Threat Reduction Agency
IOPs	Intensive Observation Periods
JU2003	Joint Urban 2003
LLNL	Lawrence Livermore National Laboratory
met	meteorological
ML	mixed layer
MMS	Meteorological Measuring Set
NNSA	National Nuclear Security Administration
OKC	Oklahoma City
RSL	roughness sub-layer
T	temperature

TKE	turbulent kinetic energy
UCL	urban canopy layer

NO. OF COPIES	ORGANIZATION
1 ELEC	ADMNSTR DEFNS TECHL INFO CTR ATTN DTIC OCP 8725 JOHN J KINGMAN RD STE 0944 FT BELVOIR VA 22060-6218
1	CHAIRMAN JOINT CHIEFS OF STAFF ATTN J5 R&D DIV WASHINGTON DC 20301
1	DARPA ATTN IXO S WELBY 3701 N FAIRFAX DR ARLINGTON VA 22203-1714
2	DIR OF DEFNS RSRCH & ENGRG ATTN DD TWP ATTN ENGRG WASHINGTON DC 20301
1 CD	OFC OF THE SECY OF DEFNS ATTN ODDRE (R&AT) THE PENTAGON WASHINGTON DC 20301-3080
1	COMMANDING OFFICER ATTN NMCB23 6205 STUART RD STE 101 FT BELVOIR VA 22060-5275
1	US ARMY RSRCH DEV AND ENGRG CMND ARMAMENT RSRCH DEV AND ENGRG CTR ARMAMENT ENGRG AND TECHNLGY CTR ATTN AMSRD AAR AEF T J MATTS BLDG 305 ABERDEEN PROVING GROUND MD 21005-5001
1	US ARMY TRADOC BATTLE LAB INTEGRATION & TECHL DIRCTRT ATTN ATCD B 10 WHISTLER LANE FT MONROE VA 23651-5850

NO. OF COPIES	ORGANIZATION
1	NATL GROUND INTLLGNC CTR ATTN RSRCH & DATA BRANCH 220 7TH STRET NE CHARLOTTESVILLE VA 22901-5396
1	PM TIMS, PROFILER (MMS-P) AN/TMQ-52 ATTN B GRIFFIES BUILDING 563 FT MONMOUTH NJ 07703
1	TECOM ATTN AMSTE CL ABERDEEN PROVING GROUND MD 21005-5057
1	US ARMY ENGRG DIV ATTN HNDED FD PO BOX 1500 HUNTSVILLE AL 35807
1	US ARMY INFO SYS ENGRG CMND ATTN AMSEL IE TD A RIVERA FT HUACHUCA AZ 85613-5300
1	US ARMY MIS & SPC INTLLGNC CTR ATTN AIAMS YDL REDSTONE ARSENAL AL 35898-5500
1	US ARMY NATICK RDEC ACTING TECHL DIR ATTN SBCN TP P BRANDLER KANSAS STREET BLDG 78 NATICK MA 01760-5056
1	US ARMY NUC & CHEML AGCY 7150 HELLER LOOP STE 101 SPRINGFIELD VA 22150-3198
1	COMMANDER US ARMY RDECOM ATTN AMSRD AMR W C MCCORKLE 5400 FOWLER RD REDSTONE ARSENAL AL 35898-5000
1	US ARMY STRTGC DEFNS CMND ATTN CSSD H MPL TECHL LIB PO BOX 1500 HUNTSVILLE AL 35807

NO. OF COPIES ORGANIZATION

1 CHIEF OF NAV OPS DEPT OF THE NAVY
ATTN OP 03EG
WASHINGTON DC 20350

1 US AIR FORCE TECH APPL CTR
ATTN HQ AFTAC/TCC
1030 SOUTH HIGHWAY A1A
PATRICK AFB FL 32925-3002

1 CENTRAL INTLLGNC AGCY DIR DB STANDARD
ATTN OSS/KPG/DHRT
1E15 OHB
WASHINGTON DC 20505

1 US GOVERNMENT PRINT OFF
DEPOSITORY RECEIVING SECTION
ATTN MAIL STOP IDAD J TATE
732 NORTH CAPITOL ST NW
WASHINGTON DC 20402

1 NATL CTR FOR ATMOS RSRCH
ATTN NCAR LIBRARY SERIALS
PO BOX 3000
BOULDER CO 80307-3000

1 US ARMY RSRCH LAB
ATTN RDRL CIM G T LANDFRIED
BLDG 4600
ABERDEEN PROVING GROUND MD 21005-5066

1 DIRECTOR
US ARMY RSRCH LAB
ATTN RDRL ROE V W D BACH
PO BOX 12211
RESEARCH TRIANGLE PARK NC 27709

COPIES ORGANIZATION

15 US ARMY RSRCH LAB
ATTN IMNE ALC HRR
MAIL & RECORDS MGMT
ATTN RDRL CIE D
D GARVEY (5 COPIES)
S CHANG
G HUYNH
C KLIPP
Y WANG
C WILLIAMSON
ATTN RDRL CIE S D LIGON
ATTN RDRL CIE P CLARK
ATTN RDRL CIM L TECHL LIB
ATTN RDRL CIM P TECHL PUB
ADELPHI MD

9 US ARMY RSRCH LAB
ATTN RDRL CIE D
D HOOCK (4 COPIES)
E CREEGAN
D S ELLIOTT
E MEASURE
G VAUCHER
ATTN RDRL CIE M
D KNAPP
BLDG 1622
WHITE SANDS MISSILE RANGE NM 88002-5501

TOTAL: 50 (1 ELEC, 1 CD, 48 HCS)